

Asymptotic Safety of Yukawa Systems

Diploma thesis presented to the
Physikalisch-Astronomische Fakultät
Friedrich Schiller Universität Jena

Submitted by
Stefan Rechenberger
born on the first of September 1983
in Dresden, Germany

First referee: Prof. Dr. Holger Gies

Second referee: Dr. Jens Braun

Day of granting of diploma: 26.03.2010

Asymptotic Safety of Yukawa Systems

Abstract

Different Yukawa systems in three and four dimensions are investigated. The four-dimensional systems are toy models and are plagued with the still unresolved triviality and hierarchy problem of the Standard Model Higgs sector. We use the functional renormalisation group equations and construct asymptotic safety scenarios for the four-dimensional models. This was recently done in a simple Yukawa system. In this thesis we expand this model and include a left-right asymmetry. For the three-dimensional model we investigate the critical behaviour of a second-order phase transition to a chiral-symmetry broken phase. The critical behaviour is investigated in terms of critical exponents.

Contents

1	Introduction	7
2	Theoretical Foundations	11
2.1	Quantum Field Theory Basics	11
2.2	Exact Renormalisation Group Equation	12
2.3	Asymptotic Safety	16
2.4	Gauge Theory Basics	17
2.5	Goldstone and Higgs Model	20
3	4D Model without Gauge Bosons	23
3.1	Constructing the Model	23
3.2	Flow Equations	26
3.2.1	Fluctuation Matrix and Regulator	26
3.2.2	Flow Equation of the Effective Potential	27
3.2.3	Flow Equation of the Yukawa Coupling	30
3.2.4	Anomalous Dimensions	33
3.3	Fixed-Point Analysis	37
3.3.1	Symmetric Regime	37
3.3.2	Spontaneously Symmetry Broken Regime	38
4	3D Model without Gauge Bosons	45
4.1	Classification	45
4.2	Flow Equations	50
4.3	Fixed-Point Analysis	52
4.3.1	Symmetric Regime	52
4.3.2	Spontaneously Symmetry Broken Regime	54
5	4D Model including Gauge Bosons	59
5.1	Extension of the Model	59
5.2	Flow Equations	63
5.2.1	Fluctuation Matrix and Regulator	64
5.2.2	Flow Equation of the Effective Potential	65
5.2.3	Flow Equation of the Yukawa Coupling	68
5.2.4	Anomalous Dimensions	69
5.3	Fixed-Point Analysis for $N_L = 2$	71

6	Conclusion and Outlook	75
A	Fluctuation Matrix	77
B	Extended Fluctuation Matrix	79
C	Threshold Functions	81

Chapter 1

Introduction

The Standard Model of particle physics was developed in the early 1970s and has been tested very well in a large number of experiments. It is a quantum field theory containing various fields (see Tab. 1.1), including six quark flavours (upper left in Tab. 1.1) and six lepton flavours (upper right in Tab. 1.1), which are the matter content of the known universe. Further included particles are eight gluons, the W- and Z-bosons and the photon (the lower part in Tab. 1.1). These particles are carrier particles and thus are responsible for the interaction of the matter particles. They belong to the strong force, the weak force and the electromagnetic force, respectively. The last particle of the Standard Model is the yet not discovered Higgs particle. This field is very important since it generates the masses of the matter particles via a Yukawa interaction in combination with the mechanism of spontaneous symmetry breaking (SSB). The Higgs field also generates the masses of the W- and Z-bosons via this mechanism. The fourth known force (gravity) and its carrier particle (graviton) are not included in the Standard Model.

The success of the Standard Model did not come all of a sudden. It took a long time from the proposition of quarks as constituents of protons and neutrons by Gell-Mann and Zweig in 1964. Important steps towards today's picture were the electroweak unification in 1967 by Weinberg, Glashow and Salam, the first observation of a quark (charmed quark) in an experiment in 1974, the experimental proof for the bottom quark in 1977, the discovery of the W- and Z-bosons in 1983, the evidence for the top quark, as the heaviest quark, in 1995 at Fermilab and the observation of the τ -neutrino in 2000 also at Fermilab. Today all the particles of the Standard Model except the Higgs boson has been observed. The hope is that this last particle has not been observed yet because of insufficient energies at the

u	d	e	ν_e	h
c	s	μ	ν_μ	
t	b	τ	ν_τ	
g	W^\pm	Z^0	γ	

Table 1.1: Particles of the Standard Model.

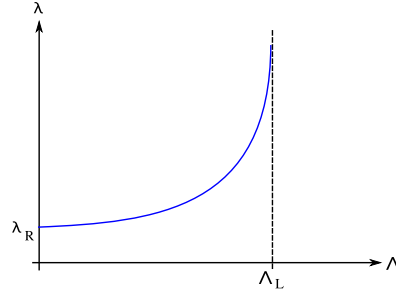


Figure 1.1: Landau pole of the perturbative $\lambda\phi^4$ theory.

experiments made till this day. If this is the case the new experiments at the Large Hadron Collider (LHC) at CERN coming up in the next few years may successfully find the last undiscovered part of the Standard Model.

In spite of the successes of this model there are still unresolved problems. First of all the unification with gravity. Furthermore there are obscurities about neutrino masses and oscillations, dark matter and energy and baryon asymmetry. However, besides these problems which are beyond the Standard Model there is also lack of knowledge inside the theory. Two problems which are still unresolved are the *triviality problem* and the *hierarchy problem*. These are the two problems which we tackle in the present work.

The easiest way to explain the triviality problem is to study the perturbative $\lambda\phi^4$ theory. The relation between the bare coupling λ and the renormalised coupling λ_R is given by

$$\frac{1}{\lambda_R} - \frac{1}{\lambda} = \beta_0 \ln \left(\frac{\Lambda}{m_R} \right), \quad \beta_0 = \text{const.} > 0.$$

Here m_R is the renormalised mass and Λ is a momentum cutoff. If the renormalised coupling is kept fixed and the momentum cutoff is send to infinity the bare coupling diverges at the *Landau pole*

$$\Lambda_L = m_R \exp \left(\frac{1}{\beta_0 \lambda_R} \right).$$

See also Fig. 1.1. On the other hand, if we fix the bare coupling λ the continuum limit ($\Lambda \rightarrow \infty$) leads to a vanishing renormalised coupling λ_R . Thus the theory becomes trivial. That is why the problem is called triviality problem. If one investigates the Standard Model, which is of course more complicated than the $\lambda\phi^4$ theory, one gets the same problem in the Higgs sector [1, 2, 3, 4, 5, 6, 7] and also in the U(1) gauge sector [8, 9, 10, 11]. The common opinion is that the Standard Model is an effective theory which means that it is only valid up to a cutoff scale Λ_{cutoff} where new physics sets in. In this spirit the Standard Model has to be considered as a low energy limit of a more fundamental theory.

The scale where the Landau pole of the U(1) sector occurs is beyond the Planck scale where gravitational contributions have to be taken into account [9]. The Landau pole of the Higgs sector occurs at a scale below the Planck scale. Thus the cutoff

scale for the Standard Model has to be below the scale of the Landau pole of the Higgs sector. That is why we are turning our attention to this triviality problem.

One might ask whether the triviality problem is a problem of the system or just a problem due to the shortcomings of perturbation theory. One hint for the latter is that near the Landau pole the interaction constant becomes very large and thus the perturbation theory predicts its own breakdown. This induced some investigations of scalar and Yukawa systems with non-perturbative lattice methods which confirmed the Landau pole in a limited set of scenarios [12, 13, 14, 15, 16, 17, 18, 19, 20, 21]. Also the gauged Yukawa system was investigated [22]. Another non-perturbative method is the functional renormalisation group which we are using in the present work.

Our aim is to construct an asymptotic safety scenario. In such a scenario one uses nontrivial fixed points instead of the trivial one of perturbation theory¹. A fixed point of this type would enable us to move the cutoff to infinity. This brings back our attention to the Planck scale where the other triviality problem occurs and also gravity sets in. In this region the search for asymptotic safety scenarios including gravity is also at work. The hope is that it might be possible to construct such a scenario including the matter content of the Standard Model and gravitation [23, 24, 25].

The inclusion of all these things is far beyond the scope of this work. We restrict ourselves to toy models which are less complicated but still have the properties of the Standard Model Higgs sector which are responsible for the triviality problem. In this way we try to find out which degrees of freedom are needed to construct an asymptotic safety scenario and hope to get a deeper insight into the problem itself.

The second problem mentioned above is the hierarchy problem of the Higgs sector. It is not a fundamental problem, like the triviality problem, but it seems unnatural. The reason is a large separation of the Higgs mass at different scales. At a ultraviolet (UV) cutoff scale (Λ_{UV}) $m^2 \sim \Lambda_{UV}^2$ holds. Let us consider the GUT scale $\Lambda_{GUT} \sim 10^{16}\text{GeV}$ as a UV cutoff scale. As an infrared (IR) scale let us use the scale of electroweak symmetry breaking $\Lambda_{EW} \sim 10^2\text{GeV}$. Again perturbation theory suffices to explain the hierarchy problem. The mass at the EW scale is expected to be given as $m_{EW}^2 = a10^4\text{GeV}^2$ where a is a constant of order one. The relation between the initial condition (m_{GUT}^2) and m_{EW}^2 is given by

$$m_{EW}^2 \sim m_{GUT}^2 - \delta m^2,$$

with δm^2 being the counterterm of perturbation theory. Since these contributions are of order of the squared cutoff we can write $\delta m^2 = b10^{32}\text{GeV}^2$. Again b is a constant of order one. Thus we get

$$m_{GUT}^2 \sim (b + a10^{-28}) 10^{32}\text{GeV}^2.$$

The second part in the parentheses indicates that the initial condition, m_{GUT}^2 , has to be given very precisely. This is called *fine tuning* of initial conditions. In our case

¹A fixed point is called trivial if all interaction constants vanish and nontrivial if at least one remains finite.

the precision has to be of order $\Lambda_{\text{EW}}^2/\Lambda_{\text{GUT}}^2 \sim 10^{-28}$. This is the point which seems unnatural as mentioned above but does not represent a problem of principle.

The question is if it is possible to circumvent the Hierarchy problem. There are different approaches on how to solve the problem, e.g., with supersymmetry. Our aim is to solve or at least weaken the hierarchy problem by using the asymptotic safety scenario. In order to explain this idea we have to use the terminology of the renormalisation group: The quadratic dependence on the cutoff scale Λ_{UV} mentioned above corresponds to the critical exponent $\theta = 2$ at a perturbative, trivial fixed point. The critical exponent specifies how fast a given coupling flows away from the fixed point. If it is possible to get an interacting, or nontrivial, fixed point it might be possible that the value of the critical exponent at this point is less than that of the trivial one. Such a *non-Gaussian* fixed point corresponds to an asymptotic safety scenario if some other conditions are fulfilled. The hierarchy problem is said to be weakened if $\theta < 2$ and is said to be solved if $\theta \ll 1$.

In summary, we aim to construct an asymptotic safety scenario for a toy model plagued by the triviality problem and the hierarchy problem. If this is possible and the critical exponent at the corresponding fixed point is less than two we would have solved the triviality problem and the hierarchy problem would be, at least, weakened.

A first step in this direction was done by Holger Gies and Michael M. Scherer in [26]. They investigated a simple Yukawa system which consists of a single real scalar field, representing the Higgs field, and N Dirac fermions. The goal of the present work is to extend this model and to construct an asymptotic safety scenario. Therefore we start, in Chap. 2, by introducing briefly the tools we are using. This includes the exact renormalisation group equation, the asymptotic safety scenario and a short introduction to gauge theories. This introduction is far away from being complete but contains the things needed in this work. Furthermore this chapter contains a section about the Goldstone and the Higgs model. In Chap. 3 we are starting by motivating the model under investigation in this chapter. Afterwards we deduce the flow equations of the system and analyse the fixed-point behaviour of this model in the symmetric regime and in the spontaneously symmetry broken regime², see also [27, 28] for this four-dimensional model. Chap. 4 is an excursion: It investigates the model of Chap. 3 in three dimensions. In the first section we give a short overview over the comparison of our model with other models like the Thirring model or the Gross-Neveu model. After motivating our three-dimensional model we are following the steps of the previous chapter and deduce the flow equations and analyse the fixed-point behaviour, see also [29]. In Chap. 5 we are turning back to our four-dimensional model of Chap. 3. We extend this model by introducing gauge degrees of freedom. Again we start with a short motivation before deducing the flow equations and analysing the fixed-point structure. In the last chapter we conclude and give a short outlook.

²We talk about regimes at ultraviolet scales and about phases at infrared scales.

Chapter 2

Theoretical Foundations

In the following chapters we use the functional renormalisation group (RG) in the formulation as put forward by C. Wetterich [30]. Here we give a short introduction. For more information see [31, 32, 33, 34, 35, 36]. The functional RG method is not restricted to weak couplings, like in perturbation theory. It is a combination of functional methods and the RG idea. Functional methods handle with generating functionals or correlation functions and try to solve them analytically. To do so one starts with microscopic interactions and has to integrate out all quantum fluctuations to understand the macroscopic physics. The RG idea is not to integrate over all momentum scales at once, but to integrate momentum shells successively (Wilson's idea). This leads to an exact differential equation. We shall recall the most important quantum field theory (QFT) basics, before we derive this RG equation. Afterwards we introduce the idea of asymptotic safety and give a very brief introduction to gauge theories. At the end of this chapter we introduce the Goldstone and the Higgs model.

2.1 Quantum Field Theory Basics

In quantum field theory all the information about a system is encoded in correlation functions. In the case of a scattering process with two incoming and $n - 2$ outgoing fields, the system is described by a n -point correlator. This correlator is defined through n field operators $\varphi(x_i)$ as $\langle \varphi(x_1) \dots \varphi(x_n) \rangle$. In Euclidean field theory and with the help of the path integral formalism this correlator can be written as

$$\langle \varphi(x_1) \dots \varphi(x_n) \rangle = \mathcal{N} \int \mathcal{D}\varphi \varphi(x_1) \dots \varphi(x_n) e^{-S[\varphi]},$$

where S is the action and \mathcal{N} is a normalisation constant. We assume that a proper definition of the measure can be given, for example with a spacetime lattice discretisation. Furthermore this measure has to preserve the symmetry of the relevant theory.

The information of all n -point correlators can be summarised in a generating functional

$$Z[J] = \int \mathcal{D}\varphi e^{-S[\varphi] + \int d^d x J(x) \varphi(x)}. \quad (2.1)$$

If this generating functional is known, all n -point functions can be determined by taking functional derivatives with respect to the fields.

$$\langle \varphi(x_1) \dots \varphi(x_n) \rangle = \frac{1}{Z[0]} \left(\frac{\delta^n Z[J]}{\delta J(x_1) \dots \delta J(x_n)} \right)_{J=0}.$$

It is also possible to use the Schwinger functional W , instead of Z . W is defined through $Z[J] = \exp(W[J])$. Another alternative (and this is the one we use) is to Legendre transform this Schwinger functional and use the so-called *effective action* Γ .

$$\Gamma[\Phi] = \sup_J \left(\int d^d x J \Phi(x) - W[J] \right). \quad (2.2)$$

All information about the system is stored in these functionals. Once $Z[J]$, $W[J]$ or $\Gamma[\Phi]$ is computed the theory is “solved”.

The next question is how to compute for example the effective action. Let J_{sup} be the value of J where $\int d^d x J \Phi - W$ reaches its supremum. At $J = J_{\text{sup}}$ the following equation holds:

$$\frac{\delta \Gamma[\Phi]}{\delta \Phi(x)} = - \int d^d y \frac{\delta W[J]}{\delta J(y)} \frac{\delta J(y)}{\delta \Phi(x)} + \int d^d y \frac{\delta J(y)}{\delta \Phi(x)} \Phi(y) + J(x) = J(x). \quad (2.3)$$

The last identity is true since

$$0 \stackrel{!}{=} \frac{\delta}{\delta J(x)} \left(\int d^d x J \Phi - W[J] \right) \Rightarrow \Phi = \frac{\delta W}{\delta J}$$

is true at $J = J_{\text{sup}}$. With Eq. (2.2), Eq. (2.3) and Eq. (2.1) we find

$$e^{-\Gamma[\Phi]} = \int \mathcal{D}\varphi \exp \left(-S[\Phi + \varphi] + \int d^d x \frac{\delta \Gamma[\Phi]}{\delta \Phi} \varphi \right).$$

Altogether we get a nonlinear first-order functional differential equation, which is a result of a functional integral, for computing the effective action. A different way for the computation is given by RG ideas, where we get the flow equation mentioned above which was first developed by C. Wetterich [30].

2.2 Exact Renormalisation Group Equation

Let us now derive this flow equation. It is called the *exact renormalisation group equation* (ERGE). Instead of the effective action, like in Eq. (2.2), we define an *effective average action* Γ_k . Let k be a momentum-shell parameter, such that

$$\Gamma_{k \rightarrow \Lambda} \simeq S_{\text{bare}} \quad \text{and} \quad \Gamma_{k \rightarrow 0} = \Gamma, \quad (2.4)$$

where S_{bare} is the bare action and Λ is an ultraviolet (UV) cutoff scale. As we did for Γ we define the generating functional, but this time we insert a *regulator term* ΔS_k , which implicitly specifies the properties of the momentum-shell integration:

$$e^{W_k[J]} \equiv Z_k[J] := \int \mathcal{D}\varphi e^{-S[\varphi] - \Delta S_k[\varphi] + \int d^d x J \varphi}. \quad (2.5)$$

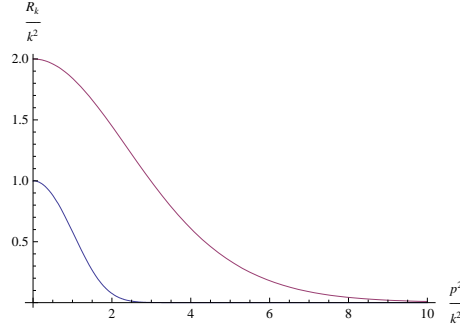


Figure 2.1: The exponential regulator $\frac{R_k(p)}{k^2} = \frac{p^2/k^2}{\exp(p^2/k^2)-1}$ (lower curve) and its derivative $\frac{\partial_t R_k}{k^2}$ (upper curve).

Let ΔS_k be quadratic in φ for acting like a k -dependent mass term:

$$\Delta S_k[\varphi] = \frac{1}{2} \int \frac{d^d p}{(2\pi)^d} \varphi(-p) R_k \varphi(p). \quad (2.6)$$

Here the *regulator function* R_k , sometimes also called *cutoff function*, has to fulfil the following conditions:

$$\lim_{p^2/k^2 \rightarrow 0} R_k(p) > 0, \quad \lim_{k^2/p^2 \rightarrow 0} R_k(p) = 0 \quad \text{and} \quad \lim_{k^2 \rightarrow \Lambda \rightarrow \infty} R_k(p) \rightarrow \infty. \quad (2.7)$$

The first condition implements an infrared (IR) regularisation, which means that the IR modes become mass like. The second condition ensures $Z_{k \rightarrow 0}[J] = Z[J]$ and the third condition ensures that we find the classical action for $k^2 \rightarrow \Lambda \rightarrow \infty$. Therefore the regularised effective average action Γ_k satisfies Eq. (2.4) if it is defined by the *average generating functional* Z_k , with a regulator function satisfying Eq. (2.7). A typical regulator and its derivative is shown in Fig. 2.1.

Since we know that the effective average action exhibits the correct limits for $k \rightarrow 0$ and $k \rightarrow \infty$ we now turn our attention to the intermediate path, the *RG trajectory*. At first we define the logarithmic scale parameter $t := \ln \frac{k}{\Lambda_{\text{ref}}}$ with a reference scale Λ_{ref} . The derivative with respect to t is then given by $\partial_t = k \frac{d}{dk}$. For receiving information about the RG trajectory let us investigate the derivative $\partial_t \Gamma_k$. Due to the insertion of the regulator the Legendre transformation has to be changed to

$$\Gamma_k[\Phi] = \sup_J \left(\int d^d x J \Phi - W_k[J] \right) - \Delta S_k[\Phi]. \quad (2.8)$$

We observe again that $\Phi(x) = \frac{\delta W[J]}{\delta J(x)}$ at $J = J_{\text{sup}}$ and we therefore obtain

$$\frac{\delta \Phi(y)}{\delta J(x')} = \frac{\delta^2 W_k[J]}{\delta J(x') \delta J(y)} =: G_k(y - x'). \quad (2.9)$$

On the other hand Eq. (2.3) changes to

$$J(x) = \frac{\delta \Gamma_k[\Phi]}{\delta \Phi(x)} + (R_k \Phi)(x)$$

and functional differentiation leads to

$$\frac{\delta J(x)}{\delta \Phi(x)} = \frac{\delta^2 \Gamma_k[\Phi]}{\delta \Phi(x) \delta \Phi(y)} + R_k(x, y) =: \Gamma_k^{(2)}[\Phi] + R_k(x, y). \quad (2.10)$$

The so defined matrix $\Gamma_k^{(2)}$ is called *fluctuation matrix*. Combining Eq. (2.9) and Eq. (2.10) we find

$$\begin{aligned} \delta(x - x') &= \frac{\delta J(x)}{\delta J(x')} = \int d^d y \frac{\delta J(x)}{\delta \Phi(y)} \frac{\delta \Phi(y)}{\delta J(x')} \\ &= \int d^d y \left(\Gamma_k^{(2)}[\Phi] + R_k \right) (x, y) G_k(y - x'). \end{aligned}$$

In operator notation this important identity reads

$$\mathbb{1} = \left(\Gamma_k^{(2)} + R_k \right) G_k. \quad (2.11)$$

$\partial_t \Gamma_k$ for fixed Φ and at $J = J_{\text{sup}}$ is given by

$$\begin{aligned} \partial_t \Gamma_k[\Phi] &= -\partial_t W_k[J]|_{\Phi} - \partial_t \Delta S_k[\Phi] + \int d^d x (\partial_t J) \Phi \\ &= - \left[\partial_t W_k[J]|_J + \int d^d x \frac{\delta W_k[J]}{\delta J(x)} \partial_t J(x) \right] + \int d^d x \Phi (\partial_t J) - \partial_t \Delta S_k[\Phi] \\ &= -\partial_t W_k[J]|_J - \partial_t \Delta S_k[\Phi]. \end{aligned}$$

$\partial_t W_k$ can be written as

$$\begin{aligned} \partial_t W_k &= \frac{\partial_t Z_k}{Z_k} = -\frac{1}{2Z_k} \int \frac{d^d p}{(2\pi)^d} \partial_t R_k \int \mathcal{D}\varphi(-p) \varphi(p) e^{-S - \Delta S + \int d^d x J \varphi} \\ &= -\frac{1}{2} \int \frac{d^d p}{(2\pi)^d} \partial_t R_k [\langle \varphi(-p) \varphi(p) \rangle - \langle \varphi(-p) \rangle \langle \varphi(p) \rangle + \langle \varphi(-p) \rangle \langle \varphi(p) \rangle] \\ &= -\frac{1}{2} \int \frac{d^d p}{(2\pi)^d} \partial_t R_k \left[\frac{\delta^2 W_k}{\delta J \delta J} + \langle \varphi(-p) \rangle \langle \varphi(p) \rangle \right] \\ &= -\frac{1}{2} \int \frac{d^d p}{(2\pi)^d} \partial_t R_k \frac{\delta^2 W_k}{\delta J \delta J} - \partial_t \Delta S_k. \end{aligned}$$

Together we find

$$\partial_t \Gamma_k = \frac{1}{2} \int \frac{d^d p}{(2\pi)^d} G_k \partial_t R_k.$$

Writing this in operator notation and using Eq. (2.11) we end up with the *Wetterich equation* (ERGE):

$$\partial_t \Gamma_k[\Phi] = \frac{1}{2} \text{Tr}[(\Gamma_k^{(2)}[\Phi] + R_k)^{-1} \partial_t R_k],$$

where the trace denotes a sum over all loop momenta and matrix indices. If the theory also contains fermionic degrees of freedom the Wetterich equation changes to

$$\partial_t \Gamma_k[\Phi] = \frac{1}{2} \text{STr}[(\Gamma_k^{(2)}[\Phi] + R_k)^{-1} \partial_t R_k]. \quad (2.12)$$

$$\partial_t \Gamma_k = \frac{1}{2} \text{ (diagram: a circle with a filled square on its left side) }$$

Figure 2.2: Graphical representation of the Wetterich equation as explained in the text below.

Here the “super-trace” (STr) is a trace in the super-field space. This super-field space is equipped with a metric which includes a minus sign for the fermions.

Comparing Eq. (2.12) and the regulator conditions, Eq. (2.7), one can see how the regulator R_k acts as a mass term and therefore cuts off all diverging small-momentum terms (see also Fig. 2.1 for an example). On the other side the derivative $\partial_t R_k$ cuts off all large-momentum terms and therefore acts as a UV regulator.

The Wetterich equation can be interpreted in a graphical language as in Fig. 2.2. The one loop structure corresponds to one momentum integral which is the trace in Eq. (2.12). The propagator line is the full propagator $(\Gamma_k^{(2)} + R_k)^{-1}$ and the filled box is the regulator insertion $\partial_t R_k$. We shall come back to this graphical language in later sections.

We have derived an exact functional differential equation, so we do not have to deal with the complicated functional integral. If the initial condition (for example the bare action at a high UV cutoff scale Λ) and the regulator function R_k are given, the solution of this equation provides us the trajectory of Γ_k in *theory space*¹ from $k = \Lambda$ down to $k = 0$, which is the full effective action. Following this trajectory is like integrating out all quantum fluctuations, momentum shell by momentum shell, like in Wilson’s idea.

There are two ingredients we have to deal with: the regulator and the initial condition. The latter one is a point in our infinite-dimensional theory space. We can not deal with infinitely many operators all at once. Thus we have to choose a *truncation* of Γ_k with a finite number of operators. How this Γ_k looks like depends on the task. One possibility is to use the so-called derivative expansion as was done in various works [37, 38, 39, 40, 41, 42]. In this case one organises the operators with respect to the power of derivatives $(\sum_n a_n (\partial_\mu \phi)^n)$ and truncates the series. At the end one has to take these parts into account which are important for the flow. Thus the choice of the operators needs to be guided with as much physical input as possible. Note that the usage of a truncation is the point where one has to use an approximation, so the solution of the exact equation is not exact anymore.

The second ingredient we have to deal with is the regulator. It only has to satisfy the conditions of Eq. (2.7). Apart from that it can be constructed with regard to the special case. Different regulators surely lead to different trajectories in theory space. Provided that the full theory is studied, the endpoint $(\Gamma_{k=0})$ does not depend on the regulator. If we deal with a truncation (not with the full theory), the variation

¹The theory space is the space of all action functionals spanned by all possible invariant operators of the field.

of the endpoint can indicate the quality of the truncation and the regulator. In our calculation we use an “optimised regulator” (see [43]) in the sense that this regulator maximises the gap $\min_{q^2 \geq 0} (\Gamma_k^{(2)} + R_k) = Ck^2 > 0$. This is the denominator of the Wetterich equation, thus the r.h.s. of Eq. (2.12) becomes as small as possible due to the choice of the regulator. Consequently the system flows as little as possible.

2.3 Asymptotic Safety

In this section we give a short introduction to the so-called *asymptotic safety scenario*. This scenario was first discussed in connection with the quantisation of general relativity by S. Weinberg in 1976 [44, 45]. The common expectation is that at very short distances (e.g. the Planck scale) the continuum QFT should be replaced by a more general theory. This is not necessary if one can construct an asymptotic safety scenario. If this is possible the theory is valid and consistent at all energy scales. Till this day asymptotic safety was used in various theories. Ranging from four-fermion models [46, 47], nonlinear sigma models in $d > 2$ dimensions [48], the Gross-Neveu model [49], the standard model without fundamental Higgs scalar [50] and extra-dimensional gauge theories [51]. Also the research with respect to gravity is still going on [52, 53, 54, 55, 56, 57, 58, 59, 60, 61, 62]. For a more detailed introduction see e.g. [45, 63]. A discussion in a historical context is given in [64].

Now we introduce the idea of asymptotic safety. Let us begin with a general effective average action $\Gamma_k(\phi_A, g_i) = \sum_i g_i \mathcal{O}_i(\phi_A)$. Here g_i are running couplings, \mathcal{O}_i are operators and ϕ_A are the fields of which the operators are constructed. The Wetterich equation, which we derived in the previous section, provides us with the flow of this effective action. If it happens that the flow cannot be integrated beyond a scale $k = \Lambda$, new physics sets in. We then talk about an *effective* QFT. The theory is called *fundamental*, if the limit $t \rightarrow \infty$ can be taken safely. We now want to study the flow of the couplings instead of the flow of Γ_k . The derivatives of the Wetterich equation with respect to the fields provide us with the flow of the g_i ’s and $\partial_t g_i = \beta_i(g_j)$ are called *beta functions*. The couplings are related to physically measurable quantities like cross sections. If one of the couplings diverges for $k \rightarrow \infty$ we expect the cross section to do the same. This problem can be avoided if there is a fixed point g_i^* where $\beta_j(g_i^*) = 0$ holds for all j . This is the first requirement for asymptotic safety. Now we distinguish between *inessential* and *essential* couplings. Therefore we first need a few definitions. Let us consider the effective action as a functional on $\mathcal{F} \times \mathcal{Q} \times \mathbb{R}^+$, where \mathcal{F} is the configuration space of the fields, \mathcal{Q} is an infinite-dimensional manifold parametrised by the g_i ’s and \mathbb{R}^+ is the space parametrised by the scale parameter k . The fields ϕ_A can be redefined without changing the physics. This redefinition can be described by a group \mathcal{G} acting on \mathcal{F} . It is possible to define an action of \mathcal{G} on \mathcal{Q} (at least locally) by

$$\Gamma_k(\phi'_B(\phi_A), g_i) = \Gamma_k(\phi_A, g'_i),$$

where primes denote the redefined fields and couplings. Now we can divide \mathcal{Q} into two subsets. The first subset $\{g_i\}$ contains all couplings which transform nontrivial

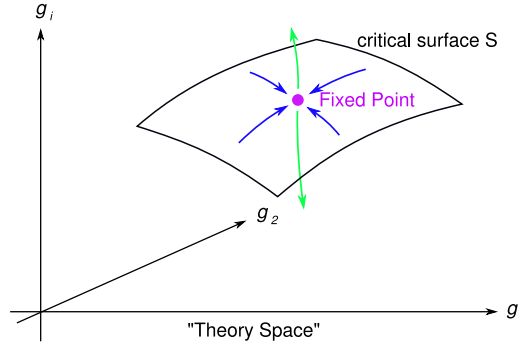


Figure 2.3: Theory space and critical surface at a fixed point.

under \mathcal{G} . These couplings are called inessential. The second subset $\{g_i\}$ contains all couplings invariant under \mathcal{G} . These are called essential couplings. We can use a field redefinition (at least locally) such that the inessential couplings g_i gain fixed values $(g_i)_0$. Furthermore there is an effective action $\bar{\Gamma}_k$ which depends only on the essential couplings:

$$\Gamma_k(\phi_A, g_i, g_{\bar{i}}) = \Gamma_k(\bar{\phi}_A, g_{\bar{i}}, (g_i)_0) =: \bar{\Gamma}_k(\bar{\phi}_A, g_{\bar{i}}).$$

This means that there is no need to restrict the flow of the inessential couplings. It does not matter whether they flow towards a fixed point or not.

Next we turn our attention to the second requirement for asymptotic safety. Let $\tilde{\mathcal{Q}}$ be the space of all essential couplings. The set of all points in $\tilde{\mathcal{Q}}$ that flow towards a fixed point for $k \rightarrow \infty$ is called the UV critical surface S . If the initial point lies on S the whole trajectory lies on S . If the critical surface is finite dimensional only a finite number of parameters have to be taken into account. These parameters can be determined in experiments. This is the second requirement.

This situation is depicted in Fig. 2.3. The blue arrows on the critical surface S indicate the so-called *UV attractive directions* corresponding to relevant parameters. The green arrows, leaving S , indicate the so-called *UV repulsive directions* corresponding to irrelevant parameters. In summary, a theory is called asymptotic safe if there exists a fixed point and the critical surface is finite dimensional.

An example for an asymptotic safe theory is a perturbatively renormalisable, asymptotically free theory (e.g. QCD). In this case the fixed point is the Gaussian one. In the present work we consider the electroweak standard model (SM). Nowadays the SM is seen as an effective theory. That means there has to be a cutoff scale Λ above which new physics sets in. If it is possible to construct an asymptotic safety scenario, such a new theory would not be necessary.

2.4 Gauge Theory Basics

In this section we shall give a very brief introduction to gauge theories. Often gauge theories are introduced via the most common one, namely electrodynamics. Here

we talk about gauge theories in general since electrodynamics is not the topic of the present work. For more information see e.g. [65] for the main ideas of gauge theory or [66] for a detailed description. There are also a lot of introductions like [67] available.

Let us start with a system containing some field ψ , which should satisfy some symmetry. Let the symmetry transformation be of the form

$$\psi \rightarrow \psi' = \exp(-ig \sum_k \theta_k(x) F_k) \psi =: U \psi. \quad (2.13)$$

Here F_k are the *generators* of the transformation and θ_k are some space-dependent parameters. Thus we have a *local* instead of a *global* symmetry (θ_k spacetime independent). First it looks like a very little change but we shall see that this has huge consequences. In the case of a global symmetry $\partial_\mu \psi \rightarrow U \partial_\mu \psi$ holds. This is not true for a local symmetry, since

$$\partial_\mu \psi \rightarrow U \partial_\mu \psi - ig \sum_k (\partial_\mu \theta_k) F_k U \psi.$$

Introducing the *gauge fields* $A_\mu^k := \partial_\mu \theta_k$ we can define a so-called *covariant derivative* as $D_\mu := \partial_\mu - ig A_\mu^k F_k$. We can not achieve $\partial_\mu \psi \rightarrow U \partial_\mu \psi$, but we can obtain $D_\mu \psi \rightarrow U D_\mu \psi$.

$$\begin{aligned} \psi' &= U \psi, & D'_\mu \psi' &\stackrel{!}{=} U (D_\mu \psi) \\ \Rightarrow (\partial_\mu - ig A_\mu^{k'} F_k) U \psi &= U (\partial_\mu - ig A_\mu^k F_k) \psi \\ \Rightarrow A_\mu^{k'} F_k &= U A_\mu^k F_k U^{-1} - \frac{i}{g} (\partial_\mu U) U^{-1}. \end{aligned} \quad (2.14)$$

Requiring the gauge fields A_μ^k to satisfy Eq. (2.14) we find the desired behaviour of ψ under these local transformations. Consider a system described by an action which is invariant under a global transformation. If we want to switch to a local symmetry we have to introduce the gauge fields and replace ∂_μ through D_μ . The new action is then invariant under the gauge transformations (2.13) and (2.14).

Due to the gauge symmetry we not only have the spacetime itself, but also have an internal space of the gauge group. The system has an additional freedom. Thereby some trouble arises while quantising a theory. Consider a theory described by an action S . Integrating path integrals of the form $\int \mathcal{D}A e^{-S[A_\mu]}$ would lead to difficulties because different A_μ 's lead to the same physics due to the internal space. Sloppy speaking it is like double counting. In order to avoid this we have to choose a *gauge* $G(A_\mu) = 0$ (e.g. the Lorentz gauge $\partial_\mu A^\mu = 0$) and implement a gauge fixing term into the path integral. This is called the *Faddeev-Popov method*. For details about this method see e.g. [68] or [69]. Let us see how it works. At first we can insert a 1 into the path integral (c.f. $1 = \int dx \delta(f(x)) |\partial f / \partial x|$):

$$1 = \int \mathcal{D}\theta(x) \delta \left(G(A_\mu^\theta) \right) \det \left(\frac{\delta G(A_\mu^\theta)}{\delta \theta} \right).$$

A_μ^θ is the transformed gauge field, defined through

$$A_\mu^{\theta k} F_k = U(\theta) A_\mu^k F_k U^{-1}(\theta) - \frac{i}{g} (\partial_\mu U(\theta)) U^{-1}(\theta).$$

As long as G is linear the determinant is independent of θ and with a change of the integration variable we get

$$I := \int \mathcal{D}A e^{-S[A_\mu]} = \left(\int \mathcal{D}\theta \right) \int \mathcal{D}A e^{-S[A_\mu]} \delta(G(A_\mu)) \det \left(\frac{\delta G(A_\mu^\theta)}{\delta \theta} \right).$$

The θ integral gives a normalisation constant \mathcal{N} , which is not important due to the fact that we are interested in quantities which are proportional to a quotient of path integrals. In the next step we introduce a spacetime-dependent function $\omega(x)$ with a Gaussian weight.

$$\begin{aligned} I &= \mathcal{N} \int \mathcal{D}\omega e^{-\int d^d x \frac{\omega^* \omega}{2\alpha}} \int \mathcal{D}A e^{-S[A_\mu]} \det \left(\frac{\delta G(A_\mu^\theta)}{\delta \theta} \right) \delta(G(A) - \omega(x)) \\ &= \mathcal{N} \int \mathcal{D}A \exp \left(-S[A_\mu] - \int d^d x \frac{G^* G}{2\alpha} \right) \det \left(\frac{\delta G(A_\mu^\theta)}{\delta \theta} \right) \\ &= \mathcal{N} \int \mathcal{D}A \mathcal{D}\bar{c} \mathcal{D}c \exp \left(-S[A_\mu] - \int d^d x \frac{G^* G}{2\alpha} + \int d^d x \bar{c}^i D^{ij} c^j \right). \end{aligned} \quad (2.15)$$

In the last line we introduced $D^{ij} = \frac{\delta G(A_\mu^\theta)}{\delta \theta}$ and complex Grassmann variables c and \bar{c} and used the following identity.

$$\det D^{ij} = \int \mathcal{D}c \mathcal{D}\bar{c} e^{-\int d^d x \bar{c}_i D^{ij} c_j}.$$

This identity is easily shown with the following definition of integration over a Grassmann variable θ . $\int d\theta (A + B\theta) := B$. Using this definition we find

$$\begin{aligned} \int d\theta_i^* d\theta_i e^{\theta_i^* B^{ij} \theta_j} &= \int d\theta_i^* d\theta_i e^{\sum_i \theta_i^* b_i \theta_i} \\ &= \int d\theta_i^* d\theta_i \left(1 + \sum_i \theta_i^* b_i \theta_i \right) = \sum_i b_i = \det B, \end{aligned}$$

where B is a hermitian matrix with eigenvalues b_i . In the second line we Taylor-expanded the exponential function and only the linear term survived, due to the properties of the Grassmann variables.

Summarising the Faddeev-Popov method we can say that with Eq.(2.15) we effectively have to replace the action

$$S \rightarrow S + \int d^d x \frac{G^* G}{2\alpha} - \int d^d x \bar{c}_i D^{ij} c_j \quad (2.16)$$

for quantising our theory. The new fields \bar{c}, c are called *ghost fields*. These new field are anti commuting fields which satisfy boson statistics and do not interact with the matter.

2.5 Goldstone and Higgs Model

One important feature of the models discussed below is the possibility of spontaneous symmetry breaking. Therefore we contemplate the spontaneous symmetry breaking in the *Goldstone model* and in the *Higgs model* in this section. These models are simple but appropriate to explain the mechanism. A more detailed description can be found in many standard textbooks like [68] or [70].

We start with the Goldstone model which consists of one dynamic, complex scalar field ϕ . The action of the Goldstone model reads

$$S = \int d^d x [(\partial_\mu \phi^*)(\partial^\mu \phi) - \mu^2 |\phi|^2 - \lambda |\phi|^4], \quad (2.17)$$

where λ and μ are parameters. The latter terms can be combined into a potential $U[\phi] = \mu^2 |\phi|^2 + \lambda |\phi|^4$. The field ϕ can be divided into its real and imaginary part $\phi(x) = \frac{1}{\sqrt{2}}[\phi_1(x) + i\phi_2(x)]$. Since the potential energy of the system should be bounded from below, $\lambda > 0$ should hold. This action is invariant under a global U(1) phase transformation:

$$\phi(x) \rightarrow \phi'(x) = \phi(x)e^{i\alpha}, \quad \phi^*(x) \rightarrow \phi^{*'}(x) = \phi^*(x)e^{-i\alpha}.$$

The system reaches its minimum of energy if ϕ minimises the potential. Whether the ground state is determined by a finite expectation value of ϕ depends on the value of μ^2 :

In the *symmetric phase* $\mu^2 > 0$ holds. The potential looks like the left one in Fig. 2.4 and reaches its minimum at $\phi(x) = 0$. This describes a complex Klein Gordon field with self-interaction $\lambda|\phi|^4$. The vacuum expectation value is given by $\langle 0|\phi(x)|0\rangle = 0$.

In the *regime of spontaneously broken symmetry* $\mu^2 < 0$ holds. The shape of the potential is depicted in the right panel of Fig. 2.4 and reaches its minimum at

$$\phi(x) = \phi_0 = \left(\frac{-\mu^2}{2\lambda}\right)^{\frac{1}{2}} e^{i\theta}, \quad 0 \leq \theta < 2\pi.$$

Here θ is an angle in the complex ϕ plane and ϕ_0 is the vacuum expectation value.

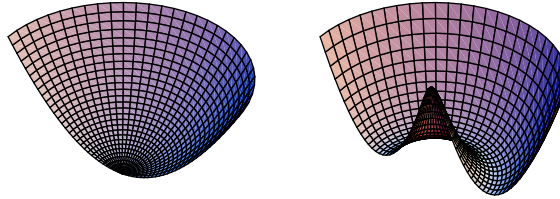


Figure 2.4: Effective potential in the symmetric phase (left panel) and the spontaneously symmetry broken phase (right panel).

The ground state is degenerated. Let us choose $\theta = 0$ and expand the field around the minimum v .

$$\phi(x) = \frac{1}{\sqrt{2}}[v + \sigma(x) + i\eta(x)]. \quad (2.18)$$

σ and η are the fluctuations around the minimum. The action of the Goldstone model (Eq. (2.17)) can be rewritten as

$$\begin{aligned} S = \int d^d x \bigg[& \frac{1}{2}(\partial_\mu \sigma)(\partial^\mu \sigma) - \frac{1}{2}(2\lambda v^2)\sigma^2 \\ & + \frac{1}{2}(\partial_\mu \eta)(\partial^\mu \eta) \\ & - \lambda v \sigma(\sigma^2 + \eta^2) - \frac{1}{4}\lambda(\sigma^2 + \eta^2)^2 + \text{const.} \bigg]. \end{aligned}$$

This can be interpreted as one massive boson (first line), one massless boson (second line) which is called *Goldstone boson* and interactions (last line). If one starts with a N -component, complex scalar field one gets one massive boson and $(2N - 1)$ massless Goldstone bosons.

Next we discuss briefly the so-called Higgs model. This model is the Goldstone model plus gauge degrees of freedom as a consequence of a local symmetry. Thus the action reads

$$S = \int d^d x \left[(D_\mu \phi)(D^\mu \phi) - U[\phi] - \frac{1}{4}F_{\mu\nu}F^{\mu\nu} \right]. \quad (2.19)$$

Here $D_\mu \phi = (\partial_\mu + igA_\mu)\phi$ and $F_{\mu\nu} = \partial_\nu A_\mu - \partial_\mu A_\nu$. As explained in Sec. 2.4 A_μ is the gauge field and g is the gauge coupling. Decomposing the bosonic field as done in Eq. (2.18) leads to

$$S = \int d^d x \left[\frac{1}{2}(\partial_\mu \sigma)(\partial^\mu \sigma) - \frac{1}{2}(2\lambda v^2)\sigma^2 \right. \quad (2.20)$$

$$\left. - \frac{1}{4}F_{\mu\nu}F^{\mu\nu} + \frac{1}{2}(gv)^2 A_\mu A^\mu \right. \quad (2.21)$$

$$\left. + \frac{1}{2}(\partial_\mu \eta)(\partial^\mu \eta) + gv A^\mu \partial_\mu \eta \right], \quad (2.22)$$

where the interaction terms are omitted for brevity. The interpretation is not that easy since the term $gv A^\mu \partial_\mu \eta$ shows that σ, η and A_μ are not independent. Another hint for the problems with the interpretation is that the vector field A_μ , the massive field σ and the massless field η together contain five degrees of freedom while Eq. (2.19) describes a system containing four degrees of freedom. Since we have only changed the variables, the number of degrees of freedom should not change. If we use the so-called *unitary gauge* the field η vanishes: $\phi(x) = \frac{1}{\sqrt{2}}[v + \sigma(x)]$. Now the action excluding the interaction terms reads

$$\begin{aligned} S = \int d^d x \bigg[& \frac{1}{2}(\partial_\mu \sigma)(\partial^\mu \sigma) - \frac{1}{2}(2\lambda v^2)\sigma^2 \\ & - \frac{1}{4}F_{\mu\nu}F^{\mu\nu} + \frac{1}{2}(gv)^2 A_\mu A^\mu \bigg]. \end{aligned}$$

Thus we have a system containing the massive boson and a massive gauge boson. The Higgs mechanism thus eliminates the massless field η of the Goldstone model and equips the gauge boson with a mass. We shall come back to these two mechanisms below.

Chapter 3

4D Model without Gauge Bosons

In this chapter we investigate a four-dimensional model which serves as a simple toy model for the Standard Model of particle physics. The goal is to solve the triviality problem. That is why the model requires to have some special properties. A simple model able to mimic the triviality problem was investigated in [26]. It consists of a real scalar field and N Dirac fermions. We extend this model and use a N -component, complex scalar field and N left-handed and one right-handed fermions. This asymmetry between left-handed and right-handed number also exists in the Standard Model. It is still a toy model but can be seen as a next step towards the Standard Model.

3.1 Constructing the Model

Before we construct the model mentioned above we recapitulate the findings of [26]. In this work the truncation of the effective action of the considered model reads

$$\Gamma_k = \int d^4x \left(\frac{Z_\phi}{2} (\partial_\mu \phi)^2 + U_k(\rho) + Z_\psi \bar{\psi} i \not{\partial} \psi + i h_k \phi \bar{\psi} \psi \right). \quad (3.1)$$

Here ϕ is a single-component real scalar field and ψ describes N Dirac fermions. Furthermore U_k is the effective potential, $\rho = \frac{1}{2}\phi^2$, Z_ϕ and Z_ψ are the wave-function renormalisations and h_k is the Yukawa coupling. Constant wave-function renormalisations correspond to the leading order derivative expansion. The system described by this truncation is invariant under a discrete Z_2 symmetry. It can be in one of two regimes, the symmetric one (SYM) or the regime of spontaneous symmetry breaking (SSB). The first corresponds to an expansion of the effective potential around zero field $\rho = \kappa = 0$ while the second corresponds to an expansion around the minimum $\rho = \kappa > 0$. In both cases the authors found no evidence for a reliable non-Gaussian fixed point for $N \in \mathbb{N}$. Thus no asymptotic safety scenario can be established. The problem occurs in the flow equation of the vacuum expectation value κ . This equation reads

$$\partial_t \kappa = -2\kappa - \text{fermionic contributions} + \text{bosonic contributions}. \quad (3.2)$$

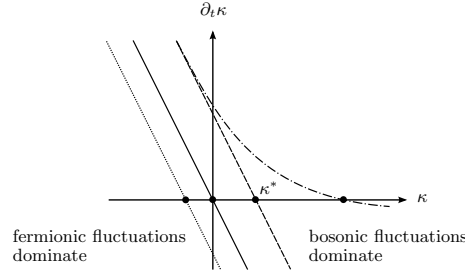


Figure 3.1: Contribution of fermionic and bosonic fluctuations to the flow equation for the vacuum expectation value κ as explained in the text below.

A possible fixed point requires a vanishing $\partial_t \kappa$. If the bosonic contributions do not compensate the fermionic contributions the term -2κ leads to a negative fixed-point value for κ . Neglecting the κ dependence of the fermionic and bosonic contributions leads to the straight lines in Fig. 3.1. The intersection with the κ axis is the fixed-point value of κ . If the fermionic contributions dominate this fixed-point value is negative. Including the κ dependence of the different contributions might lead to a change of the slope near the fixed point. For $N = 1$ it turned out that the fermionic fluctuations dominate and increasing N would make the problem more severe since the fermionic loops are proportional to the number of fermions (see Fig. 3.2). The authors showed that it is possible to get an acceptable fixed point if one decreases N sufficiently. This decreases the contribution of the fermionic fluctuations and the bosonic fluctuations dominate. Such a change corresponds to a shift of the zero to the right side in Fig. 3.1.

Since a fermionic number $N < 1$ is unphysical we try to circumvent this problem in a different way. Instead of decreasing the fermionic contribution we try to increase the bosonic ones. Thus we extend the model by introducing a N -component, complex scalar field instead of the one-component real one. The bosonic loop in Fig. 3.2 is now proportional to N . The Yukawa coupling part of the truncation of the old model is $ih_k \phi \bar{\psi} \psi$. Since we changed the bosonic field we have to change this interaction too. The interaction term has to be scalar and thus the index of the new bosonic field has to be contracted. We divide the fermionic field in its left-handed and its right-handed part. Introducing an asymmetry by using N left-handed and only one right-handed fermion the new Yukawa interaction reads $h_k (\bar{\psi}_R \phi^a \psi_L^a - \bar{\psi}_L^a \phi^{a\dagger} \psi_R)$. This left-right asymmetry is not just a mathematical trick but can also be seen in the Standard Model. The electron consists of a left-handed and a right-handed part but the neutrino only has a left-handed part. This corresponds to a vanishing neutrino mass. New experiments showed that neutrinos might have tiny masses. However, since our model is a toy model we can take the left-right asymmetry simply as a property of our model. With this new Yukawa interaction we can see in Fig. 3.2 that the fermionic loop is not proportional to N since the "incoming" boson component defines the fermionic component of the loop. Altogether our new system contains a N -component, complex scalar field, a N -component, left-handed fermionic field and one right-handed fermionic field. Therefore we denote the number of bosonic



Figure 3.2: Bosonic and fermionic contributions to the flow equation of the vacuum expectation value: Left panel: Bosonic loop. Right panel: Fermionic loop.

and left-handed, fermionic components by N_L . The symmetry we desire is a chiral $U(N_L)_L \otimes U(1)_R$ symmetry. This allows a mass term for the bosons ($m^2 \sum_a \phi^{a\dagger} \phi^a$)¹ but inhibits a mass term for the fermions. The fermions acquire a mass via the Yukawa interaction in the following way. In the SSB regime the bosonic field acquires a vacuum expectation value v . Let $\phi^1 = v$ and $\phi^i = 0$ ($\forall i > 1$). Thus, the Yukawa interactions containing ψ_i ($\forall i > 1$) vanish and these purely left-handed fermions remain massless. The Yukawa interaction containing ψ^1 does not vanish and this fermion consisting of a left-handed and a right-handed part acquires a mass:

$$h_k \bar{\psi}_R v \psi_L + c.c. = h_k v \bar{\psi} \psi, \quad \text{with} \quad \psi = (\psi_L, \psi_R)^T.$$

Furthermore we introduce bosonic self-interactions to arbitrary order $\sum_i \frac{\lambda_i}{i!} \rho^i$ where $\rho = \phi^{a\dagger} \phi^a$ and collect the mass term and the self-interactions in an effective potential U_k . Introducing kinetic terms for the fermions and the bosons we obtain the following new truncation:

$$\begin{aligned} \Gamma_k = \int d^d x \left[U_k(\rho) + Z_{\phi,k} (\partial_\mu \phi^{a\dagger}) (\partial^\mu \phi^a) + i (Z_{L,k} \bar{\psi}_L^a \not{\partial} \psi_L^a + Z_{R,k} \bar{\psi}_R^a \not{\partial} \psi_R^a) \right. \\ \left. + \bar{h}_k (\bar{\psi}_R \phi^a \psi_L^a - \bar{\psi}_L^a \phi^{a\dagger} \psi_R) \right]. \end{aligned} \quad (3.3)$$

Here the lower index k indicates the scale dependence, Z_L and Z_R are the wave-function renormalisations of the left-handed and the right-handed fermions, respectively, and \bar{h}_k is the Yukawa coupling. It is important to distinguish between $Z_{L,k}$ and $Z_{R,k}$ because in later sections we shall see that they obtain different loop contributions. The standard RG invariance of field rescaling is fixed by the definition of the renormalised fields:

$$\tilde{\phi} = Z_{\phi,k}^{1/2} \phi, \quad \tilde{\psi}_{L,R} = Z_{L,R}^{1/2} \psi_{L,R}.$$

The scale dependence of the field thus tucks in Z_ϕ , Z_L and Z_R respectively. It follows that the t derivative of the fields is proportional to the *anomalous dimensions* η_ϕ , η_L and η_R . These anomalous dimensions are given by $\eta = -\frac{\partial_t Z}{Z}$. If these anomalous dimensions become too large the derivative expansion breaks down.

¹From now on we will drop the \sum and if there is a index two times ahead the sum has to be taken.

3.2 Flow Equations

In this section our goal is to determine the flow of the effective average action Γ_k of our toy model. It is not possible to solve the Wetterich equation (2.12) exactly (as mentioned in Sec. 2.2) so we first have to truncate our action. We use the truncation (3.3). The next step is then to determine the flow equations for the different parts of our truncated action by choosing appropriate projections. If we have done this we get a system of coupled nonlinear equations, the so-called β functions.

3.2.1 Fluctuation Matrix and Regulator

At first we have to determine the fluctuation matrix and decide which regulator is appropriate for our purposes. Therefore we start by introducing some definitions which help us to simplify the calculations.

We split the complex bosonic fields into two real scalar fields:

$$\begin{aligned}\phi^a(x) &= \frac{1}{\sqrt{2}}(\phi_1^a(x) + i\phi_2^a(x)) & \phi^{a\dagger}(x) &= \frac{1}{\sqrt{2}}(\phi_1^a(x) - i\phi_2^a(x)) \\ \phi^{a\dagger}(x)\phi^a(x) &= \frac{1}{2}(\phi_1^a(x)^2 + \phi_2^a(x)^2) = \rho.\end{aligned}$$

The Fourier transform is given by

$$\phi^a(p) := \frac{1}{\sqrt{2}}(\phi_1^a(p) + i\phi_2^a(p)) \quad \phi^{a\dagger}(p) := \frac{1}{\sqrt{2}}(\phi_1^a(p) - i\phi_2^a(p)) \neq \text{FT}(\phi^{a\dagger}(x)),$$

where we used the following convention for the Fourier transformation:

$$\begin{aligned}f(x) &= \int \frac{d^d p}{(2\pi)^d} f(p) e^{ipx}, & \delta(x) &= \int \frac{d^d p}{(2\pi)^d} e^{ipx}, \\ f(p) &= \int d^d x f(x) e^{-ixp}, & \delta(p) &= \int d^d x e^{-ixp}.\end{aligned}$$

Note that $\phi_1^a(p)$ and $\phi_2^a(p)$ are no real fields. Using this we can write down the truncation (3.3) in momentum space:

$$\begin{aligned}\Gamma_k &= \int d^d x U_k(\rho) + \frac{Z_{\phi,k}}{2} \int \frac{d^d p}{(2\pi)^d} p^2 [\phi_1^a(p)\phi_1^a(-p) + \phi_2^a(p)\phi_2^a(-p)] \\ &\quad - \int \frac{d^d p}{(2\pi)^d} [Z_{L,k}\bar{\psi}_L^a(p)\not{p}\psi_L^a(p) + Z_{R,k}\bar{\psi}_R(p)\not{p}\psi_R(p)] \\ &\quad + \bar{h}_k \int \frac{d^d p}{(2\pi)^d} \int \frac{d^d q}{(2\pi)^d} \left[\bar{\psi}_R(p)\phi^a(p-q)\psi_L^a(q) - \bar{\psi}_L^a(p)\phi^{a\dagger}(p-q)\psi_R(q) \right].\end{aligned}\tag{3.4}$$

Our task is to evaluate the Wetterich equation (2.12). So far we know what Γ_k looks like. The fluctuation matrix $\Gamma_k^{(2)}$ and the regulator R_k are still missing. The next task is to evaluate the fluctuation matrix. This matrix is given by $\Gamma_k^{(2)}(p, q) = \frac{\overrightarrow{\delta}}{\delta\Phi(p)} \Gamma_k \frac{\overleftarrow{\delta}}{\delta\Phi^T(-q)}$, where we have combined all fields in one vector $\Phi(p)$. Therefore the

fluctuation matrix is a $(4N_L + 2) \times (4N_L + 2)$ matrix and can be written as

$$\Gamma_k^{(2)} = \begin{pmatrix} \Gamma_{\phi_1\phi_1} & \Gamma_{\phi_1\phi_2} & \Gamma_{\phi_1\psi_L} & \Gamma_{\phi_1\bar{\psi}_L} & \Gamma_{\phi_1\psi_R} & \Gamma_{\phi_1\bar{\psi}_R} \\ \Gamma_{\phi_2\phi_1} & \Gamma_{\phi_2\phi_2} & \Gamma_{\phi_2\psi_L} & \Gamma_{\phi_2\bar{\psi}_L} & \Gamma_{\phi_2\psi_R} & \Gamma_{\phi_2\bar{\psi}_R} \\ \Gamma_{\psi_L\phi_1} & \Gamma_{\psi_L\phi_2} & \Gamma_{\psi_L\psi_L} & \Gamma_{\psi_L\bar{\psi}_L} & \Gamma_{\psi_L\psi_R} & \Gamma_{\psi_L\bar{\psi}_R} \\ \Gamma_{\bar{\psi}_L\phi_1} & \Gamma_{\bar{\psi}_L\phi_2} & \Gamma_{\bar{\psi}_L\psi_L} & \Gamma_{\bar{\psi}_L\bar{\psi}_L} & \Gamma_{\bar{\psi}_L\psi_R} & \Gamma_{\bar{\psi}_L\bar{\psi}_R} \\ \Gamma_{\psi_R\phi_1} & \Gamma_{\psi_R\phi_2} & \Gamma_{\psi_R\psi_L} & \Gamma_{\psi_R\bar{\psi}_L} & \Gamma_{\psi_R\psi_R} & \Gamma_{\psi_R\bar{\psi}_R} \\ \Gamma_{\bar{\psi}_R\phi_1} & \Gamma_{\bar{\psi}_R\phi_2} & \Gamma_{\bar{\psi}_R\psi_L} & \Gamma_{\bar{\psi}_R\bar{\psi}_L} & \Gamma_{\bar{\psi}_R\psi_R} & \Gamma_{\bar{\psi}_R\bar{\psi}_R} \end{pmatrix}. \quad (3.5)$$

The different parts of this matrix can be found in App. A.

Next we choose an appropriate regulator R_k . As said in Sec. 2.2 the regulator has to satisfy three conditions. Recalling that the regulator contributions could be interpreted as momentum dependent masses the structure of the regulator matrix is obvious. The non-vanishing elements of the matrix should be those, which are responsible for the masses of the fields. These are the $\phi^{a\dagger}\phi^a$ term for the bosonic fields, the $\bar{\psi}_L\psi_L$ term and the $\psi_L\bar{\psi}_L$ term for the left-handed fermionic fields and the $\bar{\psi}_R\psi_R$ term and the $\psi_R\bar{\psi}_R$ term for the right-handed fermionic field. Therefore the regulator matrix is given as

$$R_k(q, p) = \delta(p - q) \begin{pmatrix} R_{kB} & 0 \\ 0 & -R_{kF} \end{pmatrix}, \quad (3.6)$$

with a $2N_L \times 2N_L$ matrix

$$R_{kB} = \begin{pmatrix} Z_{\phi,k}\delta^{ab}p^2r_{kB}(p) & 0 \\ 0 & Z_{\phi,k}\delta^{ab}p^2r_{kB}(p) \end{pmatrix}$$

for the bosonic sector and a $(2N_L + 2) \times (2N_L + 2)$ matrix

$$R_{kF} = \begin{pmatrix} 0 & Z_{L,k}\delta^{ab}\not{p}^T r_{kF}(-p) & 0 & 0 \\ Z_{L,k}\delta^{ab}\not{p} r_{kF}(p) & 0 & 0 & 0 \\ 0 & 0 & 0 & Z_{R,k}\not{p}^T r_{kF}(-p) \\ 0 & 0 & Z_{R,k}\not{p} r_{kF}(p) & 0 \end{pmatrix}$$

for the fermionic sector. Now we have all ingredients at hand that we need for our calculation of the flow equations.

3.2.2 Flow Equation of the Effective Potential

In this subsection we use the Wetterich equation, our truncation and the things we dealt with in the last subsection for a derivation of the flow equation of the effective potential. This equation will be used later for the calculation of the flow equation of the bosonic mass, the flow equation of the bosonic self interacting constants and the flow equation of the vacuum expectation value. First let us rewrite the Wetterich equation (2.12) and our truncation (3.3):

$$\partial_t \Gamma_k = \frac{1}{2} \text{STr}[(\Gamma_k^{(2)} + R_k)^{-1} \partial_t R_k],$$

$$(\partial_t U_k)_B = \frac{1}{2} \left((2N_L - 1) \begin{array}{c} \text{Goldstone} \\ \text{massless} \end{array} \right) + \begin{array}{c} \text{Goldstone} \\ \text{massless} \end{array}$$

Figure 3.3: Bosonic contributions to the flow equation of the effective potential in the spontaneously symmetry broken regime.

$$\Gamma_k = \int d^d x \left[U_k(\rho) + Z_{\phi,k} (\partial_\mu \phi^{a\dagger}) (\partial^\mu \phi^a) + i(Z_{L,k} \bar{\psi}_L^a \not{\partial} \psi_L^a + Z_{R,k} \bar{\psi}_R \not{\partial} \psi_R) + \bar{h}_k \bar{\psi}_R \phi^a \psi_L^a - \bar{h}_k \bar{\psi}_L^a \phi^{a\dagger} \psi_R \right].$$

Inserting the truncation into the Wetterich equation we see how to get the flow equation of the effective potential. We project onto constant bosonic fields and vanishing fermionic fields. If we do so only the potential term in our truncation survives. Thus the flow equation reads

$$\partial_t U_k = \frac{1}{2} \text{STr}[(\Gamma_k^{(2)} + R_k)^{-1} \partial_t R_k] \Big|_{\phi^a = \text{const}, \psi_L^a = \psi_R = 0}. \quad (3.7)$$

Comparing Eq. (3.7) with Eq. (3.6) we see that we can calculate the bosonic part (upper left block) and the fermionic part (lower right block) of $(\Gamma_k^{(2)} + R_k)^{-1} \partial_t R_k$ separately. Let us start with the bosonic part:

$$(\Gamma_k^2 + R_k)_B = \delta(p - q) \left[(Z_{\phi,k} P_B(p) + U'_k) \mathbb{1} + U''_k \begin{pmatrix} \phi_1^1 \phi_1^1 & \dots & \phi_1^1 \phi_2^{N_L} \\ \vdots & & \vdots \\ \phi_2^{N_L} \phi_1^1 & \dots & \phi_2^{N_L} \phi_2^{N_L} \end{pmatrix} \right], \quad (3.8)$$

with $P_B(p) = p^2(1 + r_{kB}(p))$, $\mathbb{1}$ being the identity matrix and primes denote the derivative with respect to ρ . Inverting the matrix, multiplying it with the derivative of the regulator and taking the STTr yields

$$(\partial_t U_k)_B = \frac{1}{2} \int \frac{d^d p}{(2\pi)^d} \partial_t (Z_{\phi,k} p^2 r_{kB}(p)) \times \left[\frac{2N_L - 1}{Z_{\phi,k} P_B(p) + U'_k} + \frac{1}{Z_{\phi,k} P_B(p) + U'_k + 2U''_k \rho} \right]. \quad (3.9)$$

This equation can be interpreted graphically as we did with the Wetterich equation in Sec. 2.2. In Fig. 3.3 one can see two different parts which correspond to the two different parts of Eq. (3.9). In the symmetric regime the vacuum expectation value of the bosonic field vanishes and thus both parts are the same and the equation becomes proportional to $2N_L$. In the symmetry broken regime both parts differ from each other. Thus we have the left loop in Fig. 3.3 which are the $2N_L - 1$

$$(\partial_t U_k)_F = - \left((N_L - 1) \text{massless} + \text{massive} \right)$$

Figure 3.4: Fermionic contributions to the flow equation of the effective potential in the spontaneously symmetry broken regime.

Goldstone modes and the right loop which corresponds to the one massive radial mode. Again the filled boxes are the regulator insertions $\partial_t R_k$.

Now let us have a look for the fermionic part. Again we first write down the $(\Gamma_k^{(2)} + R_k)_F$ matrix:

$$(\Gamma_k^{(2)} + R_k)_F = -\delta(p - q) \begin{pmatrix} 0 & A_1^T & 0 & h_k \phi^a \\ A_1 & 0 & h_k \phi^{a\dagger} & 0 \\ 0 & -h_k \phi^{b\dagger} & 0 & A_2^T \\ -h_k \phi^b & 0 & A_2 & 0 \end{pmatrix}.$$

Here we introduced $A_1 = Z_{L,k} \delta^{ab} \not{p} (1 + r_{kF}(p))$ and $A_2 = Z_{R,k} \delta^{ab} \not{p} (1 + r_{kF}(p))$, $a, b = 1, \dots, N_L$. Inverting, multiplying with the derivative of the regulator and taking the STr we find

$$\begin{aligned} (\partial_t U_k)_F = & -d_\gamma \int \frac{d^d p}{(2\pi)^d} \left\{ (N_L - 1) \frac{\not{p}}{Z_{L,k} p^2 (1 + r_{kF}(p))} \partial_t (Z_{L,k} \not{p} r_{kF}(p)) \right. \\ & + \frac{Z_{L,k} Z_{R,k} P_F(p)}{\bar{h}_k^2 \rho + Z_{L,k} Z_{R,k} P_F(p)} \frac{\not{p}}{Z_{L,k} p^2 (1 + r_{kF}(p))} \partial_t [Z_{L,k} \not{p} r_{kF}(p)] \\ & \left. + \frac{Z_{L,k} Z_{R,k} P_F(p)}{\bar{h}_k^2 \rho + Z_{L,k} Z_{R,k} P_F(p)} \frac{\not{p}}{Z_{R,k} p^2 (1 + r_{kF}(p))} \partial_t [Z_{R,k} \not{p} r_{kF}(p)] \right\}, \quad (3.10) \end{aligned}$$

with $P_F(p) = p^2 (1 + r_{kF}(p))^2$ and d_γ as the dimension of the γ matrices. This equation can again be interpreted graphically, see Fig. 3.4. The left loop corresponds to the first line in Eq. (3.10). These are the $(N_L - 1)$ massless, purely left-handed fermions. The right loop corresponds to the second and third line in Eq. (3.10). These are the left-handed and the right-handed part of the massive fermion. In the symmetric regime $\rho = 0$ holds and thus all parts become massless.

Now we just have to add the fermionic part, Eq. (3.10), and the bosonic part, Eq. (3.8). Using the threshold functions defined in App C we end up with

$$\begin{aligned} \partial_t U_k = & v_d k^d 2 \left[(2N_L - 1) l_0^d \left(\frac{U'_k}{Z_{\phi,k} k^2} \right) + l_0^d \left(\frac{U'_k + 2\rho U''_k}{Z_{\phi,k} k^2} \right) \right] \\ & - d_\gamma v_d k^d 2 \left[(N_L - 1) l_{0L}^{(F)d}(0) + l_{0L}^{(F)d} \left(\frac{\rho \bar{h}_k^2}{k^2 Z_{L,k} Z_{R,k}} \right) + l_{0R}^{(F)d} \left(\frac{\rho \bar{h}_k^2}{k^2 Z_{L,k} Z_{R,k}} \right) \right]. \quad (3.11) \end{aligned}$$

Here $v_d^{-1} = 2^{d+1}\pi^{d/2}\Gamma(d/2)$ is the volume of the d -dimensional unit sphere and again primes denote derivatives with respect to ρ . In this equation the different contributions are visible. The first line contains the $(2N_L - 1)$ Goldstone modes and the radial mode. The second line contains $(N_L - 1)$ massless fermions and the left-handed and the right-handed part of the massive fermion.

If we want to look for a fixed point it is convenient to rewrite this equation in terms of dimensionless quantities. Therefore we use the dimensionless form by running scale division. This means that we have to use the following quantities:

$$\begin{aligned}\tilde{\rho} &= Z_{\phi,k} k^{2-d} \rho, \\ h_k^2 &= Z_{\phi,k}^{-1} Z_{L,k}^{-1} Z_{R,k}^{-1} k^{d-4} \bar{h}_k^2, \\ u_k(\tilde{\rho}) &= k^{-d} U_k(\rho)|_{\rho=k^{d-2}\tilde{\rho}/Z_{\phi,k}}.\end{aligned}\tag{3.12}$$

Rewriting Eq. (3.11) with Eq. (3.12) yields

$$\begin{aligned}\partial_t u_k &= -du_k + \tilde{\rho} u'_k (d-2 + \eta_\phi) \\ &\quad + 2v_d \{ (2N_L - 1) l_0^d(u'_k) + l_0^d(u'_k + 2\tilde{\rho} u''_k) \\ &\quad - d_\gamma ((N_L - 1) l_{0,L}^{(F)d}(0) + l_{0,L}^{(F)d}(\tilde{\rho} h_k^2) + l_{0,R}^{(F)d}(\tilde{\rho} h_k^2)) \},\end{aligned}$$

where primes denote derivatives with respect to $\tilde{\rho}$. Inserting the optimised regulators (see App. C) and using the anomalous dimensions η_ϕ , η_L and η_R we end up with the dimensionless form of the flow equation for the effective potential:

$$\begin{aligned}\partial_t u_k &= -du_k + \tilde{\rho} u'_k (d-2 + \eta_\phi) \\ &\quad + \frac{4v_d}{d} \left[\frac{2N_L - 1}{1 + u'_k} \left(1 - \frac{\eta_\phi}{d+2} \right) + \frac{1}{1 + u'_k + 2\tilde{\rho} u''_k} \left(1 - \frac{\eta_\phi}{d+2} \right) \right. \\ &\quad \left. - d_\gamma \left(1 - \frac{\eta_L}{d+1} \right) \left((N_L - 1) + \frac{1}{1 + \tilde{\rho} h_k^2} \right) + \left(1 - \frac{\eta_R}{d+1} \right) \frac{d_\gamma}{1 + \tilde{\rho} h_k^2} \right].\end{aligned}\tag{3.13}$$

3.2.3 Flow Equation of the Yukawa Coupling

Now we determine the flow equation of the Yukawa coupling h^2 . As we did with the effective potential we start with our truncation and project onto the coupling. The truncation reads

$$\begin{aligned}\Gamma_k &= \int d^d x U_k(\rho) + \frac{Z_{\phi,k}}{2} \int \frac{d^d p}{(2\pi)^d} p^2 [\phi_1^a(p) \phi_1^a(-p) + \phi_2^a(p) \phi_2^a(-p)] \\ &\quad - \int \frac{d^d p}{(2\pi)^d} [Z_{L,k} \bar{\psi}_L^a(p) \not{p} \psi_L^a(p) + Z_{R,k} \bar{\psi}_R(p) \not{p} \psi_R(p)] \\ &\quad + \bar{h}_k \int \frac{d^d p}{(2\pi)^d} \int \frac{d^d q}{(2\pi)^d} [\bar{\psi}_R(p) \phi^a(p-q) \psi_L^a(q) - \bar{\psi}_L^a(p) \phi^{a\dagger}(p-q) \psi_R(q)].\end{aligned}$$

For the projection we divide our bosonic field into two parts: the vacuum expectation value (vev), which is zero in the SYM regime and greater than zero in the SSB

regime, and the fluctuation around the vev ($\Delta\phi$). The vev acts as a mass term for the fermionic fields and the fluctuation contributes to the interaction via Yukawa coupling. Precisely we divide the bosonic field as follows:

$$\phi = \frac{1}{\sqrt{2}} \begin{pmatrix} \phi_1^1(p) + i\phi_2^1(p) \\ \phi_1^2(p) + i\phi_2^2(p) \\ \vdots \\ \phi_1^{N_L}(p) + i\phi_2^{N_L}(p) \end{pmatrix} = \frac{\delta(p)}{\sqrt{2}} \begin{pmatrix} \phi_{\text{vev}} \\ 0 \\ \vdots \\ 0 \end{pmatrix} + \frac{1}{\sqrt{2}} \begin{pmatrix} \Delta\phi_1^1(p) + i\Delta\phi_2^1(p) \\ \Delta\phi_1^2(p) + i\Delta\phi_2^2(p) \\ \vdots \\ \Delta\phi_1^{N_L}(p) + i\Delta\phi_2^{N_L}(p) \end{pmatrix}. \quad (3.14)$$

Here we rotated the coordinate system such that the vev points into the direction of the first real axis. Inserting this into our truncation we see that a possible projection rule is

$$\left. \frac{\vec{\delta}}{\delta\bar{\psi}_L^1(p)} \frac{\sqrt{2}\vec{\delta}}{\delta\Delta\phi_1^1(p')} \Gamma_k \frac{\overleftarrow{\delta}}{\delta\psi_R(q)} \right|_{\substack{\psi_R^a = \psi_L^a = \Delta\phi = 0 \\ p' = p = q = 0}} = -\bar{h}_k \delta(0).$$

Using this projection for the Wetterich equation we obtain the flow of the Yukawa coupling:

$$-\delta(0)\partial_t \bar{h}_k = \frac{1}{2} \frac{\vec{\delta}}{\delta\bar{\psi}_L^1(p)} \frac{\sqrt{2}\vec{\delta}}{\delta\Delta\phi_1^1(p')} \text{STr}[\tilde{\partial}_t \ln(\Gamma_k^{(2)} + R_k)] \frac{\overleftarrow{\delta}}{\delta\psi_R(q)} \Big|_{\substack{\psi_R^a = \psi_L^a = \Delta\phi = 0 \\ p' = p = q = 0}}.$$

Here we introduced the operator $\tilde{\partial}_t$ which is the the same as ∂_t , but it just acts on the regulator R_k . One may ask why we use this new operator and the logarithm instead of the old operator. The answer is that it may look a little bit more complicated at the moment but it helps us during the following calculations. At first we divide the term $\Gamma_k^{(2)} + R_k$ into two parts as we did with our bosonic fields. The first part is called $\Gamma_{k,0}^{(2)} + R_k$ and only contains the components which are independent of the fluctuating fields ($\Delta\phi, \psi_L, \psi_R, \bar{\psi}_L, \bar{\psi}_R$). The second part contains just those fluctuating fields. This one is called $\Delta\Gamma_k^{(2)}$.

First we note that only those parts survive the projection which contain exactly one $\Delta\phi_1^1$, one $\bar{\psi}_L^1$ and one ψ_R . That is why we can drop the other terms. At first we expand the logarithm:

$$\begin{aligned} \tilde{\partial}_t \ln(\Gamma_k^{(2)} + R_k) &= \tilde{\partial}_t \ln(\Gamma_{k,0}^{(2)} + R_k + \Delta\Gamma_k^{(2)}) \\ &= \tilde{\partial}_t \ln[(\Gamma_{k,0}^{(2)} + R_k)(1 + (\Gamma_{k,0}^{(2)} + R_k)^{-1} \Delta\Gamma_k^{(2)})] \\ &= \tilde{\partial}_t \ln(\Gamma_{k,0}^{(2)} + R_k) + \tilde{\partial}_t \ln[1 + (\Gamma_{k,0}^{(2)} + R_k)^{-1} \Delta\Gamma_k^{(2)}]. \end{aligned} \quad (3.15)$$

The first term does not survive the projection so we can drop it. For the second part we use the Taylor expansion of the logarithm $\ln(1+x) = x - \frac{1}{2}x^2 + \frac{1}{3}x^3 - \dots$. Just the part to the third power survives the projection. Together we obtain

$$-\delta(0)\partial_t \bar{h}_k = \frac{1}{6} \frac{\vec{\delta}}{\delta\bar{\psi}_L^1(p)} \frac{\sqrt{2}\vec{\delta}}{\delta\Delta\phi_1^1(p')} \text{STr} \left[\tilde{\partial}_t \left(\frac{\Delta\Gamma_k^{(2)}}{\Gamma_{k,0}^{(2)} + R_k} \right)^3 \right] \frac{\overleftarrow{\delta}}{\delta\psi_R(q)} \Big|_{\substack{\psi_R^a = \psi_L^a = \Delta\phi = 0 \\ p' = p = q = 0}}.$$

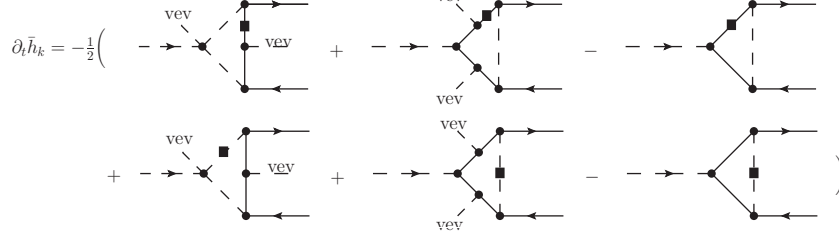


Figure 3.5: Different contributions to the flow equation of the Yukawa coupling.

Performing the matrix calculations and taking the super-trace we find:

$$\begin{aligned}
 \partial_t \bar{h}_k = & -\frac{\bar{h}_k^3}{2} \int \frac{d^d p}{(2\pi)^d} \tilde{\partial}_t \times \\
 & \left[\frac{1}{Z_L Z_R P_F + \frac{\bar{h}_k^2}{2} \phi_{\text{vev}}^2} \left(\frac{U''_{k\text{vev}} \phi_{\text{vev}}^2}{(Z_\phi P_B + U'_{k\text{vev}})^2} - \frac{3U''_{k\text{vev}} \phi_{\text{vev}}^2 + U'''_{k\text{vev}} \phi_{\text{vev}}^4}{(Z_\phi P_B + U'_{k\text{vev}} + U''_{k\text{vev}} \phi_{\text{vev}}^2)^2} \right) \right. \\
 & + \frac{\bar{h}_k^2 \phi_{\text{vev}}^2}{(Z_L Z_R P_F + \frac{\bar{h}_k^2}{2} \phi_{\text{vev}}^2)^2} \left(\frac{1}{Z_\phi P_B + U'_{k\text{vev}}} - \frac{1}{Z_\phi P_B + U'_{k\text{vev}} + U''_{k\text{vev}} \phi_{\text{vev}}^2} \right) \\
 & \left. - \frac{1}{Z_L Z_R P_F + \frac{\bar{h}_k^2}{2} \phi_{\text{vev}}^2} \left(\frac{1}{Z_\phi P_B + U'_{k\text{vev}}} - \frac{1}{Z_\phi P_B + U'_{k\text{vev}} + U''_{k\text{vev}} \phi_{\text{vev}}^2} \right) \right]. \quad (3.16)
 \end{aligned}$$

For a better readability we dropped the k index of the wave-function renormalisations and used the shortcut $U_{k\text{vev}}$ for $U_k(\phi_{\text{vev}}^2)$. Primes again denote derivatives with respect to ρ . As we did for the flow equation of the effective potential we can write down this equation in terms of Feynman diagrams. This time the derivative with respect to the fields at the projection onto the coupling corresponds to external legs in the graph. Therefore all graphs contain one external, bosonic leg and two external, fermionic legs. The $\tilde{\partial}_t$ operator converts n propagators to $(n+1)$ propagators and one regulator insertion. Note that $\frac{1}{P_F}$ is proportional to two fermionic propagators. In Fig. 3.5 we can see six diagrams corresponding to the three lines in Eq. (3.16). We do not separate the loops for the Goldstone and the radial mode and ignore the term proportional to U'''_k in this figure. The first two graphs (corresponding to the first line in Eq. (3.16)) contain three Yukawa couplings where one of them couples the fermions to the vev. Furthermore they contain one ϕ^4 coupling with three fluctuating bosonic fields coupling to the vev. Both graphs differ only by the regulator insertion. The second two graphs (corresponding to the second line in Eq. (3.16)) couple two times to the vev too but contain five times the Yukawa coupling. The third two graphs do not couple to the vev and contain three times the Yukawa coupling.

Using the threshold functions defined in the App. C we find:

$$\begin{aligned}
 \partial_t \bar{h}_k^2 = & -4v_d \bar{h}_k^4 \times \\
 & \left[-\frac{U''_{k\text{vev}} \phi_{\text{vev}}^2}{k^{6-d} Z_{L,k} Z_{R,k} Z_{\phi,k}^2} l_{1,2}^{(\text{FB})d} \left(\frac{\bar{h}_k^2 \phi_{\text{vev}}^2}{2k^2 Z_{L,k} Z_{R,k}}, \frac{U'_{k\text{vev}}}{k^2 Z_{\phi,k}} \right) \right. \\
 & + \frac{3U''_{k\text{vev}} \phi_{\text{vev}}^2 + U'''_{k\text{vev}} \phi_{\text{vev}}^4}{k^{6-d} Z_{L,k} Z_{R,k} Z_{\phi,k}^2} l_{1,2}^{(\text{FB})d} \left(\frac{\bar{h}_k^2 \phi_{\text{vev}}^2}{2k^2 Z_{L,k} Z_{R,k}}, \frac{U'_{k\text{vev}} + U''_{k\text{vev}} \phi_{\text{vev}}^2}{k^2 Z_{\phi,k}} \right) \\
 & + \frac{1}{k^{4-d} Z_{L,k} Z_{R,k} Z_{\phi,k}} l_{1,1}^{(\text{FB})d} \left(\frac{\bar{h}_k^2 \phi_{\text{vev}}^2}{2k^2 Z_{L,k} Z_{R,k}}, \frac{U'_{k\text{vev}}}{k^2 Z_{\phi,k}} \right) \\
 & - \frac{1}{k^{4-d} Z_{L,k} Z_{R,k} Z_{\phi,k}} l_{1,1}^{(\text{FB})d} \left(\frac{\bar{h}_k^2 \phi_{\text{vev}}^2}{2k^2 Z_{L,k} Z_{R,k}}, \frac{U'_{k\text{vev}} + U''_{k\text{vev}} \phi_{\text{vev}}^2}{k^2 Z_{\phi,k}} \right) \\
 & - \frac{\bar{h}_k^2 \phi_{\text{vev}}^2}{k^{6-d} Z_{L,k}^2 Z_{R,k} Z_{\phi,k}} l_{2,1}^{(\text{FB})d} \left(\frac{\bar{h}_k^2 \phi_{\text{vev}}^2}{2k^2 Z_{L,k} Z_{R,k}}, \frac{U'_{k\text{vev}}}{k^2 Z_{\phi,k}} \right) \\
 & \left. + \frac{\bar{h}_k^2 \phi_{\text{vev}}^2}{k^{6-d} Z_{L,k}^2 Z_{R,k} Z_{\phi,k}} l_{2,1}^{(\text{FB})d} \left(\frac{\bar{h}_k^2 \phi_{\text{vev}}^2}{2k^2 Z_{L,k} Z_{R,k}}, \frac{U'_{k\text{vev}} + U''_{k\text{vev}} \phi_{\text{vev}}^2}{k^2 Z_{\phi,k}} \right) \right].
 \end{aligned}$$

Using the dimensionless quantities in Eq. (3.12) and writing $u_{k\text{vev}}$ as a short cut for $u_k(\kappa_k/Z_{\phi,k}k^{2-d})$ we end up with

$$\begin{aligned}
 \partial_t h_k^2 = & (\eta_\phi + \eta_L + \eta_R + d - 4) h_k^2 - 4v_d h_k^4 [\\
 & -2u''_{k\text{vev}} \kappa_k l_{1,2}^{(\text{FB})d} (\kappa_k h_k^2, u'_{k\text{vev}}) \\
 & + (6u''_{k\text{vev}} \kappa_k + 4u'''_{k\text{vev}} \kappa_k^2) l_{1,2}^{(\text{FB})d} (\kappa_k h_k^2, u'_{k\text{vev}} + 2u''_{k\text{vev}} \kappa_k) \\
 & + l_{1,1}^{(\text{FB})d} (\kappa_k h_k^2, u'_{k\text{vev}}) \\
 & - l_{1,1}^{(\text{FB})d} (\kappa_k h_k^2, u'_{k\text{vev}} + 2u''_{k\text{vev}} \kappa_k) \\
 & - 2\kappa_k h_k^2 l_{2,1}^{(\text{FB})d} (\kappa_k h_k^2, u'_{k\text{vev}}) \\
 & + 2\kappa_k h_k^2 l_{2,1}^{(\text{FB})d} (\kappa_k h_k^2, u'_{k\text{vev}} + 2u''_{k\text{vev}} \kappa_k)]. \quad (3.17)
 \end{aligned}$$

This time primes denote derivatives with respect to $\tilde{\rho}$. Since our choice of the regulator is hidden in the threshold functions this is the general result. Now we move on with the determination of the anomalous dimensions.

3.2.4 Anomalous Dimensions

In this section we calculate the equation for the anomalous dimensions depending on the bosonic self-interactions, the Yukawa coupling and the other anomalous dimensions. Because of $\eta_i = -\partial_t Z_i/Z_i$ we have to turn our attention to the flow of the wave-function renormalisations. Let us start with the bosonic one. At first we divide our bosonic field according to Eq. (3.14) into two parts. One part contains

the vev and the other one the fluctuating fields. If we look at our truncation

$$\begin{aligned}\Gamma_k = & \int d^d x U_k(\rho) + \frac{Z_{\phi,k}}{2} \int \frac{d^d p}{(2\pi)^d} p^2 [\phi_1^a(p) \phi_1^a(-p) + \phi_2^a(p) \phi_2^a(-p)] \\ & - \int \frac{d^d p}{(2\pi)^d} [Z_{L,k} \bar{\psi}_L^a(p) \not{p} \psi_L^a(p) + Z_{R,k} \bar{\psi}_R(p) \not{p} \psi_R(p)] \\ & + \bar{h}_k \int \frac{d^d p}{(2\pi)^d} \int \frac{d^d q}{(2\pi)^d} [\bar{\psi}_R(p) \phi^a(p-q) \psi_L^a(q) - \bar{\psi}_L^a(p) \phi^{a\dagger}(p-q) \psi_R(q)],\end{aligned}$$

we see how to project onto $Z_{\phi,k}$:

$$\delta(0) \partial_t Z_{\phi,k} = \frac{\partial}{\partial(p^2)} \frac{\delta}{\delta \Delta \phi_1^1(p')} \frac{\delta}{\delta \Delta \phi_1^1(q')} \frac{1}{2} \text{STr} \left(\tilde{\partial}_t \ln(\Gamma_k^{(2)} + R_k) \right) \Big|_{\substack{\Delta \phi = \psi_L^a = \psi_R = 0 \\ p' = q' = 0}}.$$

The first step is analogous to the one in Subsec. 3.2.3: We rewrite the logarithm as we did in Eq. (3.15) and use the Taylor expansion. This time, however, we just need those parts which contain two fields. Thus we just have to pick up the quadratic term:

$$\delta(0) \partial_t Z_{\phi,k} = \frac{\partial}{\partial(p^2)} \frac{\delta}{\delta \Delta \phi(p')} \frac{\delta}{\delta \Delta \phi(q')} \frac{-1}{4} \text{STr} \left[\tilde{\partial}_t \left(\frac{\Delta \Gamma_k^{(2)}}{\Gamma_{k,0}^{(2)} + R_k} \right)^2 \right] \Big|_{\substack{\Delta \phi = \psi_L^a = \psi_R = 0 \\ p' = q' = 0}}.$$

Since the matrix calculation is not straightforward let us remark on those things which are a little bit more involved. First, it is important to realise that the matrix multiplications contain “momentum indices”. In our case the $\Delta \Gamma_k^{(2)}$ part is proportional to $\delta(p-q)$ and the inverse matrix $(\Gamma_{k,0}^{(2)} + R_k)^{-1}$ is proportional to $\Delta \phi_1^1(p-q)$. Because of the square inside the super-trace four matrices are involved in the multiplication. The result is proportional to

$$\int \frac{d^d p}{(2\pi)^d} \int \frac{d^d r}{(2\pi)^d} \int \frac{d^d s}{(2\pi)^d} \int \frac{d^d t}{(2\pi)^d} \delta(p-r) \Delta \phi_1^1(r-s) \delta(s-t) \Delta \phi_1^1(t-p),$$

where the p integration belongs to the STTr.

In the fermionic part of the supertrace the following term appears:

$$\begin{aligned} & \int \frac{d^d p}{(2\pi)^d} \frac{d}{dp^2} \frac{1}{Z_{L,k} Z_{R,k} P_F(p) + \frac{\bar{h}_k}{2} \phi_{\text{vev}}^2} \times \\ & \left(\frac{1}{Z_{L,k} Z_{R,k} P_F(p+p') + \frac{\bar{h}_k}{2} \phi_{\text{vev}}^2} + \frac{1}{Z_{L,k} Z_{R,k} P_F(p-p') + \frac{\bar{h}_k}{2} \phi_{\text{vev}}^2} \right). \quad (3.18)\end{aligned}$$

As a shortcut let us write the fraction as a function f depending on p , $p+p'$ and $p-p'$ respectively. Eq. (3.18) then reads $\int \frac{d^d p}{(2\pi)^d} \frac{d}{dp^2} f(p) (f(p+p') + f(p-p'))$. Now

let us rewrite this term by using the Taylor expansion:

$$\begin{aligned}
 \int \frac{d^d p}{(2\pi)^d} \frac{d}{dp^2} f(p) (f(p+p') + f(p-p')) &= \int \frac{d^d p}{(2\pi)^d} \frac{d}{dp^2} f(p) p'^\mu p'^\nu \partial_\mu \partial_\nu f(p) \\
 &= -\frac{d}{dp^2} p'^\mu p'^\nu \int \frac{d^d p}{(2\pi)^d} \partial_\mu f(p) \partial_\nu f(p) \\
 &= -\frac{d}{dp^2} p'^\mu p'^\nu \int \frac{d^d p}{(2\pi)^d} 4p_\mu p_\nu \left(\frac{d}{dp^2} \tilde{f}(p^2) \right)^2 = -\frac{4}{d} \int \frac{d^d p}{(2\pi)^d} p^2 \left(\frac{d}{dp^2} \tilde{f}(p^2) \right)^2.
 \end{aligned}$$

Apart from these things the matrix calculation can be performed as discussed above. If one calculates the bosonic and the fermionic part separately one gets the following two contributions to the flow of $Z_{\phi,k}$. The bosonic part reads

$$\begin{aligned}
 (\partial_t Z_{\phi,k})_B &= \frac{1}{d} \int \frac{d^d p}{(2\pi)^d} \tilde{\partial}_t \times \\
 &\left[(3U''_{k\text{vev}} \phi_{\text{vev}} + U'''_{k\text{vev}} \phi_{\text{vev}}^3)^2 p^2 Z_{\phi,k}^2 \left(\frac{\frac{\partial}{\partial p^2} P(p)}{(Z_{\phi,k} P(p) + U'_{k\text{vev}} + U''_{k\text{vev}} \phi_{\text{vev}}^2)^2} \right)^2 \right. \\
 &\quad \left. + (2N_L - 1) (U''_{k\text{vev}} \phi_{\text{vev}})^2 p^2 Z_{\phi,k}^2 \left(\frac{\frac{\partial}{\partial p^2} P(p)}{(Z_{\phi,k} P(p) + U'_{k\text{vev}})^2} \right)^2 \right]
 \end{aligned}$$

and the fermionic part reads

$$\begin{aligned}
 (\partial_t Z_{\phi,k})_F &= \frac{d_\gamma}{d} \int \frac{d^d p}{(2\pi)^d} \tilde{\partial}_t \left[2\bar{h}_k^2 p^4 Z_{L,k} Z_{R,k} \left(\frac{\partial}{\partial p^2} \frac{(1 + r_{kF}(p))}{Z_{L,k} Z_{R,k} P_F(p) + \frac{\bar{h}_k^2}{2} \phi_{\text{vev}}^2} \right)^2 \right. \\
 &\quad \left. - \bar{h}_k^4 \phi_{\text{vev}}^2 p^2 \left(\frac{\partial}{\partial p^2} \frac{1}{Z_{L,k} Z_{R,k} P_F(p) + \frac{\bar{h}_k^2}{2} \phi_{\text{vev}}^2} \right)^2 \right].
 \end{aligned}$$

This again can be interpreted graphically, see Fig. 3.6. We do not separate the different contributions of the Goldstone modes and the radial modes in the bosonic loop. Adding both parts and using the threshold functions as well as $\eta_\phi = -\partial_t Z_{\phi,k}/Z_{\phi,k}$ we obtain

$$\begin{aligned}
 \eta_\phi &= \frac{4v_d}{d} (18u''_{k\text{vev}} \kappa_k + 24u''_{k\text{vev}} u'''_{k\text{vev}} \kappa_k^2 + 8u'''_{k\text{vev}} \kappa_k^3) m_{22}^d (u'_{k\text{vev}} + 2\kappa_k u''_{k\text{vev}}) \\
 &\quad + \frac{(2N_L - 1)8v_d}{d} \kappa_k u''_{k\text{vev}} m_{22}^d (u'_{k\text{vev}}) \\
 &\quad + \frac{8v_d d_\gamma}{d} h_k^2 m_4^{(F)d} (\kappa_k h_k^2) - \frac{8v_d d_\gamma}{d} \kappa_k h_k^4 m_2^{(F)d} (\kappa_k h_k^2). \tag{3.19}
 \end{aligned}$$

Again the choice of the regulator is hidden in the threshold functions defined in App. C.

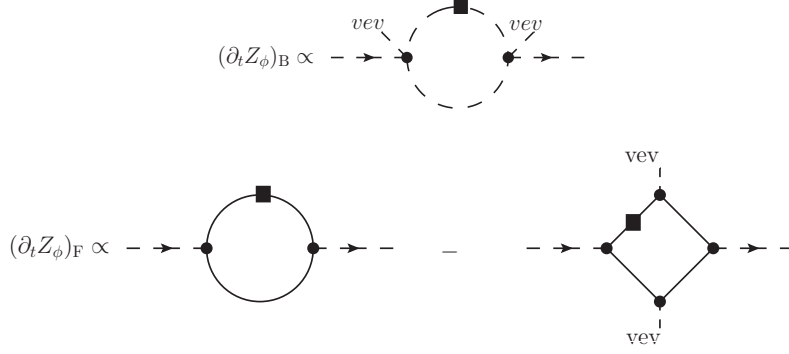


Figure 3.6: Graphical interpretation of the flow equation for Z_ϕ . Bosonic contribution on the top and fermionic contribution below.

Now there are just η_L and η_R missing. The calculation can be performed along the lines to η_ϕ and that is why we discuss this part very briefly. The projection rules are

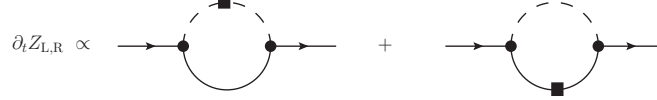
$$\delta(0)\partial_t Z_{L,k} = \frac{\text{tr}\gamma^\mu}{4dd_\gamma} \frac{\partial}{\partial p'^\mu} \frac{\vec{\delta}}{\delta\bar{\psi}_L^1(p')} \text{STr} \left[\tilde{\partial}_t \left(\frac{\Delta\Gamma_k^{(2)}}{\Gamma_{k,0}^{(2)} + R_k} \right)^2 \right] \frac{\overleftarrow{\delta}}{\delta\psi_L^1(q')} \Bigg|_{\substack{\Delta\phi=\psi_L=\psi_R=0 \\ p'=q'=0}}$$

and

$$\delta(0)\partial_t Z_{R,k} = \frac{\text{tr}\gamma^\mu}{4dd_\gamma} \frac{\partial}{\partial p'^\mu} \frac{\vec{\delta}}{\delta\bar{\psi}_R(p')} \text{STr} \left[\tilde{\partial}_t \left(\frac{\Delta\Gamma_k^{(2)}}{\Gamma_{k,0}^{(2)} + R_k} \right)^2 \right] \frac{\overleftarrow{\delta}}{\delta\psi_R(q')} \Bigg|_{\substack{\Delta\phi=\psi_L=\psi_R=0 \\ p'=q'=0}}$$

for $Z_{L,k}$ and $Z_{R,k}$ respectively. Using the Taylor expansion as above we get the following flow equations for $Z_{L,k}$ and $Z_{R,k}$:

$$\begin{aligned} \partial_t Z_{L,k} &= \frac{2\bar{h}_k^2}{d} \int \frac{d^d p}{(2\pi)^d} p^2 \tilde{\partial}_t \left[\frac{Z_{L,k}(1 + r_{kF}(p))}{Z_{L,k}Z_{R,k}P_F(p) + \frac{\bar{h}_k^2}{2}\phi_{\text{vev}}^2} Z_{\phi,k} \times \right. \\ &\quad \left. \frac{\partial}{\partial p^2} P(p) \left(\frac{1}{(Z_{\phi,k}P(p) + U'_{k\text{vev}} + U''_{k\text{vev}}\phi_{\text{vev}}^2)^2} + \frac{1}{(Z_{\phi,k}P(p) + U'_{k\text{vev}})^2} \right) \right], \\ \partial_t Z_{R,k} &= \frac{2\bar{h}_k^2}{d} \int \frac{d^d p}{(2\pi)^d} p^2 \tilde{\partial}_t \left[\frac{Z_{R,k}(1 + r_{kF}(p))}{Z_{L,k}Z_{R,k}P_F(p) + \frac{\bar{h}_k^2}{2}\phi_{\text{vev}}^2} Z_{\phi,k} \times \right. \\ &\quad \left. \frac{\partial}{\partial p^2} P(p) \left(\frac{1}{(Z_{\phi,k}P(p) + U'_{k\text{vev}} + U''_{k\text{vev}}\phi_{\text{vev}}^2)^2} + \frac{1}{(Z_{\phi,k}P(p) + U'_{k\text{vev}})^2} \right) \right. \\ &\quad \left. + \frac{2(N_L - 1)Z_{R,k}(1 + r_{kF}(p))}{Z_{L,k}Z_{R,k}P_F(p)} Z_{\phi,k} \frac{\partial}{\partial p^2} P(p) \frac{1}{(Z_{\phi,k}P(p) + U'_{k\text{vev}})^2} \right]. \end{aligned}$$


 Figure 3.7: Graphical interpretation of the flow equation for $Z_{L,R}$.

The graphical representation is shown in Fig. 3.7. The graph for the left-handed and the right-handed wave-function renormalisation is the same but the right-handed one contains massive and massless fermionic propagators as internal lines and the left-handed one only contains massive propagators.

Using $\eta_i = -\partial_t Z_i / Z_i$, the threshold functions defined in App. C and the dimensionless quantities in Eq. (3.12) we find

$$\eta_L = \frac{8v_d}{d} h_k^2 [m_{12}^{(\text{FB})d} (h_k^2 \kappa_k, u'_{\text{kvev}} + 2\kappa_k u''_{\text{kvev}}) + m_{12}^{(\text{FB})d} (h_k^2 \kappa_k, u'_{\text{kvev}})] \quad (3.20)$$

and

$$\begin{aligned} \eta_R = \frac{8v_d}{d} h_k^2 [m_{12}^{(\text{FB})d} (h_k^2 \kappa_k, u'_{\text{kvev}} + 2\kappa_k u''_{\text{kvev}}) + m_{12}^{(\text{FB})d} (h_k^2 \kappa_k, u'_{\text{kvev}}) \\ + 2(N_L - 1)m_{12}^{(\text{FB})d}(0, u'_{\text{kvev}})]. \end{aligned} \quad (3.21)$$

Now we are equipped with the flow equation of the Yukawa coupling (Eq. (3.17)), the anomalous dimensions η_ϕ , η_L and η_R (Eq. (3.19), Eq. (3.20) and Eq. (3.21)) and the flow equation for the potential (Eq. (3.13)). In the symmetric regime the latter one provides us with the flow equations for the mass and the bosonic self-interactions. In the regime of spontaneous symmetry breaking it provides us with the flow equation for the vacuum expectation value and the bosonic self-interactions. Altogether we are equipped with a system of coupled differential equations which we have to solve.

3.3 Fixed-Point Analysis

In this section we analyse the fixed-point structure of the symmetric regime and the regime of spontaneous symmetry breaking separately. At first we give some constraints for the parameters. Afterwards we try to find some fixed points in the different regimes which fulfil these constraints.

3.3.1 Symmetric Regime

The parameters of our system are the mass m^2 and the self-interactions λ_i of the effective potential. Furthermore we have the Yukawa coupling h and the anomalous dimensions η_ϕ, η_L and η_R . Due to the derivative expansion $\eta_\phi, \eta_L, \eta_R \lesssim O(1)$ should hold. The squared Yukawa coupling should be positive since a vanishing h^2 would lead to a decoupling of the bosonic and the fermionic part. It is clear that m^2 has to be positive and furthermore the highest non vanishing coefficient λ_i should be positive too. Otherwise the potential is not bounded from below.

Here it suffices to investigate the flow for the Yukawa coupling and the anomalous dimensions. In four dimensions and at vanishing κ (symmetric regime) the flow equations read

$$\begin{aligned}\partial_t h^2 &= (\eta_\phi + \eta_L + \eta_R) h^2, \\ \eta_\phi &= \frac{1}{4\pi^2} h^2 \left(1 - \frac{\eta_L + \eta_R}{8} \right), \\ \eta_L &= \frac{1}{16\pi^2} h^2 \left(1 - \frac{\eta_\phi}{5} \right) \frac{2}{(1 + m^2)^2}, \\ \eta_R &= \frac{1}{16\pi^2} h^2 \left(1 - \frac{\eta_\phi}{5} \right) \frac{2N_L}{(1 + m^2)^2}.\end{aligned}$$

At a fixed point the flow of the Yukawa coupling has to vanish ($\partial_t h_k^2 = 0$). The first conclusion is, that in leading order of the derivative expansion (vanishing anomalous dimensions) this is the case. In next to leading order the sum of the anomalous dimensions has to vanish. There has to be a relative minus sign. This is only possible if $\eta_\phi > 5$ or $\eta_L + \eta_R > 8$. These constraints are not compatible with the assumption of small anomalous dimensions. Thus the only possibility is a vanishing Yukawa coupling.

Our fixed-point Yukawa coupling vanishes in the symmetric regime ($h_k^{*2} = 0$). Since the flow of h_k^2 is proportional to itself this leads to a decoupling of bosons and fermions at every scale. Altogether, there is no reliable fixed point in the symmetric regime of the present truncation.

3.3.2 Spontaneously Symmetry Broken Regime

The parameters of the SSB regime differ from those of the SYM regime. We still have the Yukawa coupling and the anomalous dimensions but we expand our effective potential differently. The general expansion is given by

$$u_k = \sum_{n=1}^{N_p} \frac{\lambda_n}{n!} (\tilde{\rho} - \kappa_k)^n = \frac{\lambda_1}{1!} (\tilde{\rho} - \kappa_k) + \frac{\lambda_2}{2!} (\tilde{\rho} - \kappa_k)^2 + \frac{\lambda_3}{3!} (\tilde{\rho} - \kappa_k)^3 + \dots$$

In the symmetric regime we expand around zero field ($\kappa_k = 0$) and set $\lambda_1 = m^2$. In the symmetry broken regime we expand around the vacuum expectation value κ_k where the first derivative of the effective potential has to vanish ($\lambda_1 = 0$). The vev κ and the self-interaction λ_2 have to be positive. Otherwise the curvature at the minimum of the potential is not positive. Furthermore the potential should be bounded from below and thus the highest order λ_i should be positive too.

A first approximation is given by leading order in the derivative expansion (vanishing anomalous dimensions) and leading order in the polynomial expansion of the effective potential ($N_p = 2$). Thus our parameters are h_k, κ_k and λ_2 . The flow equation for λ_2 can be derived by using $u_k''(\tilde{\rho})|_{\kappa_k} = \lambda_2$. As mentioned above the first derivative of the potential at κ_k has to vanish and therefore the flow has to vanish

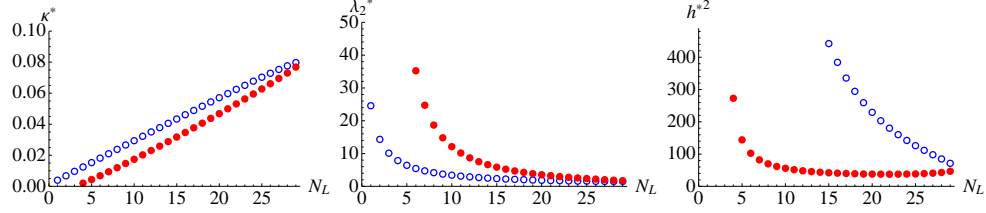


Figure 3.8: Appropriate fixed-point values for κ , λ_2 and h^2 in leading order derivative expansion as well as leading order polynomial expansion of the potential as a function of N_L .

as well:

$$\begin{aligned} 0 = \partial_t u'_k(\kappa_k) &= \partial_t u'_k(\tilde{\rho})|_{\tilde{\rho}=\kappa_k} + (\partial_t \kappa_k) u''_k(\kappa_k) \\ \Rightarrow \partial_t \kappa_k &= -\frac{1}{u''_k(\kappa_k)} \partial_t u'_k(\tilde{\rho})|_{\tilde{\rho}=\kappa_k}. \end{aligned} \quad (3.22)$$

This is how we get the flow equation for κ_k . Together with the flow equation of h_k in four dimensions we get

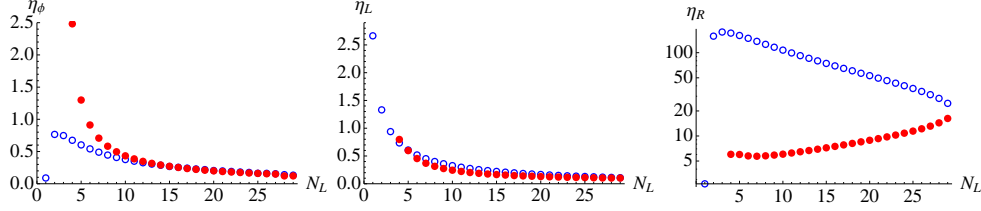
$$\begin{aligned} \partial_t \kappa &= -2\kappa + \frac{1}{32\pi^2} (2N_L - 1) + \frac{3}{32\pi^2} \frac{1}{(1 + 2\kappa\lambda_2)^2} - \frac{1}{4\pi^2} \frac{h^2}{\lambda_2(1 + \kappa h^2)^2}, \\ \partial_t \lambda_2 &= \frac{1}{16\pi^2} (2N_L - 1) \lambda_2^2 + \frac{1}{16\pi^2} \frac{9\lambda_2^2}{(1 + 2\kappa\lambda_2)^3} - \frac{1}{2\pi^2} \frac{h^4}{(1 + \kappa h^2)^3}, \\ \partial_t h^2 &= \frac{1}{16\pi^2} \frac{h^4}{(1 + \kappa h^2)} \left\{ 2\lambda_2 \kappa \left(\frac{1}{1 + \kappa h^2} + 2 \right) - \left(\frac{1}{1 + \kappa h^2} + 1 \right) \right. \\ &\quad - \frac{6\kappa\lambda_2}{(1 + 2\kappa\lambda_2)^2} \left(\frac{1}{1 + \kappa h^2} + \frac{2}{1 + 2\kappa\lambda_2} \right) \\ &\quad + \frac{1}{(1 + 2\kappa\lambda_2)} \left(\frac{1}{1 + \kappa h^2} + \frac{1}{1 + 2\kappa\lambda_2} \right) + \frac{2\kappa h^2}{(1 + \kappa h^2)} \left(\frac{2}{1 + \kappa h^2} + 1 \right) \\ &\quad \left. - \frac{2\kappa h^2}{(1 + \kappa h^2)(1 + 2\kappa\lambda_2)} \left(\frac{2}{1 + \kappa h^2} + \frac{1}{1 + 2\kappa\lambda_2} \right) \right\}. \end{aligned}$$

If there is a fixed point $(\kappa^*, \lambda_2^*, h^{*2})$ the flow of all parameters has to vanish.

$$\begin{aligned} \partial_t \kappa_k(\kappa^*, \lambda_2^*, h^{*2}) &= 0, \\ \partial_t \lambda_{2,k}(\kappa^*, \lambda_2^*, h^{*2}) &= 0, \\ \partial_t h_k^2(\kappa^*, \lambda_2^*, h^{*2}) &= 0. \end{aligned}$$

This nonlinear system of equations can be solved analytically. Many solutions can be excluded by the constraints given above. For $1 \leq N_L < 4$ there exists one reliable fixed point. For $4 \leq N_L \leq 29$ there exist two reliable fixed points and for some (but not all) $N_L > 29$ there exists one appropriate fixed point, see Fig. 3.8.

The next question is whether it is possible to extend this solution to higher orders in the derivative expansion. In other words, are the anomalous dimensions


 Figure 3.9: Estimates for anomalous dimensions depending on N_L .

small enough? The equations of the anomalous dimensions are given in Eq. (3.19) for η_ϕ , in Eq. (3.20) for η_L and in Eq. (3.21) for η_R . A first estimate can be given by inserting the fixed-point values for κ, h^2 and λ_2 . It does not consider the back coupling of the nonzero anomalous dimensions to the fixed-point values. These estimates depending on N_L are given in Fig. 3.9. For $N_L > 5$, $\eta_\phi < 1$ and $\eta_L < 1$ holds but η_R is much bigger than one. This is due to the large values of h^2 and the contributions of the massless Goldstone bosons. These contributions are large because they are not damped by a mass. Moreover they are proportional to N_L . If one trusts this estimate the leading order derivative expansion is not self consistent. Nevertheless we do not know the real value of the anomalous dimensions.

A consistent calculation of the real values requires a solution of the following system:

$$\begin{aligned}
 \partial_t \kappa_k(\kappa^*, \lambda_2^*, h^{*2}, \eta_\phi^*, \eta_L^*, \eta_R^*) &= 0, \\
 \partial_t \lambda_{2,k}(\kappa^*, \lambda_2^*, h^{*2}, \eta_\phi^*, \eta_L^*, \eta_R^*) &= 0, \\
 \partial_t h_k^2(\kappa^*, \lambda_2^*, h^{*2}, \eta_\phi^*, \eta_L^*, \eta_R^*) &= 0, \\
 \eta_\phi^*(\kappa^*, \lambda_2^*, h^{*2}, \eta_\phi^*, \eta_L^*, \eta_R^*) &= \eta_\phi(\kappa^*, \lambda_2^*, h^{*2}, \eta_\phi^*, \eta_L^*, \eta_R^*), \\
 \eta_L^*(\kappa^*, \lambda_2^*, h^{*2}, \eta_\phi^*, \eta_L^*, \eta_R^*) &= \eta_L(\kappa^*, \lambda_2^*, h^{*2}, \eta_\phi^*, \eta_L^*, \eta_R^*), \\
 \eta_R^*(\kappa^*, \lambda_2^*, h^{*2}, \eta_\phi^*, \eta_L^*, \eta_R^*) &= \eta_R(\kappa^*, \lambda_2^*, h^{*2}, \eta_\phi^*, \eta_L^*, \eta_R^*).
 \end{aligned}$$

We are not able to solve this highly nonlinear system analytically but tackle this problem numerically. We use Newton methods with the leading order fixed point as a starting point but are not able to find a suitable fixed point with non-vanishing anomalous dimensions. Due to the non linearity of the system a systematic search is computationally expensive and thus beyond the scope of this work.

To get an idea of the behaviour of the system we switched on the anomalous dimensions step by step and realised that the leading order fixed point vanishes if the anomalous dimensions become sufficiently large.

Comparing our model with the Standard Model one realises that the Goldstone bosons which are responsible for the large anomalous dimensions in our model are not present in the Standard Model (see Sec. 2.5). Thus it might be possible that this problem is just a problem of our toy model. Although our leading order fixed points are not self consistent regarding the derivative expansion it might be interesting to investigate the behaviour of such a fixed point in more detail. As an example we choose $N_L = 10$ and the red points in Fig. 3.8 since it has no extreme coupling

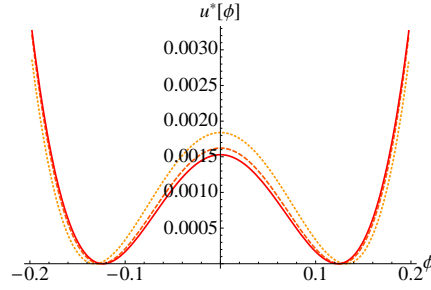


Figure 3.10: Dimensionless effective potential for different expansions. Dotted line: Expansion up to λ_2 . Dashed line: Expansion up to λ_4 . Solid line: Expansion up to λ_6 .

values. The first question is if the polynomial expansion of the potential is reliable. Therefore we can draw the effective potential for $N_P = 2, 4, 6$ (N_P is the highest order in the expansion), see Fig. 3.10. The quantitative form of the potential does not change in the vicinity of the expansion point κ . Thus the fixed point should be stable when higher order bosonic self-interactions are taken into account. If we calculate the fixed-point values for different orders of the expansion the stability can be shown. For $N_P = 2, 4, 6$ the results are given in Tab. 3.1. One can see that the fixed-point values converge satisfactorily as we expected due to the form of the effective potential.

Now we are interested in the vicinity of the fixed point. There the flow equations of the different coupling constants can be linearised:

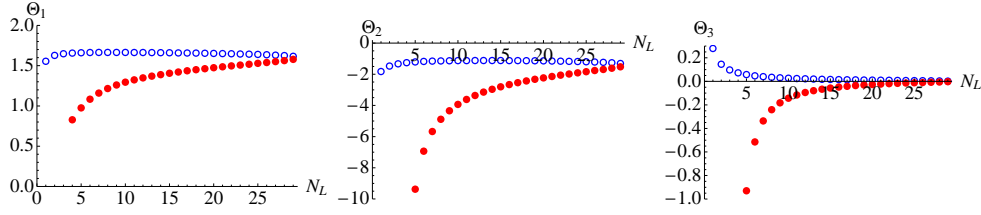
$$\partial_t g_i = B_i^j (g_j^* - g_j) + \dots, \quad B_i^j = \left. \frac{\partial \beta_{g_i}}{\partial g_j} \right|_{g=g^*}.$$

In our case the g_i represents $\kappa, \lambda_2, \lambda_3, \dots$ and h^2 . The negative of the eigenvalues of the stability matrix B_i^j are the so-called *critical exponents* θ^I . As mentioned above they describe how fast the system leaves the fixed-point regime. If the real part of a critical exponent $\Re(\theta^I) < 0$ the contributions in this direction die out towards the IR. These directions are the irrelevant directions. On the other hand if $\Re(\theta^I) > 0$ the corresponding direction is relevant and the respective physical parameter has to be fixed by experiment. The asymptotic safety scenario is thus predictive if the number of positive critical exponents is finite.

The calculation of the stability matrix and the corresponding critical exponents of our model is straightforward. The results are given in Fig. 3.11 depending on N_L

$N_L = 10$	h_*^2	κ_*	λ_2^*	λ_3^*	λ_4^*	λ_5^*	λ_6^*
$N_P = 2$	55.8	0.0174	12.11	-	-	-	-
$N_P = 4$	56.0	0.0158	12.09	-115	$1.30 \cdot 10^4$	-	-
$N_P = 6$	57.4	0.0152	12.13	-152	$1.20 \cdot 10^4$	$-8.76 \cdot 10^5$	$1.44 \cdot 10^8$

Table 3.1: Fixed-point values for different orders in the polynomial expansion of the effective potential.


 Figure 3.11: Critical exponents depending on N_L .

and in Tab. 3.2 for $N_L = 10$. The first result is that the critical exponents converge like the fixed-point values. The higher order critical exponents do not converge that fast but they do. The second result is that the maximal critical exponent is smaller than two and thus the hierarchy problem is weakened. The third result is that the number of relevant directions do not change if one increases the order of the polynomial expansion. There is just one relevant direction corresponding to one physical parameter which has to be fixed.

Now we can compare our toy model to the Standard Model. Our massive fermion can be interpreted as the top quark with mass m_{top} . The massless fermions are bottom quark like. The bosonic field contains the massless Goldstone bosons which have no counterpart in the Standard Model and the massive radial mode can be interpreted as the Higgs boson with mass m_{Higgs} . The bosonic field exhibits a vacuum expectation value κ which has its counterpart $v^2 = 2\phi^{a\dagger}\phi^a$ in the Standard Model. These different parameters can be connected to the dimensionless parameters κ and λ_2 of our model:

$$v = \sqrt{2\kappa} k, \quad m_{\text{top}} = \sqrt{h^2} v, \quad m_{\text{Higgs}} = \sqrt{\lambda_2} v.$$

The top mass and the vacuum expectation value are known from experiments: $m_{\text{top}} = 173\text{GeV}$ and $v = 246\text{GeV}$. These experimental data are values at an IR scale and thus to compare these parameters with our model we have to integrate out the flow. This can be done numerically. The starting point is an UV point for which we choose $t = 16$ corresponding to $k = e^{16}\text{GeV}$ since $t = \ln k$. As an IR scale we choose $t = 2$ corresponding to $k = e^2\text{GeV}$. Since κ is a relevant parameter different IR values flow to the same UV fixed point. The same has to hold for v as depicted in Fig. 3.12. Our goal is to end up at the IR scale with the measured value $v = 246\text{GeV}$.

At the UV scale κ still flows and thus differs from the fixed-point value κ^* . We can slightly perturb our initial value for κ at the UV scale. Changing this starting point results in different values for κ at the IR scale and thus for v . Therefore

$N_L = 10$	Θ_1	Θ_2	Θ_3	Θ_4	Θ_5	Θ_6	Θ_7
$N_p = 2$	1.294	-0.143	-3.94	-	-	-	-
$N_p = 4$	1.167	-0.170	-2.50	-5.53	-13.61	-	-
$N_p = 6$	1.056	-0.175	-2.35	-4.97	-8.49	-14.02	-25.54

Table 3.2: Critical exponents in the polynomial expansion of the effective potential.

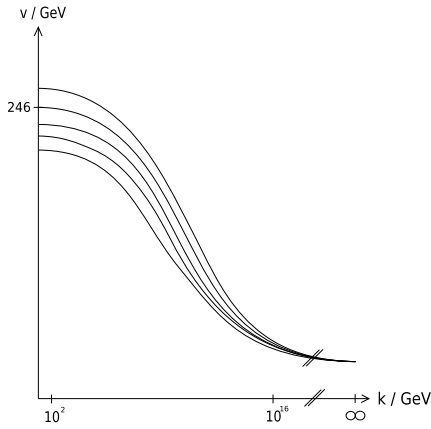


Figure 3.12: Different possible flows of v towards the IR.

we can fine-tune the starting point so that we end up at $v = 246\text{GeV}$. Solving the flow equations provides us with the IR values of κ, h^2 and λ_2 . The other two parameters are predictions since there is only one relevant direction. Thus our asymptotic safety scenario "predicts" the top mass and the Higgs mass. These "predictions" are $m_{\text{top}} = 5.78v$ and $m_{\text{Higgs}} = 0.97v$. The top mass is far above the expected value. The problems are the strong Yukawa coupling and the Goldstone-boson contributions which are not included in the Standard Model, see Sec. 2.5. As expected the predictions of our model are special for our toy model and have to be taken with care.

However, we showed that it is possible to construct an asymptotic safety scenario which weakens the hierarchy problem, i.e. highest critical exponent is lower than two, solves the triviality problem by construction and is predictable (only one parameter has to be fixed by experiment).

Chapter 4

3D Model without Gauge Bosons

In this chapter we take a little side trip to a three-dimensional model. The model we investigated in the previous chapter resembles the Standard Model. Furthermore it resembles statistical physics models like the Nambu-Jona-Lasinio (NJL) model or the Thirring model in three dimensions. For a comparison of the different models we start by introducing a very general fermionic model which obeys some symmetries and then determine all possible terms satisfying these symmetries. These terms can be used to classify different models. Included in this classification is for example the NJL model.

After this classification we use the techniques of the previous chapter to find fixed points and critical exponents. This time the goal is not the construction of an asymptotic safety scenario, but to investigate the critical behaviour of the model corresponding to the phase transition between the symmetric and the symmetry broken phase. Information about the critical behaviour are stored in the critical exponents which can be calculated at the fixed point.

4.1 Classification

On the next few pages we construct the above mentioned, general model. Therefore we start to investigate chiral symmetries. Since our model contains fermions we have to think about a representation of the Dirac algebra

$$\{\gamma_\mu, \gamma_\nu\} = 2\delta_{\mu\nu}.$$

This algebra could be realised by an irreducible representation in terms of (2×2) matrices. Such a representation inhibits chiral symmetry since there exists no fifth γ matrix. Thus we use a reducible representation with (4×4) matrices. These matrices are given by

$$\gamma_\mu = \begin{pmatrix} 0 & -i\sigma_\mu \\ i\sigma_\mu & 0 \end{pmatrix}, \quad \mu = 1, 2, 3.$$

Here σ_1, σ_2 and σ_3 are the (2×2) Pauli matrices. Using these γ matrices we are able to construct two fifth γ matrices as

$$\gamma_4 = \begin{pmatrix} 0 & \mathbb{1} \\ \mathbb{1} & 0 \end{pmatrix} \quad \text{and} \quad \gamma_5 = \gamma_1 \gamma_2 \gamma_3 \gamma_4 = \begin{pmatrix} \mathbb{1} & 0 \\ 0 & -\mathbb{1} \end{pmatrix}.$$

These matrices anticommute with each other as well as with the γ_μ matrices. Furthermore we can construct the generators of the Lorentz transformations

$$\sigma_{\mu\nu} = \frac{i}{2} [\gamma_\mu, \gamma_\nu] \quad (\mu < \nu).$$

Altogether the sixteen matrices $\{\mathbb{1}, \gamma_\mu, \sigma_{\mu\nu}, i\gamma_\mu \gamma_4, i\gamma_\mu \gamma_5, i\gamma_4 \gamma_5, \gamma_4, \gamma_5\}$ form a complete basis of the Dirac algebra. Since we would like to discuss chiral symmetries we have to define the chiral projectors. We choose $P_{L/R} = \frac{1}{2}(\mathbb{1} \pm \gamma_5)$ but note that we could have chosen different projectors by replacing the γ_5 matrix in the definition by γ_4 or $i\gamma_4 \gamma_5$. Note that the chirality is conserved under Lorentz transformations since $[\gamma_5, \sigma_{\mu\nu}] = 0$ holds. These chiral projectors define the four-dimensional left-handed and right-handed Weyl spinors ψ_L and ψ_R of the Dirac fermion ψ as

$$\psi_{L/R} = P_{L/R} \psi, \quad \bar{\psi}_{L/R} = \bar{\psi} P_{R/L}.$$

These left-handed and right-handed fermions are the constituents of our model. To be specific, the system contains N_L left-handed and N_R right-handed fermions where N_L and N_R do not have to be identical. We demand the system to be $U(N_L)_L \otimes U(N_R)_R$ symmetric. This means that it is invariant under the chiral transformations

$$\begin{aligned} U(N_L)_L : \quad \psi_L^a &\mapsto U_L^{ab} \psi_L^b, & \bar{\psi}_L^a &\mapsto \bar{\psi}_L^b (U_L^\dagger)^{ba}, \\ U(N_R)_R : \quad \psi_R^a &\mapsto U_R^{ab} \psi_R^b, & \bar{\psi}_R^a &\mapsto \bar{\psi}_R^b (U_R^\dagger)^{ba}. \end{aligned}$$

The field transformations act independently on the left-handed and right-handed parts. U_L and U_R are unitary ($N_L \times N_L$) and ($N_R \times N_R$) matrices respectively. The symmetry can be splitted as

$$U(N_L)_L \otimes U(N_R)_R \cong SU(N_L)_L \otimes SU(N_R)_R \otimes U(1)_A \otimes U(1)_V,$$

where for the $U(1)_A$ axial transformations $U_L^{ab} = e^{i\alpha} \delta^{ab}$ and $U_R^{ab} = e^{-i\alpha} \delta^{ab}$ holds and for the $U(1)_V$ vector rotations holds $U_L^{ab} = e^{i\alpha} \delta^{ab} = U_R^{ab}$.

Besides the invariance under these chiral transformations we expect the system to be invariant under some discrete transformations as it is the case for the NJL model and the Thirring model. These are the charge conjugation \mathcal{C} , the parity transformation \mathcal{P} and the time reversal \mathcal{T} . Due to the reducible representation of the Dirac algebra these transformations are ambiguous (see also [29] and [71]). For these transformations we use the following conventions. The coordinates (x_1, x_2, x_3) , where the first two parts are the space coordinates and the last one is the Euclidean time coordinate, change under parity transformation as

$$(x_1, x_2, x_3) \mapsto (-x_1, x_2, x_3) =: \tilde{x}.$$

	\mathcal{C}	\mathcal{P}	\mathcal{T}
$\bar{\psi}_L^a \psi_R^b$	$\bar{\psi}_R^b \psi_L^a$	$\bar{\psi}_R^a \psi_L^b$	$\bar{\psi}_R^a \psi_L^b$
$\bar{\psi}_L^a \gamma_\mu \psi_L^b$	$-\bar{\psi}_L^b \gamma_\mu \psi_L^a$	$\bar{\psi}_L^a \tilde{\gamma}_\mu \psi_L^b$	$-\bar{\psi}_L^a \hat{\gamma}_\mu \psi_L^b$
$\bar{\psi}_L^a \sigma_{\mu\nu} \psi_R^b$	$-\bar{\psi}_R^b \sigma_{\mu\nu} \psi_L^a$	$\bar{\psi}_L^a \tilde{\sigma}_{\mu\nu} \psi_R^b$	$-\bar{\psi}_L^a \hat{\sigma}_{\mu\nu} \psi_R^b$
$\bar{\psi}_L^a \gamma_4 \psi_L^b$	$\bar{\psi}_L^b \gamma_4 \psi_L^a$	$-\bar{\psi}_L^a \gamma_4 \psi_L^b$	$\bar{\psi}_L^a \gamma_4 \psi_L^b$
$\bar{\psi}_L^a i\gamma_\mu \gamma_4 \psi_R^b$	$\bar{\psi}_R^b i\gamma_\mu \gamma_4 \psi_L^a$	$-\bar{\psi}_L^a i\tilde{\gamma}_\mu \gamma_4 \psi_R^b$	$\bar{\psi}_L^a i\hat{\gamma}_\mu \gamma_4 \psi_R^b$

Table 4.1: Properties of fermion bilinears under discrete transformations. The arguments of the transformed fields are $\tilde{x} = (-x_1, x_2, x_3)$ in the case of parity transformation and $\hat{x} = (x_1, x_2, -x_3)$ in the case of time reversal. The bilinears with $(L \leftrightarrow R)$ transform analogously.

The time reversal is defined via

$$(x_1, x_2, x_3) \mapsto (x_1, x_2, -x_3) =: \hat{x}.$$

The three discrete transformations are given by

$$\begin{aligned} \mathcal{C} &: \psi_{L/R}^a \mapsto \left(\bar{\psi}_{L/R}^a C \right)^T, \quad \bar{\psi}_{L/R}^a \mapsto - \left(C^\dagger \psi_{L/R}^a \right)^T, \\ \mathcal{P} &: \psi_{L/R}^a(x) \mapsto P \psi_{L/R}^a(\tilde{x}), \quad \bar{\psi}_{L/R}^a(x) \mapsto \bar{\psi}_{L/R}^a(\tilde{x}) P^\dagger, \\ \mathcal{T} &: \psi_{L/R}^a(x) \mapsto T \psi_{L/R}^a(\hat{x}), \quad \bar{\psi}_{L/R}^a(x) \mapsto \bar{\psi}_{L/R}^a(\hat{x}) T^\dagger. \end{aligned}$$

The unitary matrices C, P and T are given as $C = \gamma_2 \gamma_5, P = \gamma_1 \gamma_4$ and $T = \gamma_2 \gamma_3$. Since there exists an ambiguity this is just one possible choice.

In summary we expect our system to be invariant under Lorentz transformation, chiral $U(N_L)_L \otimes U(N_R)_R$ transformations, \mathcal{C} charge conjugation, \mathcal{P} parity transformation and \mathcal{T} time reversal. All these symmetries together forbid fermionic bilinears to zeroth order in derivatives. For example the $\bar{\psi}_L^a \psi_R^a$ term and the $\bar{\psi}_R^a \psi_L^a$ term is not allowed due to chiral invariance. The terms $\bar{\psi}_L^a \gamma_4 \psi_L^a$ and $\bar{\psi}_R^a \gamma_4 \psi_R^a$ are excluded due to \mathcal{P} parity transformation. Terms like $\bar{\psi}_L \psi_L$ vanish since $P_L P_R = 0$, see also Tab.4.1 for transformation properties of all nonvanishing bilinears. In leading order in derivatives the only combinations which are invariant are the standard kinetic terms

$$\bar{\psi}_L^a i\partial_\mu \gamma_\mu \psi_L^a \quad \text{and} \quad \bar{\psi}_R^a i\partial_\mu \gamma_\mu \psi_R^a. \quad (4.1)$$

Although all bilinears to zeroth order in derivatives are forbidden there exist some *four-Fermi terms*¹ invariant under all considered transformations. These invariant terms are

$$\begin{aligned} \left(\bar{\psi}_L^a \gamma_A \psi_L^b \right) \left(\bar{\psi}_L^b \gamma_A \psi_L^a \right), \quad & \left(\bar{\psi}_R^a \gamma_A \psi_R^b \right) \left(\bar{\psi}_R^b \gamma_A \psi_R^a \right) \quad \text{with} \quad \gamma_A \in \{\gamma_\mu, \gamma_4\}, \\ & \left(\bar{\psi}_L^a \gamma_B \psi_R^b \right) \left(\bar{\psi}_R^b \gamma_B \psi_L^a \right) \quad \text{with} \quad \gamma_B \in \{\mathbb{1}, i\gamma_\mu \gamma_4\} \end{aligned}$$

¹Four-Fermi terms are combinations of two bilinears.

or with inverse flavor structure

$$\begin{aligned} & (\bar{\psi}_L^a \gamma_A \psi_L^a) (\bar{\psi}_L^b \gamma_A \psi_L^b), \quad (\bar{\psi}_R^a \gamma_A \psi_R^a) (\bar{\psi}_R^b \gamma_A \psi_R^b), \\ & (\bar{\psi}_R^a \gamma_A \psi_R^a) (\bar{\psi}_L^b \gamma_A \psi_L^b). \end{aligned}$$

Terms with $\gamma_A \in \{\mathbb{1}, \gamma_5, i\gamma_\mu \gamma_4, \sigma_{\mu\nu}\}$ or $\gamma_B \in \{\gamma_\mu, i\gamma_\mu \gamma_5, \gamma_4, i\gamma_4 \gamma_5\}$ vanish since $P_R P_L = P_L P_R = 0$ holds. If $\gamma_A \in \{i\gamma_\mu \gamma_5, i\gamma_4 \gamma_5\}$ or $\gamma_B \in \{\gamma_5, \sigma_{\mu\nu}\}$ no new terms appear since ψ_L and ψ_R are eigenvectors of γ_5 and $\sigma_{\mu\nu}$ is given as $\sigma_{\mu\nu} = -i\epsilon_{\mu\nu\rho} \gamma_\rho \gamma_4 \gamma_5$. Furthermore the terms with the inverse flavor structure are not independent of the terms above. They are related to each other by the so-called *Fierz transformations*. These transformations read

$$(\bar{\psi}_L^a \gamma_\mu \psi_L^a) (\bar{\psi}_L^b \gamma_\mu \psi_L^b) = \frac{1}{2} (\bar{\psi}_L^a \gamma_\mu \psi_L^b) (\bar{\psi}_L^b \gamma_\mu \psi_L^a) + \frac{3}{2} (\bar{\psi}_L^a \gamma_4 \psi_L^b) (\bar{\psi}_L^b \gamma_4 \psi_L^a), \quad (4.2)$$

$$(\bar{\psi}_L^a \gamma_4 \psi_L^a) (\bar{\psi}_L^b \gamma_4 \psi_L^b) = \frac{1}{2} (\bar{\psi}_L^a \gamma_\mu \psi_L^b) (\bar{\psi}_L^b \gamma_\mu \psi_L^a) - \frac{1}{2} (\bar{\psi}_L^a \gamma_4 \psi_L^b) (\bar{\psi}_L^b \gamma_4 \psi_L^a), \quad (4.3)$$

$$(\bar{\psi}_R^a \gamma_\mu \psi_R^a) (\bar{\psi}_L^b \gamma_\mu \psi_L^b) = -\frac{3}{2} (\bar{\psi}_R^a \psi_L^b) (\bar{\psi}_L^b \psi_R^a) - \frac{1}{2} (\bar{\psi}_R^a i\gamma_\mu \gamma_4 \psi_L^b) (\bar{\psi}_L^b i\gamma_\mu \gamma_4 \psi_R^a), \quad (4.4)$$

$$(\bar{\psi}_R^a \gamma_4 \psi_R^a) (\bar{\psi}_L^b \gamma_4 \psi_L^b) = -\frac{1}{2} (\bar{\psi}_R^a \psi_L^b) (\bar{\psi}_L^b \psi_R^a) + \frac{1}{2} (\bar{\psi}_R^a i\gamma_\mu \gamma_4 \psi_L^b) (\bar{\psi}_L^b i\gamma_\mu \gamma_4 \psi_R^a). \quad (4.5)$$

Analogous equations hold for the case ($L \leftrightarrow R$). In summary we have six independent four-Fermi terms which are invariant under Lorentz transformation, chiral $U(N_L)_L \otimes U(N_R)_R$ transformations, \mathcal{C} charge conjugation, \mathcal{P} parity transformation and \mathcal{T} time reversal. These are

$$(\bar{\psi}_L^a \psi_R^b) (\bar{\psi}_R^b \psi_L^a), \quad (4.6)$$

$$(\bar{\psi}_L^a \gamma_4 \psi_L^b) (\bar{\psi}_L^b \gamma_4 \psi_L^a), \quad (\bar{\psi}_R^a \gamma_4 \psi_R^b) (\bar{\psi}_R^b \gamma_4 \psi_R^a), \quad (4.7)$$

$$(\bar{\psi}_L^a \gamma_\mu \psi_L^b) (\bar{\psi}_L^b \gamma_\mu \psi_L^a), \quad (\bar{\psi}_R^a \gamma_\mu \psi_R^b) (\bar{\psi}_R^b \gamma_\mu \psi_R^a), \quad (4.8)$$

$$(\bar{\psi}_L^a i\gamma_\mu \gamma_4 \psi_L^b) (\bar{\psi}_R^b i\gamma_\mu \gamma_4 \psi_L^a). \quad (4.9)$$

Now we can construct our general theory by combining the standard kinetic terms Eq. (4.1) and one or some of the four-Fermi terms of Eqs. (4.6)-(4.9) into one action. If one chooses the four fermi term of Eq. (4.6) the action reads

$$S = \int d^3x \left[i\bar{\psi}_L^a \not{\partial} \psi_L^a + i\bar{\psi}_R^a \not{\partial} \psi_R^a + \frac{\lambda}{N} (\bar{\psi}_L^a \psi_R^b) (\bar{\psi}_R^b \psi_L^a) \right].$$

Here λ is a coupling constant and N is the number of fermion flavors. This action describes the $U(N)_L \otimes U(N)_R$ symmetric Nambu-Jona-Lasinio model which was introduced in 1961 by Yoichiro Nambu and Giovanni Jona-Lasinio [72, 73] and is used to describe low-energy quantum chromodynamics (QCD).

Combining the left parts of Eq. (4.7) and Eq. (4.8) as in Eq. (4.2) and also combining Eq. (4.6) and Eq. (4.9) as in Eq. (4.4) leads to $(\bar{\psi}_L^a \gamma_\mu \psi_L^a) (\bar{\psi}_L^b \gamma_\mu \psi_L^b)$ and

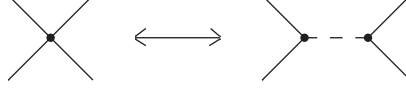


Figure 4.1: Four-Fermi vertex and the corresponding bosonised graph.

$(\bar{\psi}_R^a \gamma_\mu \psi_R^a) (\bar{\psi}_L^b \gamma_\mu \psi_L^b)$. These terms can be combined and the resulting action then reads

$$S = \int d^3x \left[i\bar{\psi}^a \not{\partial} \psi^a + \frac{g}{2N} (\bar{\psi}^a \gamma_\mu \psi^a) (\bar{\psi}^b \gamma_\mu \psi^b) \right],$$

where g and N are constant. This is the Thirring model which was introduced by Walter Thirring in 1958 [74]. This model is used to investigate for example high T_c cuprate superconductors [75] and electronic properties of graphene [76].

If we want to study the critical behaviour of our model it is convenient to include bosonic degrees of freedom. This can be done by a *Hubbard-Stratonovich transformation*. This transformation corresponds to a partial bosonisation of a theory which can be interpreted as the replacement of a four-Fermi vertex by two Yukawa interactions as indicated in Fig. 4.1. We have the scalar channel in Eq. (4.6) and the pseudo-scalar channel in Eq. (4.7). Furthermore there is a vector-boson channel in Eq. (4.8) and a pseudo-vector-boson channel in Eq. (4.9). We choose the four-Fermi term in Eq. (4.6) for our model. Furthermore N_R has to be one for our purposes. Thus the action in three dimensions reads

$$S_{4\text{-fermi}} = \int d^3x \left[i\bar{\psi}_L^a \not{\partial} \psi_L^a + i\bar{\psi}_R \not{\partial} \psi_R + 2\lambda (\bar{\psi}_L^a \psi_R) (\bar{\psi}_R \psi_L^a) \right],$$

where λ is the coupling constant. We rewrite this purely fermionic action as a partially bosonised action:

$$S = \int d^3x \left[\frac{1}{2\lambda} \phi^{a\dagger} \phi^a + i\bar{\psi}_L^a \not{\partial} \psi_L^a + i\bar{\psi}_R \not{\partial} \psi_R + \phi^{a\dagger} \bar{\psi}_R \psi_L^a - \phi^a \bar{\psi}_L^a \psi_R \right].$$

The equivalence can be seen by the equations of motion for the bosonic field ϕ .

$$\phi^a = -2\lambda \bar{\psi}_R \psi_L^a, \quad \phi^{a\dagger} = 2\lambda \bar{\psi}_L^a \psi_R.$$

It is also possible to see this equivalence with the help of the path integral. The path integral including the bosonic fields can be written as

$$\begin{aligned} \int \mathcal{D}\phi \mathcal{D}\psi \mathcal{D}\bar{\psi} e^{-S[\phi, \psi, \bar{\psi}]} = \\ \int \mathcal{D}\psi \mathcal{D}\bar{\psi} e^{-S_{4\text{-fermi}}[\psi, \bar{\psi}]} \int \mathcal{D}\phi \exp \left(-\frac{1}{2\lambda} (\phi^{a\dagger} - 2\lambda \bar{\psi}_L^a \psi_R) (\phi^a + 2\lambda \bar{\psi}_R \psi_L^a) \right). \end{aligned}$$

Here the bosonic path integral in the second line gives us an unimportant constant. From the definition of the new bosonic fields the transformation properties under chiral transformations follow:

$$\phi^a \mapsto U_L^{ab} \phi^b U_R^\dagger, \quad \phi^{a\dagger} \mapsto U_R \phi^{b\dagger} (U_L^\dagger)^{ba}.$$

Including kinetic and self-interaction terms for the bosons we end up with the action of the system we studied in the last chapter in four dimensions. The corresponding effective action reads

$$\Gamma_k = \int d^d x \left[U_k(\rho) + Z_{\phi,k}(\partial_\mu \phi^{a\dagger})(\partial^\mu \phi^a) + i(Z_{L,k}\bar{\psi}_L^a \not{\partial} \psi_L^a + Z_{R,k}\bar{\psi}_R^a \not{\partial} \psi_R^a) + \bar{h}_k \bar{\psi}_R \phi^a \psi_L^a - \bar{h}_k \bar{\psi}_L^a \phi^{a\dagger} \psi_R \right]. \quad (4.10)$$

For comparison see also Eq. (3.3). This is the starting point for the application of the exact renormalisation group equation.

4.2 Flow Equations

Now we have to derive the flow equations for the effective potential, the Yukawa coupling and the equations for the anomalous dimensions. First we see that the flow equation of the effective potential does not change besides the change of the dimension compared to the flow equation in four dimensions. Thus we can use Eq. (3.13) and find:

$$\begin{aligned} \partial_t u_k = & -du_k + \tilde{\rho} u'_k (d-2 + \eta_\phi) \\ & + \frac{4v_d}{d} \left[\frac{2N_L - 1}{1 + u'_k} \left(1 - \frac{\eta_\phi}{d+2} \right) + \frac{1}{1 + u'_k + 2\tilde{\rho} u''_k} \left(1 - \frac{\eta_\phi}{d+2} \right) \right. \\ & \left. - d_\gamma \left(1 - \frac{\eta_L}{d+1} \right) \left((N_L - 1) + \frac{1}{1 + \tilde{\rho} h_k^2} \right) + \left(1 - \frac{\eta_R}{d+1} \right) \frac{d_\gamma}{1 + \tilde{\rho} h_k^2} \right]. \end{aligned} \quad (4.11)$$

In comparison to the equation in four dimensions d and v_d change. Otherwise it remains unchanged. Again the effective potential can be in the symmetric regime and in the regime with broken symmetry.

For the flow equation of the Yukawa coupling we divide the bosonic field again into its vacuum expectation value and the deviation thereof:

$$\phi = \frac{1}{\sqrt{2}} \begin{pmatrix} \phi_1^1(p) + i\phi_2^1(p) \\ \phi_1^2(p) + i\phi_2^2(p) \\ \vdots \\ \phi_1^{N_L}(p) + i\phi_2^{N_L}(p) \end{pmatrix} = \frac{\delta(p)}{\sqrt{2}} \begin{pmatrix} \phi_{\text{vev}} \\ 0 \\ \vdots \\ 0 \end{pmatrix} + \frac{1}{\sqrt{2}} \begin{pmatrix} \Delta\phi_1^1(p) + i\Delta\phi_2^1(p) \\ \Delta\phi_1^2(p) + i\Delta\phi_2^2(p) \\ \vdots \\ \Delta\phi_1^{N_L}(p) + i\Delta\phi_2^{N_L}(p) \end{pmatrix}.$$

This time we are mainly interested in the coupling between the fermions and the Goldstone modes instead of the coupling between the fermions and the radial mode. This is essential since the four-dimensional model should mimic the Higgs sector of the Standard Model. The contributions of the massive radial mode in the IR are negligible compared to the ones of the Goldstone modes. That is why we are interested in the coupling between fermions and Goldstone bosons. Therefore we have to change our projection. We do not project onto $\Delta\phi_1^1$ but onto $\Delta\phi_2^1$. Thus our projection now reads

$$\partial_t \bar{h}_k = -\frac{i}{2} \frac{\vec{\delta}}{\delta \bar{\psi}_L(p)} \frac{\sqrt{2} \vec{\delta}}{\delta \Delta\phi_2^1(p')} \text{STr} \left[\tilde{\partial}_t \ln(\Gamma_k^{(2)} + R_k) \right] \frac{\overleftarrow{\delta}}{\delta \psi_R(q)} \Bigg|_{\substack{\psi_R^a = \psi_L^a = \Delta\phi = 0 \\ p' = p = q = 0}}.$$

The following calculation is analogous to the one of the four-dimensional model. At first we split $(\Gamma_k^{(2)} + R_k)$ into the fluctuation part and the propagator part. After expanding the logarithm only the third power survives the projection. As in the previous chapter the matrix calculation is tedious but straightforward and the result can be given in dimensionful quantities:

$$\partial_t \bar{h}_k^2 = \int \frac{d^d p}{(2\pi)^d} \tilde{\partial}_t \frac{h_k^4 U_k'' \phi_{\text{vev}}^2}{(Z_\phi P_B + U'_k + U_k'' \phi_{\text{vev}}^2) (Z_\phi P_B + U'_k) \left(Z_L Z_R P_F + \frac{\bar{h}_k^2}{2} \phi_{\text{vev}}^2 \right)}.$$

Here the potential is evaluated at the minimum $\frac{1}{2}\phi_{\text{vev}}^2$. Changing to dimensionless quantities

$$\begin{aligned} \tilde{\rho} &= Z_{\phi,k} k^{2-d} \rho, \\ \kappa_k &= \frac{1}{2} Z_{\phi,k} k^{2-d} \phi_{\text{vev}}^2 \\ h_k^2 &= Z_{\phi,k}^{-1} Z_{L,k}^{-1} Z_{R,k}^{-1} k^{d-4} \bar{h}_k^2, \\ u_k(\tilde{\rho}) &= k^{-d} U_k(\rho)|_{\rho=k^{d-2}\tilde{\rho}/Z_{\phi,k}} \end{aligned}$$

and using the threshold functions defined in App. C we get

$$\begin{aligned} \partial_t h_k^2 &= (\eta_\phi + \eta_L + \eta_R + d - 4) h_k^2 \\ &\quad - 8v_d h_k^4 \kappa_k u_k'' l_{111}^{(\text{FB})d} (\kappa_k h_k^2, u'_k + 2\kappa_k u_k'', u'_k). \end{aligned} \quad (4.12)$$

For the derivation of the bosonic anomalous dimension we project again onto $\Delta\phi_2^1$ instead of $\Delta\phi_1^1$. After splitting $(\Gamma_k^{(2)} + R_k)$ into the fluctuation part and the propagator part we expand the logarithm and the second power is the only one which survives the projection. The matrix calculation is the same as for the four-dimensional model. Using dimensionless quantities and the threshold functions defined in App. C we end up with

$$\eta_\phi = \frac{16v_d}{d} u_k'' \kappa_k m_{22}^d (u'_k + 2\kappa_k u_k'', u'_k) + \frac{8v_d d_\gamma}{d} \left[\kappa_k h_k^4 m_2^{(\text{F})d} (\kappa_k h_k^2) + h_k^2 m_4^{(\text{F})d} (\kappa_k h_k^2) \right]. \quad (4.13)$$

The derivation of the equations for the fermionic anomalous dimensions does not change. Thus we can use the results of the preceding chapter (Eqs. (3.20) and (3.21)).

$$\eta_L = \frac{8v_d}{d} h_k^2 [m_{12}^{(\text{FB})d} (h_k^2 \kappa_k, u'_{k\text{vev}} + 2\kappa_k u''_{k\text{vev}}) + m_{12}^{(\text{FB})d} (h_k^2 \kappa_k, u'_{k\text{vev}})] \quad (4.14)$$

and

$$\begin{aligned} \eta_R &= \frac{8v_d}{d} h_k^2 [m_{12}^{(\text{FB})d} (h_k^2 \kappa_k, u'_{k\text{vev}} + 2\kappa_k u''_{k\text{vev}}) + m_{12}^{(\text{FB})d} (h_k^2 \kappa_k, u'_{k\text{vev}}) \\ &\quad + 2(N_L - 1) m_{12}^{(\text{FB})d} (0, u'_{k\text{vev}})]. \end{aligned} \quad (4.15)$$

4.3 Fixed-Point Analysis

In this section we investigate possible fixed points of our system. Therefore we study our system in two different regimes: the symmetric regime and the spontaneously broken regime. The first one corresponds to an expansion of the effective potential around vanishing vacuum expectation value:

$$u_k = \sum_{n=1}^{N_P} \frac{\lambda_n}{n!} \tilde{\rho}^n = m^2 \tilde{\rho} + \frac{\lambda_2}{2!} \tilde{\rho}^2 + \frac{\lambda_3}{3!} \tilde{\rho}^3 + \dots \quad (4.16)$$

On the other hand the spontaneously broken regime corresponds to an expansion of the effective potential around non-vanishing vacuum expectation value κ_k :

$$u_k = \sum_{n=1}^{N_P} \frac{\lambda_n}{n!} (\tilde{\rho} - \kappa_k)^n = \frac{\lambda_1}{1!} (\tilde{\rho} - \kappa_k) + \frac{\lambda_2}{2!} (\tilde{\rho} - \kappa_k)^2 + \frac{\lambda_3}{3!} (\tilde{\rho} - \kappa_k)^3 + \dots \quad (4.17)$$

4.3.1 Symmetric Regime

We are equipped with the flow equation for the effective potential Eq. (4.11), the flow equation for the squared Yukawa coupling Eq. (4.12) and the equations for the anomalous dimensions Eqs. (4.13)-(4.15). If we write down the flow equation for the squared Yukawa coupling in $d = 3$ dimensions in the symmetric regime we get

$$\partial_t h^2 = (\eta_\phi + \eta_L + \eta_R - 1) h^2.$$

Thus for an interacting fixed point ($h \neq 0$) the following sum rule for the anomalous dimensions has to hold:

$$\eta_\phi + \eta_L + \eta_R = 1. \quad (4.18)$$

The equations for the anomalous dimensions in the symmetric regime and for $d = 3$ dimensions read

$$\begin{aligned} \eta_\phi &= \frac{h^2}{3\pi^2} (5 - \eta_L - \eta_R), \\ \eta_L &= \frac{h^2}{6\pi^2} (4 - \eta_L) \frac{1}{(1 + m^2)^2}, \\ \eta_R &= N_L \frac{h^2}{6\pi^2} (4 - \eta_L) \frac{1}{(1 + m^2)^2}. \end{aligned}$$

If we consider h^2 and m^2 as parameters this system of linear equations can be solved depending on these two parameters. The solution can be given as

$$\eta_\phi = \frac{2h^2(2h^2(N_L + 1) - 15\pi^2(1 + m^2)^2)}{h^4(N_L + 1) - 18\pi^4(1 + m^2)^2}, \quad (4.19)$$

$$\eta_L = \frac{h^2(5h^2 - 12\pi^2)}{h^4(N_L + 1) - 18\pi^4(1 + m^2)^2}, \quad (4.20)$$

$$\eta_R = N_L \frac{h^2(5h^2 - 12\pi^2)}{h^4(N_L + 1) - 18\pi^4(1 + m^2)^2}. \quad (4.21)$$

This solution depending on h^2 and m^2 can be inserted into Eq. (4.18). The result is an equation which can be interpreted as h^2 depending on m^2 or the other way round. We consider the first case. We get a quadratic equation for h^2 and thus get two solutions. For the solution with the positive square root we were not able to find an appropriate fixed point and thus we only consider the solution with the negative square root which reads

$$h_{\text{cond}}^2 = \frac{3\pi^2}{8(N_L + 1)} \left\{ 7 + 5m(2 + m) + 2N_L \right. \\ \left. - \sqrt{33 + m(2 + m)(54 + 25m(2 + m)) + 12N_L + 4m(2 + m)N_L + 4N_L^2} \right\}.$$

The index "cond" reflects that h_{cond}^2 still depends on m^2 and thus is a conditional fixed point.

So far we considered the anomalous dimensions and the Yukawa coupling. The effective potential and thus the couplings $m^2, \lambda_2, \lambda_3, \dots$ are still missing. The flow equations for these couplings can be derived, as for the four-dimensional model, by taking derivatives of the flow equation of the effective potential with respect to $\bar{\rho}$. We observe that the flow equation for λ_n only depends on $h^2, m^2, \lambda_2, \dots, \lambda_{n+1}$. Inserting Eqs. (4.19)-(4.21) and the conditional fixed point for h^2 into these equations leads to a nonlinear system of equations for m^2 and the λ_i . Expanding the potential (4.16) for example up to $N_P = 4$ leads to

$$\begin{aligned} \partial_t m^2 &= \beta_m(m, \lambda_2), \\ \partial_t \lambda_2 &= \beta_2(m, \lambda_2, \lambda_3), \\ \partial_t \lambda_3 &= \beta_3(m, \lambda_2, \lambda_3, \lambda_4), \\ \partial_t \lambda_4 &= \beta_4(m, \lambda_2, \lambda_3, \lambda_4, \lambda_5 = 0). \end{aligned}$$

Solving this system leads to fixed points for $N_L \in \{1, 2\}$. The results for $N_P = 6$ can be read of from Tab. 4.2. For higher N_L no reliable fixed points exist.

At these existing fixed points we can calculate the stability matrix as in the previous chapter. Let ω_I be the eigenvalues of the stability matrix. The critical exponents θ_I are the negative of these eigenvalues. The Index I labels the critical exponents starting with the largest real part θ_0 corresponding to ω_0 . Since our model resembles the $O(N)$ model we define $\nu = -\frac{1}{\omega_0}$ according to the notation of critical phenomena in $O(N)$ models. In such models ν characterises the critical exponent of the correlation length near the critical temperature. Note that ν corresponds to the largest critical exponent θ_0 and thus to the strongest relevant direction. The second largest critical exponent θ_1 corresponds to the second smallest eigenvalue $\omega_1 \equiv \omega$. The results for ν and ω can be read of from Tab. 4.2 for $N_P = 6$.

Due to the polynomial expansion of the effective potential an error occurs. To estimate this error we restrict ourselves to the case $N_L = 2$. In Fig. 4.2 the fixed-point values of h^2, m^2, λ_2, ν and ω are depicted depending on N_P . The results show that these quantities vary only on a 1% level on the highest depicted N_P . Nevertheless the results for λ_4 vary much more at this level but are expected to converge for higher orders of the expansion. Thus the error of the expansion of the effective potential is

N_L	h_*^2	m_*^2	λ_2^*	η_ϕ^*	η_L^*	η_R^*	ν	ω
1	4.496	0.326	5.099	0.716	0.142	0.142	1.132	0.786
2	3.364	0.104	3.643	0.512	0.162	0.325	1.100	0.809

Table 4.2: Fixed-point values and critical exponents in the SYM regime for an expansion of the effective potential up to $N_P = 6$.

controllable. The error due to the derivative expansion is much harder to control. Since our model resembles the $O(N)$ model we can compare results of this model to our results. We are using the next to leading order derivative expansion since we included the anomalous dimensions in our calculation. In [77] is shown that to this order the critical exponent ν of the $O(N)$ model differs from the best known value only on the 3% level. Thus we expect our results to be reliable at least for this leading critical exponent. The other critical exponents as well as the anomalous dimensions are less well approximated.

4.3.2 Spontaneously Symmetry Broken Regime

Now we turn our attention to the regime of spontaneous symmetry breaking. Here we expand the effective potential around a non-vanishing vacuum expectation value κ_k as in Eq. (4.17). This expansion and the flow equation of the effective potential, Eq. (4.11), provides us with the flow equation for the different coupling constants $\lambda_2, \lambda_3, \dots$. The flow equation for the vacuum expectation value κ_k can be derived by using Eq. (3.22). Furthermore we have the flow equation for the Yukawa coupling, Eq. (4.12), and the equations for the anomalous dimensions, Eqs. (4.13)-(4.15). If we expand the potential for example up to $N_P = 2$ we have to solve a system of

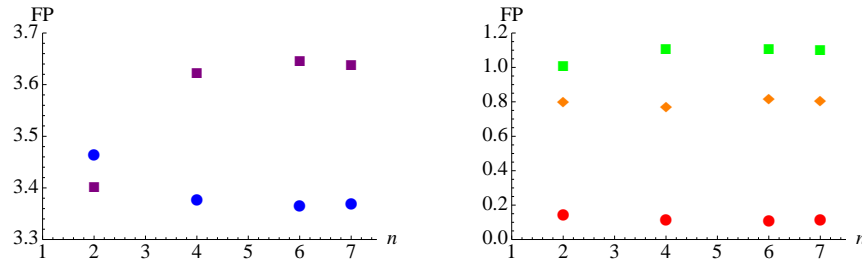


Figure 4.2: Fixed-point values for $N_L = 2$ depending on $N_P \equiv n$. Left panel: h_*^2 (blue dots) and λ_2^* (purple squares). Right panel: m_*^2 (red dots), ν (green squares) and ω (orange diamonds).

coupled nonlinear equations.

$$\begin{aligned}
 \partial_t \kappa(\kappa^*, \lambda_2^*, h^{2*}, \eta_\phi^*, \eta_L^*, \eta_R^*) &= 0 \\
 \partial_t \lambda_2(\kappa^*, \lambda_2^*, h^{2*}, \eta_\phi^*, \eta_L^*, \eta_R^*) &= 0 \\
 \partial_t h^2(\kappa^*, \lambda_2^*, h^{2*}, \eta_\phi^*, \eta_L^*, \eta_R^*) &= 0 \\
 \eta_\phi(\kappa^*, \lambda_2^*, h^{2*}, \eta_\phi^*, \eta_L^*, \eta_R^*) &= \eta_\phi^* \\
 \eta_L(\kappa^*, \lambda_2^*, h^{2*}, \eta_\phi^*, \eta_L^*, \eta_R^*) &= \eta_L^* \\
 \eta_R(\kappa^*, \lambda_2^*, h^{2*}, \eta_\phi^*, \eta_L^*, \eta_R^*) &= \eta_R^*.
 \end{aligned} \tag{4.22}$$

We were not able to solve this system analytically. However we studied this system numerically as we shall discuss below. Before introducing the numerics it is necessary to compare our system to the $O(N)$ model.

Our model consist of N_L complex bosonic fields which can be divided into their real parts and imaginary parts. Thus they can be described as $2N_L$ real bosons. These bosons are coupled via a Yukawa interaction to N_L left-handed and one right-handed fermion. For vanishing Yukawa coupling $h = 0$ the bosons and fermions decouple and thus our system corresponds to a purely bosonic system. This is the $O(2N_L)$ model. This system was investigated for example in [77] and is known to exhibit a fixed point in the spontaneous symmetry broken regime. We expect our system to differ slightly from the behaviour of the purely bosonic model due to the contributions of the fermionic fluctuations. As a first hint the solution of the $O(2N_L)$ model may be interesting. Thus we solve the system (4.22) for vanishing fermionic contributions which can be done analytically. The corresponding fixed point can be used as a starting point for our numerical solution of the whole system (4.22). Since we expect our system to behave similarly to the bosonic model we use the Newton method to solve our system. As a starting point we use the fixed point of the purely bosonic system. The solutions of the numerical calculation are given in Tab. 4.3. In Fig. 4.3 we show the fixed-point values of κ^* and h^{2*} and in Fig. 4.4 for the anomalous dimensions.

In the left panel of Fig. 4.3 we can see the fixed-point values of the dimensionless vacuum expectation value depending on N_L for our system (red dots). For comparison the fixed-point values of the $O(2N_L)$ model are given as well. Note that for

N_L	h_*^2	κ_*	λ_2^*	η_ϕ^*	η_L^*	η_R^*	ν	ω
3	2.718	0.009	2.967	0.371	0.154	0.487	0.883	0.675
4	2.713	0.042	2.954	0.279	0.125	0.637	1.043	0.678
5	2.519	0.079	2.717	0.204	0.100	0.746	1.124	0.715
10	1.452	0.256	1.506	0.075	0.046	0.913	1.092	0.872
20	0.739	0.597	0.752	0.032	0.022	0.963	1.043	0.942
50	0.296	1.612	0.298	0.012	0.009	0.986	1.017	0.978
100	0.148	3.301	0.149	0.006	0.004	0.993	1.008	0.989

Table 4.3: Fixed-point values and critical exponents in the SSB regime.

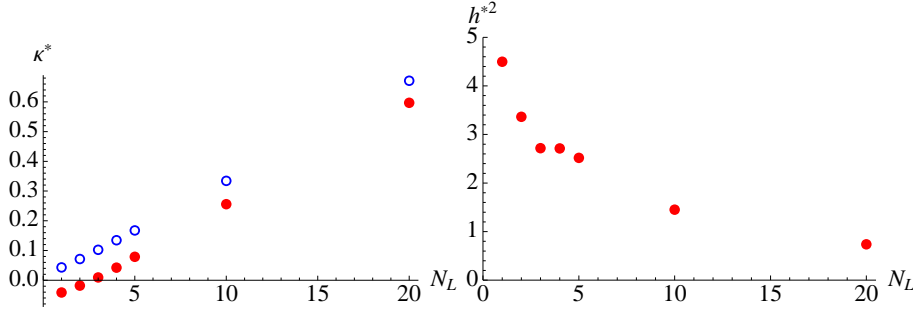


Figure 4.3: Left panel: Dimensionless vacuum expectation value κ^* in our $U(N_L)_L \otimes U(1)_R$ model (red dots) compared with those of the $O(2N_L)$ model (blue circles). Right panel: Fixed-point values of h^2 depending on N_L .

$N_L \in \{1, 2\}$ the fixed-point values of κ are negative and thus unphysical. Therefore we do not have any reliable fixed point in the case $N_L \in \{1, 2\}$ but recall that we have suitable fixed points in the symmetric regime. The unphysical fixed points for $N_L < 3$ cause a kink of the fixed-point values for h^2 between $N_L = 2$ and $N_L = 3$. Furthermore we see that the fixed-point values for κ only differ slightly from those of the purely bosonic model as expected.

In the left panel of Fig. 4.5 we show the fixed-point values of η_ϕ for our model (red dots) and for the bosonic model (blue circles). For small N_L they differ due to the fermionic contributions. For large N_L both values approach each other. This is due to the decreasing fixed-point value of h^2 which corresponds to a decoupling. In the right panel the fermionic anomalous dimensions are plotted which are identical for $N_L = 1$. This corresponds to a left-right symmetry. For larger N_L the fixed-point values of η_R increase due to the contribution proportional to N_L in Eq. (4.15).

As we did in the symmetric regime we can calculate the critical exponents. In Fig. 4.5 the exponents ν and ω are plotted depending on N_L . For comparison the values for the $O(2N_L)$ model are plotted as well. We find that the difference is

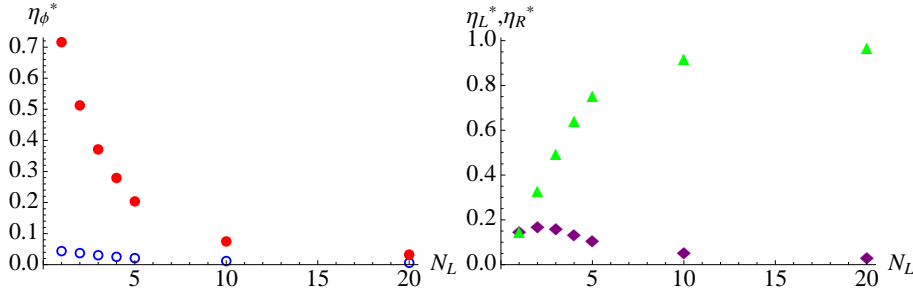


Figure 4.4: Left panel: η_ϕ^* in the $U(N_L)_L \otimes U(1)_R$ model (red dots) compared with that of the analogous $O(2N_L)$ model (blue circles). Right panel: η_L^* (purple diamonds) and η_R^* (green triangles) depending on N_L .

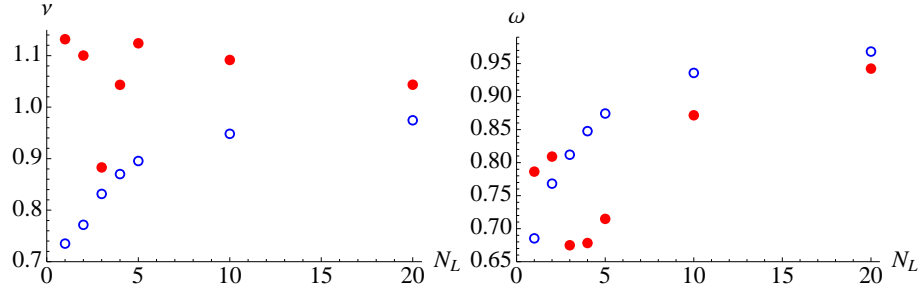


Figure 4.5: Critical exponents as a function of N_L in the chiral $U(N_L)_L \otimes U(1)_R$ model (red dots) compared to those of the corresponding $O(2N_L)$ model (blue circles).

sizeable for small N_L . For large N_L , however, the difference decreases. This is caused by the fact that for large N_L the Yukawa coupling h decreases and thus our model resembles more and more the purely bosonic $O(2N_L)$ model.

In summary we have found that our model exhibits non-trivial fixed points for various values of N_L in next to leading order. For $N_L \in \{1, 2\}$ the fixed point lies in the symmetric regime while it lies in the spontaneously broken regime for larger N_L .

Chapter 5

4D Model including Gauge Bosons

In this chapter we turn our attention to the four-dimensional model again. In Chap.3 we realised that our four-dimensional model exhibits a fixed point in the spontaneously broken regime but only in leading order. The extension to next to leading order was inhibited by the contributions of the Goldstone modes. We already mentioned that these Goldstone modes do not exist in the Standard Model. They vanish because of the Higgs mechanism explained in Sec.2.5. That is why we shall introduce gauge bosons and investigate the effects of this extension of the model. We determine the new flow equations and at the end of this chapter we study whether fixed points of this new system exist which allow a construction of an asymptotic safety scenario.

5.1 Extension of the Model

So far we have investigated the model with the truncation of Eq. (3.3):

$$\Gamma_k = \int d^d x \left[U_k(\rho) + Z_{\phi,k} (\partial_\mu \phi^a)^\dagger (\partial^\mu \phi^a) + i(Z_{L,k} \bar{\psi}_L^a \not{\partial} \psi_L^a + Z_{R,k} \bar{\psi}_R \not{\partial} \psi_R) \right. \\ \left. + \bar{h}_k \bar{\psi}_R \phi^a \psi_L^a - \bar{h}_k \bar{\psi}_L^a \phi^{a\dagger} \psi_R \right].$$

This system is invariant under global $U(N_L)_L \otimes U(1)_R$ transformations. The group $U(N_L)_L$ can be divided into $SU(N_L)_L \otimes U(1)$.

The gauge group of the Standard Model is $SU(3) \times SU(2) \times U(1)$ where the $SU(3)$ corresponds to the gluons, the $SU(2)$ corresponds to the W- and Z- gauge bosons and the $U(1)$ corresponds to the photon. We are interested in the Higgs mechanism. That is why we investigate the electroweak sector of the Standard Model. This sector corresponds to $SU(N) \otimes U(1)$ with $N = 2$. In this case $2N - 1 = 3$ Goldstone modes appear. These 3 Goldstone modes are removed from the spectrum of the theory by the $N^2 - 1 = 3$ gauge bosons¹ which acquire a mass. The gauge boson corresponding to the abelian group $U(1)$ (the photon) remains massless.

¹ $SU(N)$ has dimension $N^2 - 1$ and thus $N^2 - 1$ gauge bosons appear.

In our model N_L is arbitrary and thus can be bigger than two. As an example let $N_L = 3$. In this case $2N_L - 1 = 5$ Goldstone modes appear. If we introduce a local symmetry and the corresponding gauge degrees of freedom we get $N_L^2 - 1 = 8$ gauge bosons. They remove the Goldstone bosons and some of them but not all acquire a mass. Thus we have to have a look for the $SU(N_L)_L$ symmetry. We replace this global transformation by the local variant thereof. Elements of this group can be given as

$$U(x) = e^{-ig\alpha^i(x)T^i} \text{ with } (i = 1, \dots, N_L^2 - 1).$$

Here g is the gauge coupling constant, T^i are the generators and α^i depends on the position. The gauge field is given as $W_\mu^i = \partial_\mu \alpha^i$. Thus the partial derivative can be replaced by the covariant derivative:

$$\partial_\mu \rightarrow D_\mu = \partial_\mu - igW_\mu^i T^i.$$

The different fields (ϕ^a, ψ_L^a, ψ_R and W_μ^i) transform under the $SU(N_L)_L$ like

$$\phi^a \rightarrow U\phi^a, \quad \psi_L^a \rightarrow U\psi_L^a, \quad \psi_R \rightarrow \psi_R \quad \text{and} \quad W_\mu^i T^i \rightarrow UW_\mu^i T^i U^{-1} - \frac{i}{g}(\partial_\mu U)U^{-1}.$$

The question is how our truncation changes by switching from a global to a local symmetry. At first we have to replace the partial derivative by the covariant derivative. In our truncation this affects the kinetic term of the bosons and the kinetic term of the left-handed fermions:

$$\begin{aligned} Z_{\phi,k}(\partial_\mu \phi^a)^\dagger (\partial^\mu \phi^a) &\rightarrow Z_{\phi,k}((\partial_\mu - igW_\mu^i T^i)\phi^a)^\dagger ((\partial_\mu - igW_\mu^i T^i)\phi^a), \\ iZ_{L,k}\bar{\psi}_L^a \not{\partial} \psi_L^a &\rightarrow iZ_{L,k}\bar{\psi}_L^a (\not{\partial} - igW_\mu^i T^i)\psi_L^a. \end{aligned}$$

This covariant derivatives provide us with a Yukawa interaction between the left-handed fermions and the gauge bosons ($gZ_{L,k}\bar{\psi}_L^a W_\mu^i T^i \psi_L^a$). Besides including the covariant derivatives we have to include a kinetic term for the gauge bosons. Therefore we use the term $\frac{Z_F}{4}F_{\mu\nu}^i F^{i\mu\nu}$ with

$$F_{\mu\nu}^i = \partial_\mu W_\nu - \partial_\nu W_\mu + gf^{jki}W_\mu^j W_\nu^k.$$

Here f^{jki} are the structure constants and thus are given by $[T^i, T^j] = if^{ijk}T^k$.

As explained in Eq. (2.16) we also have to include a gauge fixing term. For the choice of this term we recall Eq. (2.20) of the section about the Higgs model.

$$\begin{aligned} S = \int d^d x &\left[\frac{1}{2}(\partial_\mu \sigma)(\partial^\mu \sigma) - \frac{1}{2}(2\lambda v^2)\sigma^2 \right. \\ &- \frac{1}{4}F_{\mu\nu}F^{\mu\nu} + \frac{1}{2}(qv)^2 A_\mu A^\mu \\ &\left. + \frac{1}{2}(\partial_\mu \eta)(\partial^\mu \eta) + qvA^\mu \partial_\mu \eta \right]. \end{aligned}$$

The last term was the one that was eliminated in the unitary gauge in Sec. 2.5. We choose the gauge fixing term in a way that this term will be eliminated. First

we identify the corresponding term in our model. The bosonic field ϕ of the Higgs model corresponds to the field ϕ^a in our model and the gauge fields are A_μ and W_μ^i respectively. The decomposition into the vacuum expectation value (v), the Goldstone mode (η) and radial mode (σ) in Eq. (2.18) corresponds to the decomposition in Eq. (3.14) into ϕ_{vev} , the radial mode ($\Delta\phi_1^1$) and the Goldstone modes. For explicit explanations we use $N_L = 2$ and go back to the classical action of our model. Using the covariant derivative and the kinetic term for the gauge bosons the action reads

$$S = \int d^d x \left[U(\rho) + (\partial_\mu \phi^a)^\dagger (\partial_\mu \phi^a) + g^2 W_\mu^i W_\mu^j \phi^{a\dagger} T_{ab}^i T_{bc}^j \phi^c + \frac{1}{4} F_{\mu\nu}^2 - ig W_\mu^i (\partial_\mu \phi^{a\dagger}) T_{ab}^i \phi^b + ig W_\mu^i \phi^{a\dagger} T_{ab}^i (\partial_\mu \phi^b) \right].$$

The bosonic field can be separated into the vacuum expectation value (vev) and the fluctuations around the vev:

$$\phi = \begin{pmatrix} 0 \\ v \end{pmatrix} + \frac{1}{\sqrt{2}} \begin{pmatrix} \Delta\phi_1^1 + i\Delta\phi_2^1 \\ \Delta\phi_1^2 + i\Delta\phi_2^2 \end{pmatrix}.$$

Inserting this into the action and rewriting all terms gives us

$$S = \int d^d x \left\{ \frac{1}{4} F_{\mu\nu}^2 + 2g^2 v^2 W_\mu^i W_\mu^j T_{Na}^i T_{aN}^j + \frac{1}{2} (\partial_\mu \Delta\phi_1^2)^2 + \lambda v^2 (\Delta\phi_1^2)^2 + \frac{1}{2} [(\partial_\mu \Delta\phi_1^1)^2 + (\partial_\mu \Delta\phi_2^1)^2 + (\partial_\mu \Delta\phi_2^2)^2] - gv W_\mu^i (\partial_\mu \Delta\phi_2^1) (T_{1N}^i + T_{N1}^i) + igv W_\mu^i (\partial_\mu \Delta\phi_1^1) (T_{N1}^i - T_{1N}^i) - 2gv W_\mu^i (\partial_\mu \Delta\phi_2^2) T_{22}^i \right\},$$

with $N = 2$. The first line corresponds to massive gauge fields, the second to the massive Higgs field and the third line corresponds to the massless Goldstone bosons, see Sec. 2.5. The last two lines contain the terms we would like to eliminate. We use $G(W_\mu^i) = \partial_\mu W_\mu^i + 2i\alpha vg T_{Na}^i (\Delta\phi_1^a + i\Delta\phi_2^a) = 0$ as a gauge with α as a parameter but exclude the term with $\Delta\phi_1^2$. We refer to this gauge as R_α gauge². Thus the gauge fixing term is given as

$$\begin{aligned} & \frac{1}{2\alpha} (\partial_\mu W_\mu^i + 2i\alpha vg T_{Na}^i (\Delta\phi_1^a + i\Delta\phi_2^a)) (\partial_\mu W_\mu^i - 2i\alpha vg (\Delta\phi_1^a - i\Delta\phi_2^a) T_{aN}^i) \\ &= \frac{1}{2\alpha} (\partial_\mu W_\mu^i)^2 + 2\alpha v^2 g^2 T_{Na}^i (\Delta\phi_1^a + i\Delta\phi_2^a) (\Delta\phi_1^b - i\Delta\phi_2^b) T_{bN}^i \\ &+ ivg (\partial_\mu W_\mu^i) \Delta\phi_1^a (T_{Na}^i - T_{aN}^i) - vg (\partial_\mu W_\mu^i) \Delta\phi_2^a (T_{Na}^i + T_{aN}^i). \end{aligned}$$

The last two lines cancel the unwanted terms in the action since the sign changes

²In many textbooks ξ is used instead of α and the gauge is called R_ξ gauge.

by partial integration. Adding this gauge fixing term to the action leads us to

$$\begin{aligned}
 S = \int d^d x \Big\{ & \frac{1}{4} F_{\mu\nu}^2 + 2g^2 v^2 W_\mu^i W_\mu^j T_{Na}^i T_{aN}^j + \frac{1}{2\alpha} (\partial_\mu W_\mu^i)^2 \\
 & + \frac{1}{2} (\partial_\mu \Delta\phi_1^2)^2 + \lambda v^2 (\Delta\phi_1^2)^2 \\
 & + \frac{1}{2} [(\partial_\mu \Delta\phi_1^1)^2 + (\partial_\mu \Delta\phi_2^1)^2 + (\partial_\mu \Delta\phi_2^2)^2] \\
 & + 2\alpha v^2 g^2 T_{Na}^i (\Delta\phi_1^a + i\Delta\phi_2^a) (\Delta\phi_1^b - i\Delta\phi_2^b) T_{bN}^i \Big\}.
 \end{aligned}$$

The first line corresponds to the gauge bosons with the kinetic term

$$\frac{1}{4} F_{\mu\nu}^2 + \frac{1}{2\alpha} (\partial_\mu W_\mu^i)^2 = -\frac{1}{2} W_\mu^i \left(\partial^2 \delta_{\mu\nu} - \partial_\mu \partial_\nu \left(1 - \frac{1}{\alpha} \right) \right) W_\nu^i,$$

the second line corresponds to the Higgs boson and the third line corresponds to the Goldstone bosons. The last line vanishes in the case of *Landau gauge* ($\alpha \rightarrow 0$). Note that the Goldstone bosons do not vanish since this only can be observed in unitary gauge.

Considering Eq. (2.16) we have to include one more ingredient into our truncation, namely the ghost term. The ghost fields are called c^i and \bar{c}^i . Thus the ghost term reads $-\bar{c}^i D^{ij} c^j$ with

$$D^{ij} = \frac{\delta G^i(W^\beta)}{\delta \beta^j} = -\partial_\mu^2 \delta^{ij} - g \partial_\mu W^{k\mu} f^{ikj} + 2\alpha v g^2 T_{Na}^i T_{ab}^j \phi_b.$$

Summarising all these terms we obtain the following truncation:

$$\begin{aligned}
 \Gamma_k = \int d^d x \Big[& U_k(\rho) + Z_{\phi,k} (D^\mu \phi)^\dagger (D_\mu \phi) + i(Z_{L,k} \bar{\psi}_L^a \not{D} \psi_L^a + Z_{R,k} \bar{\psi}_R \not{D} \psi_R) \\
 & + \bar{h}_k \bar{\psi}_R \phi^{a\dagger} \psi_L^a - \bar{h}_k \bar{\psi}_L^a \phi^a \psi_R + \frac{Z_F}{4} F_{\mu\nu}^i F^{i\mu\nu} - \bar{c}^i D^{ij} c^j \\
 & + \frac{Z_\phi}{2\alpha} (\partial_\mu W_\mu^i + 2i\alpha v g T_{Na}^i \Delta\phi^a) (\partial_\mu W_\mu^i - 2i\alpha v g \Delta\phi^{a\dagger} T_{aN}^i) \Big] \\
 = \int d^d x \Big[& U_k(\rho) + Z_{\phi,k} (\partial^\mu \phi)^\dagger (\partial_\mu \phi) + i(Z_{L,k} \bar{\psi}_L^a \not{\partial} \psi_L^a + Z_{R,k} \bar{\psi}_R \not{\partial} \psi_R) \\
 & + \frac{Z_F}{2} W_\mu^i \left(-\partial^2 \delta^{\mu\nu} + \partial_\mu \partial_\nu \left(1 - \frac{Z_\phi}{\alpha Z_F} \right) \right) W_\nu^i - \bar{c}^i D_{ij} c^j \\
 & + \bar{h}_k \bar{\psi}_R \phi^{a\dagger} \psi_L^a - \bar{h}_k \bar{\psi}_L^a \phi^a \psi_R + Z_\phi 2\alpha v^2 g^2 T_{Na}^i \Delta\phi^a \Delta\phi^{b\dagger} T_{bN}^i \\
 & + Z_F g (\partial_\mu W_\nu^i) f^{jki} W_\mu^j W_\nu^k + \frac{Z_F}{4} g^2 f^{jki} f^{lmi} W_\mu^j W_\nu^k W_\mu^l W_\nu^m \\
 & + Z_\phi g^2 W_\mu W_\nu^j \phi^{a\dagger} T_{ac}^i T_{cb}^j \phi^b \\
 & - iZ_\phi g W_\mu^i (\partial_\mu \phi^{a\dagger}) T_{ab}^i \phi^b + iZ_\phi g W_\mu^i \phi^{a\dagger} T_{ab}^i (\partial_\mu \phi^b) \\
 & + iZ_\phi v g W_\mu^i (\partial_\mu \phi^{a\dagger}) T_{aN}^i - iZ_\phi v g W_\mu^i T_{Na}^i (\partial_\mu \phi^a) \Big],
 \end{aligned}$$

with $\Delta\phi^a = \frac{1}{\sqrt{2}}(\Delta\phi_1^a + i\Delta\phi_2^a)$ excluding the term with $\Delta\phi_1^N$. The vacuum expectation value v is chosen to be in the N_L direction. We use this truncation to repeat the investigations of Chap. 3.

Before doing so we shall discuss briefly the Landau gauge and the unitary gauge. The propagator of the Higgs boson is given by

$$\Delta_{\text{Higgs}} = \frac{1}{p^2 + m_{\text{Higgs}}^2},$$

with m_{Higgs}^2 proportional to λv^2 . The propagator of the Goldstone bosons is given by

$$\Delta_{\text{Gold}} = \frac{1}{p^2 + \alpha m_{\text{Gold}}^2},$$

with m_{Gold}^2 proportional to $g^2 v^2$. Using the projection operators P_T and P_L the gauge-boson propagator is given by

$$\Delta_{\text{GB}} = -\frac{P_T}{p^2 + m_{\text{GB}}^2} - \frac{\alpha P_L}{p^2 + \alpha m_{\text{GB}}^2} = -\frac{1}{p^2 + m_{\text{GB}}^2} \left(\delta^{\mu\nu} - (1 - \alpha) \frac{p^\mu p^\nu}{p^2 + \alpha m_{\text{GB}}^2} \right),$$

with m_{GB}^2 proportional to $g^2 v^2$. P_T and P_L are associated with the longitudinal and the transversal modes of the gauge bosons. In the following we shall use the Landau gauge ($\alpha \rightarrow 0$) since it simplifies the calculation. This corresponds to massless Goldstone bosons. The unitary gauge on the other hand corresponds to $\alpha \rightarrow \infty$ and thus the Goldstone modes become infinitely heavy and decouple. Including the changes of the gauge-boson propagator in the unitary gauge corresponds to gauge bosons which remove the Goldstone bosons from the spectrum of the theory.

5.2 Flow Equations

In this section we start with the calculation of the fluctuation matrix. Afterwards we calculate the various flow equations. We shall see that there are new contributions due to the gauge fields and the ghost fields. The flow equation of the gauge coupling will not be considered. This is beyond the scope of this work. Thus we compute the flow equations for the effective potential and the Yukawa coupling which depend on the gauge coupling as an external parameter. The equations for the anomalous dimensions will also depend on the gauge coupling.

5.2.1 Fluctuation Matrix and Regulator

At first we can use the Fourier transformation as in Chap.3 and write down the truncation in momentum space. The result reads

$$\begin{aligned}
 \Gamma_k = & \int d^d x U_k(\rho) + \int \frac{d^d p}{(2\pi)^d} \left\{ \frac{Z_\phi p^2}{2} (\phi_1^a(p) \phi_1^a(-p) + \phi_2^a(p) \phi_2^a(-p)) - Z_L \bar{\psi}_L^a \not{p} \psi_L^a \right. \\
 & - Z_R \bar{\psi}_R \not{p} \psi_R + \frac{Z_F}{2} W_\mu^i(p) \left(p^2 \delta^{\mu\nu} - p_\mu p_\nu \left(a - \frac{Z_\phi}{\alpha Z_F} \right) \right) - \bar{c}^i(p) p^2 c^i(p) \\
 & + \int \frac{d^d q}{(2\pi)^d} [i g \bar{c}^i(p) q_\mu W_\mu^k(q) f^{ikj} c^j(p-q) - 2\alpha v g^2 \bar{c}^i(p) T_{Na}^i T_{ab}^i \phi^b(q) c^j(p-q)] \\
 & + \int \frac{d^d q}{(2\pi)^d} \bar{h}_k [\bar{\psi}_R(p) \phi^{a\dagger}(p-q) \psi_L^a(q) - \bar{\psi}_L^a(p) \phi^a(p-q) \psi_R(q)] \\
 & + \int \frac{d^d q}{(2\pi)^d} Z_L g \bar{\psi}_L^a(p) W^i(q) T_{ab}^i \psi_L(p-q) \\
 & + \int \frac{d^d q}{(2\pi)^d} i Z_F g f^{jki} p_\mu W_\nu^i(p) W_\mu^j(q) W_\nu^k(-p-q) \\
 & + \int \frac{d^d q}{(2\pi)^d} \int \frac{d^d r}{(2\pi)^d} \frac{Z_F}{4} g^2 f^{jki} f^{lmi} W_\mu^j(p) W_\nu^k(q) W_\mu^l(r) W_\nu^m(-p-q-r) \\
 & + \int \frac{d^d q}{(2\pi)^d} \int \frac{d^d r}{(2\pi)^d} Z_\phi g^2 W_\mu^i(p) W_\mu^j(q) \phi^{a\dagger}(r) T_{ab}^i T_{bc}^j \phi^c(-p-q-r) \\
 & + Z_\phi v g W_\mu^i(p) \left(p_\mu \phi^{a\dagger}(-p) T_{aN}^i - p_\mu T_{Na}^i \phi^a(-p) \right) \\
 & \left. + \int \frac{d^d q}{(2\pi)^d} Z_\phi g W_\mu^i(p) \left(q_\mu \phi^{a\dagger}(q) T_{ab}^i \phi^b(-p-q) - q_\mu \phi^{a\dagger}(-p-q) T_{ab}^i \phi^b(q) \right) \right\}.
 \end{aligned}$$

Here we neglected terms proportional to α . The first two lines contain the kinetic terms of all fields, the third line contains interactions which include ghost fields, the fourth line includes all Yukawa interactions and the rest represents higher order interaction terms.

Next we have to look at the fluctuation matrix. This was a $(4N_L + 2) \times (4N_L + 2)$ matrix in our first model, see Eq. (3.5). Now the matrix is a $(3N_L^2 + 4N_L - 1) \times (3N_L^2 + 4N_L - 1)$ matrix. It can be given as

$$\begin{pmatrix}
 \Gamma_{\phi_1 \phi_1} & \Gamma_{\phi_1 \phi_2} & \Gamma_{\phi_1 \psi_L} & \Gamma_{\phi_1 \bar{\psi}_L} & \Gamma_{\phi_1 \psi_R} & \Gamma_{\phi_1 \bar{\psi}_R} & \Gamma_{\phi_1 W} & \Gamma_{\phi_1 c} & \Gamma_{\phi_1 \bar{c}} \\
 \Gamma_{\phi_2 \phi_1} & \Gamma_{\phi_2 \phi_2} & \Gamma_{\phi_2 \psi_L} & \Gamma_{\phi_2 \bar{\psi}_L} & \Gamma_{\phi_2 \psi_R} & \Gamma_{\phi_2 \bar{\psi}_R} & \Gamma_{\phi_2 W} & \Gamma_{\phi_2 c} & \Gamma_{\phi_2 \bar{c}} \\
 \Gamma_{\psi_L \phi_1} & \Gamma_{\psi_L \phi_2} & \Gamma_{\psi_L \psi_L} & \Gamma_{\psi_L \bar{\psi}_L} & \Gamma_{\psi_L \psi_R} & \Gamma_{\psi_L \bar{\psi}_R} & \Gamma_{\psi_L W} & \Gamma_{\psi_L c} & \Gamma_{\psi_L \bar{c}} \\
 \Gamma_{\bar{\psi}_L \phi_1} & \Gamma_{\bar{\psi}_L \phi_2} & \Gamma_{\bar{\psi}_L \psi_L} & \Gamma_{\bar{\psi}_L \bar{\psi}_L} & \Gamma_{\bar{\psi}_L \psi_R} & \Gamma_{\bar{\psi}_L \bar{\psi}_R} & \Gamma_{\bar{\psi}_L W} & \Gamma_{\bar{\psi}_L c} & \Gamma_{\bar{\psi}_L \bar{c}} \\
 \Gamma_{\psi_R \phi_1} & \Gamma_{\psi_R \phi_2} & \Gamma_{\psi_R \psi_L} & \Gamma_{\psi_R \bar{\psi}_L} & \Gamma_{\psi_R \psi_R} & \Gamma_{\psi_R \bar{\psi}_R} & \Gamma_{\psi_R W} & \Gamma_{\psi_R c} & \Gamma_{\psi_R \bar{c}} \\
 \Gamma_{\bar{\psi}_R \phi_1} & \Gamma_{\bar{\psi}_R \phi_2} & \Gamma_{\bar{\psi}_R \psi_L} & \Gamma_{\bar{\psi}_R \bar{\psi}_L} & \Gamma_{\bar{\psi}_R \psi_R} & \Gamma_{\bar{\psi}_R \bar{\psi}_R} & \Gamma_{\bar{\psi}_R W} & \Gamma_{\bar{\psi}_R c} & \Gamma_{\bar{\psi}_R \bar{c}} \\
 \Gamma_{W \phi_1} & \Gamma_{W \phi_2} & \Gamma_{W \psi_L} & \Gamma_{W \bar{\psi}_L} & \Gamma_{W \psi_R} & \Gamma_{W \bar{\psi}_R} & \Gamma_{WW} & \Gamma_{Wc} & \Gamma_{W\bar{c}} \\
 \Gamma_{c \phi_1} & \Gamma_{c \phi_2} & \Gamma_{c \psi_L} & \Gamma_{c \bar{\psi}_L} & \Gamma_{c \psi_R} & \Gamma_{c \bar{\psi}_R} & \Gamma_{cW} & \Gamma_{cc} & \Gamma_{c\bar{c}} \\
 \Gamma_{\bar{c} \phi_1} & \Gamma_{\bar{c} \phi_2} & \Gamma_{\bar{c} \psi_L} & \Gamma_{\bar{c} \bar{\psi}_L} & \Gamma_{\bar{c} \psi_R} & \Gamma_{\bar{c} \bar{\psi}_R} & \Gamma_{\bar{c}W} & \Gamma_{\bar{c}c} & \Gamma_{\bar{c}\bar{c}}
 \end{pmatrix}.$$

The relevant parts which differ from the old fluctuation matrix are given in App. B.

Besides the fluctuation matrix we have to look at the regulator. The old regulator matrix, Eq. (3.6), has to be replaced by a bigger matrix containing the parts for the gauge bosons ($R_{k\text{GB}}$) and the ghost fields ($R_{k\text{G}}$):

$$R_k(q, p) = \delta(p - q) \begin{pmatrix} R_{kB} & 0 & 0 & 0 \\ 0 & -R_{kF} & 0 & 0 \\ 0 & 0 & R_{k\text{GB}} & 0 \\ 0 & 0 & 0 & R_{k\text{G}} \end{pmatrix}.$$

As before, the regulators for the bosons and the fermions are given as before by

$$R_{kB} = \begin{pmatrix} Z_{\phi,k} \delta^{ab} p^2 r_{kB}(p) & 0 \\ 0 & Z_{\phi,k} \delta^{ab} p^2 r_{kB}(p) \end{pmatrix}$$

and

$$R_{kF} = \begin{pmatrix} 0 & Z_{L,k} \delta^{ab} \not{p}^T r_{kF}(-p) & 0 & 0 \\ Z_{L,k} \delta^{ab} \not{p} r_{kF}(p) & 0 & 0 & 0 \\ 0 & 0 & 0 & Z_{R,k} \not{p}^T r_{kF}(-p) \\ 0 & 0 & Z_{R,k} \not{p} r_{kF}(p) & 0 \end{pmatrix}.$$

The new parts are given by

$$R_{k\text{G}} = \begin{pmatrix} 0 & p^2 \delta^{ij} r_{k\text{G}}(p) \\ -p^2 \delta^{ij} r_{k\text{G}}(p) & 0 \end{pmatrix}$$

and

$$R_{k\text{GB}} = Z_F(p^2 P_T + \frac{p^2 Z_\phi}{\alpha Z_F} P_L) \delta^{ij} r_{k\text{GB}}(p),$$

with the longitudinal and transversal projectors

$$P_T = \delta^{\mu\nu} - \frac{p^\mu p^\nu}{p^2} \quad \text{and} \quad P_L = \frac{p^\mu p^\nu}{p^2}.$$

These are all ingredients we need to calculate the flow equations.

5.2.2 Flow Equation of the Effective Potential

In this subsection we discuss how the flow equation of the effective potential changes by introducing the gauge field and the ghosts. First of all we have to project our truncation onto the potential. This can be done by expanding around constant bosonic fields and vanishing fermionic, gauge-bosonic and ghost fields.

$$\delta(0) \partial_t U_k = \partial_t \Gamma_k \Big|_{\substack{\psi, W, c=0 \\ \phi=const}} = \frac{1}{2} \text{STr} \left(\frac{\partial_t R_k}{\Gamma_k^{(2)} + R_k} \right) \Big|_{\substack{\psi, W, c=0 \\ \phi=const}}.$$

Using this projection the fluctuation matrix becomes block diagonal. Thus the bosonic part, the fermionic part, the gauge bosonic part and the ghost part can be calculated separately. Since we use the Landau gauge ($\alpha = 0$) the bosonic part and

$$(\partial_t U_k)_G = -(N_L^2 - 1) \text{ (loop diagram with a ghost vertex)} \quad \text{Figure 5.1}$$

Figure 5.1: Ghost contributions to the flow equation of the effective potential.

the fermionic part do not change. The ghost part can be computed very easily and reads

$$(\partial_t U_k)_G = -(N_L^2 - 1) \int \frac{d^d p}{(2\pi)^d} \frac{\partial_t(p^2 r_G)}{P_G(p)}$$

with $P_G(p) = p^2(1 + r_G)$. This corresponds to the graph in Fig. 5.1.

The gauge-boson part is not that trivial. So let us do it step by step. Due to the gauge bosons $\Gamma_k^{(2)} + R_k$ is now given by

$$\begin{aligned} & (\Gamma_k^{(2)} + R_k)_{ij}^{\rho\gamma} \\ &= \delta^{ij} \left[\left(Z_F p^2 P_T + \frac{Z_\phi}{\alpha} p^2 P_L \right) (1 + r_{GB}) + Z_\phi g^2 \delta^{\rho\gamma} \phi^{a\dagger} \{T^i, T^j\}_{ab} \phi^b \right] \delta(p - q) \\ &= \left[\delta^{ij} \left(Z_F p^2 P_T + \frac{Z_\phi}{\alpha} p^2 P_L \right) (1 + r_{GB}) + \delta^{\rho\gamma} \sum_{A=1}^{N_L^2-1} m_A^2 P_A^{ij} \right] \delta(p - q). \end{aligned}$$

Here we diagonalised the matrix $Z_\phi g^2 \phi^{a\dagger} \{T^i, T^j\}_{ab} \phi^b$. Since P_A, P_T and P_L are projectors we can write down the inverse as

$$\begin{aligned} & \left((\Gamma_k^{(2)} + R_k)_{ij}^{\rho\gamma} \right)^{-1} \\ &= \delta(p - q) \sum_A P_A^{ij} \left[P_T^{\rho\gamma} \frac{1}{Z_F p^2 (1 + r_{GB}) + m_A^2} + P_L^{\rho\gamma} \frac{1}{\frac{Z_\phi}{\alpha} p^2 (1 + r_{GB}) + m_A^2} \right]. \end{aligned}$$

Using $\text{Tr}_{\rho\gamma} P_T = d - 1$, $\text{Tr}_{\rho\gamma} P_L = 1$ and $\text{Tr}_{ij} P_A^{ij} = 1$ we get the gauge bosonic part of the flow equation of the effective potential as

$$(\partial_t U_k)_{GB} = \frac{1}{2} \int \frac{d^d p}{(2\pi)^d} \sum_A \left[\frac{(d-1) \partial_t (Z_F p^2 r_{GB})}{Z_F p^2 (1 + r_{GB}) + m_A^2} + \frac{\partial_t \left(\frac{Z_\phi}{\alpha} p^2 r_{GB} \right)}{\frac{Z_\phi}{\alpha} p^2 (1 + r_{GB}) + m_A^2} \right].$$

The graphical interpretation of this equation is given in Fig. 5.2. Here we combined all longitudinal and transversal modes of all gauge bosons in one loop diagram.

Altogether we have the following flow equation for the effective potential:

$$\begin{aligned} \partial_t U_k = & v_d k^d 2 \left[(2N_L - 1) l_0^d \left(\frac{U'_k}{Z_\phi k^2} \right) + l_0^d \left(\frac{U'_k + 2\rho U''_k}{Z_\phi k^2} \right) \right] \\ & - d_\gamma v_d k^d 2 \left[(N_L - 1) l_{0L}^{(F)d}(0) + l_{0L}^{(F)d} \left(\frac{\rho \bar{h}_k^2}{k^2 Z_L Z_R} \right) + l_{0R}^{(F)d} \left(\frac{\rho \bar{h}_k^2}{k^2 Z_L Z_R} \right) \right] \\ & + \frac{1}{2} \sum_A \int \frac{d^d p}{(2\pi)^d} \left[(d-1) \frac{\partial_t (Z_F p^2 r_{GB}(p))}{Z_F P_{GB}(p) + m_A^2} + \frac{\partial_t (Z_\phi p^2 r_{GB}(p))}{Z_\phi P_{GB}(p) + \alpha m_A^2} \right] \\ & - (N_L^2 - 1) \int \frac{d^d p}{(2\pi)^d} \frac{p^2 \partial_t r_G(p)}{P_G(p)}. \end{aligned}$$

We introduced $P_G = p^2(1 + r_G)$ and $P_{GB} = p^2(1 + r_{GB})$. Rewriting this equation by using the threshold functions as defined in App. C leads to

$$\begin{aligned} \partial_t U_k = & v_d k^d 2 \left[(2N_L - 1) l_0^d \left(\frac{U'_k}{Z_\phi k^2} \right) + l_0^d \left(\frac{U'_k + 2\rho U''_k}{Z_\phi k^2} \right) \right] \\ & - d_\gamma v_d k^d 2 \left[(N_L - 1) l_{0L}^{(F)d}(0) + l_{0L}^{(F)d} \left(\frac{\rho \bar{h}_k^2}{k^2 Z_L Z_R} \right) + l_{0R}^{(F)d} \left(\frac{\rho \bar{h}_k^2}{k^2 Z_L Z_R} \right) \right] \\ & + 2v_d k^d \sum_A \left[(d-1) l_{0T}^{(GB)d} \left(\frac{m_A^2}{Z_F k^2} \right) + l_{0L}^{(GB)d} \left(\frac{\alpha m_A^2}{Z_\phi k^2} \right) \right] \\ & - 4v_d k^d (N_L^2 - 1) l_0^{(G)d}(0). \end{aligned}$$

The last step is to introduce dimensionless quantities and use the specific regulators as discussed in App. C. Using the dimensionless quantities

$$\tilde{\rho} = Z_\phi k^{2-d} \rho, \quad \tilde{h}_k^2 = \frac{k^{d-4} h_k^2}{Z_\phi Z_L Z_R}, \quad \tilde{u}_k = U_k k^{-d}, \quad \tilde{m}_A^2 = \frac{m_A^2}{Z_F k^2}, \quad \tilde{g}^2 = \frac{g^2}{Z_F k^{4-d}}, \quad (5.1)$$

the flow equation for the effective potential reads:

$$\begin{aligned} \partial_t u_k = & -du_k + \tilde{\rho} u'_k (d-2 + \eta_\phi) \\ & + \frac{4v_d}{d} \left[\frac{2N_L - 1}{1 + u'_k} \left(1 - \frac{\eta_\phi}{d+2} \right) + \frac{1}{1 + u'_k + 2\tilde{\rho} u''_k} \left(1 - \frac{\eta_\phi}{d+2} \right) \right] \\ & - d_\gamma \left(1 - \frac{\eta_L}{d+1} \right) \left((N_L - 1) + \frac{1}{1 + \tilde{\rho} \bar{h}_k^2} \right) + \left(1 - \frac{\eta_R}{d+1} \right) \frac{d_\gamma}{1 + \tilde{\rho} \bar{h}_k^2} \\ & + \frac{4v_d}{d} \sum_A \left[(d-1) \frac{\left(1 - \frac{\eta_F}{d+2} \right)}{(1 + \tilde{m}_A^2)} + \left(1 - \frac{\eta_\phi}{d+2} \right) \right] - \frac{8v_d}{d} (N_L^2 - 1). \quad (5.2) \end{aligned}$$

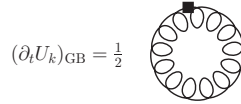


Figure 5.2: Gauge boson contributions to the flow equation of the effective potential.



Figure 5.3: New contributions to the flow equation of the Yukawa coupling.

5.2.3 Flow Equation of the Yukawa Coupling

Next we derive the flow equation for the Yukawa coupling. Therefore we start as in Chap. 3 by dividing our bosonic field into vacuum expectation value and fluctuations. This time we choose the vacuum expectation value to be in the N_L direction and call it v :

$$\phi(p) = \frac{1}{\sqrt{2}} \begin{pmatrix} \phi_1^1(p) + i\phi_2^1(p) \\ \phi_1^2(p) + i\phi_2^2(p) \\ \vdots \\ \phi_1^{N_L}(p) + i\phi_2^{N_L}(p) \end{pmatrix} = \begin{pmatrix} 0 \\ \vdots \\ 0 \\ v \end{pmatrix} \delta(p) + \frac{1}{\sqrt{2}} \begin{pmatrix} \Delta\phi_1^1(p) + i\Delta\phi_2^1(p) \\ \Delta\phi_1^2(p) + i\Delta\phi_2^2(p) \\ \vdots \\ \Delta\phi_1^{N_L}(p) + i\Delta\phi_2^{N_L}(p) \end{pmatrix}. \quad (5.3)$$

We are again interested in the Yukawa coupling between the radial mode $\Delta\phi_1^{N_L}$ and the fermions. Thus the projection onto the coupling constant \bar{h}_k can be given as

$$\left. \frac{\vec{\delta}}{\delta\bar{\psi}_L^{N_L}(p)} \frac{\sqrt{2}\vec{\delta}}{\delta\Delta\phi_1^{N_L}(p')} \Gamma_k \frac{\overleftarrow{\delta}}{\delta\psi_R(q)} \right|_{\substack{\psi=\Delta\phi=W=c=0 \\ p'=p=q=0}} = -\bar{h}_k \delta(0).$$

Now we can go on as in our first model by dividing $\Gamma_k^{(2)} + R_k$ into the propagator part and the fluctuation part. Expanding the logarithm as in Eq. (3.15) only the third power survives and thus we get

$$\delta(0)\partial_t \bar{h}_k = -\frac{\sqrt{2}}{6} \frac{\vec{\delta}}{\delta\bar{\psi}_L^{N_L}(p)} \frac{\vec{\delta}}{\delta\Delta\phi(p')} \text{STr} \left[\tilde{\partial}_t \left(\frac{\Delta\Gamma_k^{(2)}}{(\Gamma_{k0}^{(2)} + R_k)} \right)^3 \right] \frac{\overleftarrow{\delta}}{\delta\psi_R(q)} \Big|_{\substack{\psi=\Delta\phi=W=c=0 \\ p'=p=q=0}}.$$

The matrix calculations are tedious again but straightforward. The result shows that the old contributions remain unchanged and an additional term occurs. This new term corresponds to the graph in Fig. 5.3. The flow equation reads

$$\begin{aligned}
 \partial_t \bar{h}_k = & - \int \frac{d^d p}{(2\pi)^d} \tilde{\partial}_t \times \\
 & \left[\frac{v \bar{h}^3}{Z_L Z_R P_F(p) + v^2 \bar{h}^2} \left(\frac{v U''}{(Z_\phi P(p) + U')^2} - \frac{3v U'' + 2v^3 U'''}{(Z_\phi P(p) + U' + 2v^2 U'')^2} \right) \right. \\
 & + \frac{v^2 \bar{h}^5}{(Z_L Z_R P_F(p) + v^2 \bar{h}^2)^2} \left(\frac{1}{Z_\phi P(p) + U'} - \frac{1}{Z_\phi P(p) + U' + 2v^2 U''} \right) \\
 & - \frac{\frac{1}{2} \bar{h}^3}{Z_L Z_R P_F(p) + v^2 \bar{h}^2} \left(\frac{1}{Z_\phi P(p) + U'} - \frac{1}{Z_\phi P(p) + U' + 2v^2 U''} \right) \\
 & \left. - \bar{h} \sum_{a=1}^N \sum_{i=1}^{N^2-1} \frac{Z_\phi Z_L Z_R g^2 p^2 d_\gamma (1 + r_{kF}) T_{Na}^i T_{aN}^i}{(Z_\phi P + U')(Z_L Z_R P_F + v^2 \bar{h}^2 \delta^{aN})} \frac{(d-1)}{Z_F P_{GB} + m_i^2} \right].
 \end{aligned}$$

Using the threshold functions defined in App. C and the dimensionless quantities of Eq. (5.1) we get

$$\begin{aligned}
 \partial_t \tilde{h}_k^2 = & (\eta_\phi + \eta_L + \eta_R + d - 4) \tilde{h}_k^2 - 4v_d \tilde{h}_k^4 \times \\
 & [-2\tilde{u}_{k\text{vev}}'' \kappa_k l_{1,2}^{(\text{FB})d} (\kappa_k \tilde{h}_k^2, \tilde{u}_{k\text{vev}}') \\
 & + (6\tilde{u}_{k\text{vev}}'' \kappa_k + 4\tilde{u}_{k\text{vev}}''' \kappa_k^2) l_{1,2}^{(\text{FB})d} (\kappa_k \tilde{h}_k^2, \tilde{u}_{k\text{vev}}' + 2\tilde{u}_{k\text{vev}}'' \kappa_k) \\
 & + l_{1,1}^{(\text{FB})d} (\kappa_k \tilde{h}_k^2, \tilde{u}_{k\text{vev}}') \\
 & - l_{1,1}^{(\text{FB})d} (\kappa_k \tilde{h}_k^2, \tilde{u}_{k\text{vev}}' + 2\tilde{u}_{k\text{vev}}'' \kappa_k) \\
 & - 2\kappa_k \tilde{h}_k^2 l_{2,1}^{(\text{FB})d} (\kappa_k \tilde{h}_k^2, \tilde{u}_{k\text{vev}}') \\
 & + 2\kappa_k \tilde{h}_k^2 l_{2,1}^{(\text{FB})d} (\kappa_k \tilde{h}_k^2, \tilde{u}_{k\text{vev}}' + 2\tilde{u}_{k\text{vev}}'' \kappa_k)] \\
 & - \tilde{h}_k^2 \sum_{a=1}^N \sum_{i=1}^{N^2-1} \tilde{g}^2 d_\gamma T_{Na}^i T_{aN}^i (d-1) 8v_d m_{1,1}^{(\text{FBE})} (\tilde{u}', \kappa \tilde{h}_k^2 \delta^{aN}, \tilde{m}_i^2), \quad (5.4)
 \end{aligned}$$

where we used $\kappa = \tilde{\rho}(\rho = v^2)$. We use this flow equation for our fixed-point analysis in the subsequent section.

5.2.4 Anomalous Dimensions

Finally we have to derive the equations for the anomalous dimensions. We start with the bosonic anomalous dimension. The projection onto the wave-function renormalisation is given by

$$\delta(0) \partial_t Z_\phi = \frac{\partial}{\partial(p'^2)} \frac{\delta}{\delta \Delta \phi(p')} \frac{\delta}{\delta \Delta \phi(q')} \frac{-1}{4} \text{STr} \left[\tilde{\partial}_t \left(\frac{\Delta \Gamma_k^{(2)}}{\Gamma_{k,0}^{(2)} + R_k} \right)^2 \right] \Bigg|_{\substack{\Delta \phi = \psi = W = c = 0 \\ p' = q' = 0}},$$

where we divided the bosonic field as in Eq. (5.3) into its vacuum expectation value and the fluctuations. We also expanded the logarithm and this time the second power is the only one which survives the projection. The matrix calculation is straightforward and the only thing we have to care about are the momenta as in

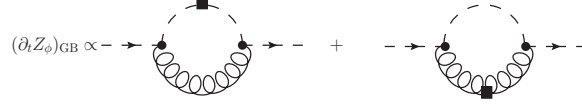


Figure 5.4: New contributions to the bosonic anomalous dimension.

Eq. (3.18). A calculation similar to that of Subsec. 3.2.4 leads to the bosonic part and the fermionic part as in our first model and contains a gauge bosonic part which reads

$$\begin{aligned}
 (\partial_t Z_{\phi,k})_{\text{GB}} = & -\frac{1}{d} \int \frac{d^d p}{(2\pi)^d} \tilde{\partial}_t \left\{ \frac{Z_\phi^2 g^2}{2} \sum_{a=1}^N \sum_{i=1}^{N^2-1} T_{Na}^i T_{aN}^i \left[\frac{2d}{(Z_\phi P_B + U')(Z_F P_{\text{GB}} + m_i^2)} \right. \right. \\
 & \left. \left. + \frac{12p^2 Z_F \frac{\partial}{\partial p^2} P_{\text{GB}}}{(Z_\phi P_B + U')(Z_F P_{\text{GB}} + m_i^2)^2} - \frac{4p^4 Z_\phi Z_F \left(\frac{\partial}{\partial p^2} P_B \right) \left(\frac{\partial}{\partial p^2} P_{\text{GB}} \right)}{(Z_\phi P_B + U')^2 (Z_F P_{\text{GB}} + m_i^2)^2} \right] \right\}.
 \end{aligned}$$

This new contribution can be interpreted graphically as in Fig. 5.4. Introducing the threshold functions defined in App. C and switching to dimensionless quantities leads to

$$\begin{aligned}
 \eta_\phi = & \frac{4v_d}{d} (18\tilde{u}''^2 \kappa_k + 24\tilde{u}''\tilde{u}''' \kappa_k^2 + 8\tilde{u}'''^2 \kappa_k^3) m_{22}^d (\tilde{u}' + 2\kappa_k \tilde{u}'') \\
 & + \frac{(2N_L - 1)8v_d}{d} \kappa_k \tilde{u}''^2 m_{22}^d (\tilde{u}') \\
 & + \frac{8v_d d_\gamma}{d} \tilde{h}_k^2 m_4^{(F)d} (\kappa_k \tilde{h}_k^2) - \frac{8v_d d_\gamma}{d} \kappa_k \tilde{h}_k^4 m_2^{(F)d} (\kappa_k \tilde{h}_k^2) \\
 & - \frac{8v_d}{d} \tilde{g}^2 \sum_{a=1}^N \sum_{i=1}^{N^2-1} T_{Na}^i T_{aN}^i \times \\
 & \left[dl_{1,1}^{(\text{BGB})d}(\tilde{u}', \tilde{m}_i^2) + 3m_{1,2}^{(\text{BGB})d}(\tilde{u}', \tilde{m}_i^2) - m_4^{(\text{BGB})d}(\tilde{u}', \tilde{m}_i^2) \right]. \quad (5.5)
 \end{aligned}$$

The calculation for the anomalous dimension of the left-handed fermion can be performed along the lines to the one for our first model. We split the bosonic field into the vacuum expectation value and fluctuations. The projection then reads

$$\delta(0) \partial_t Z_L = \frac{1}{4dd_\gamma} \text{tr} \gamma_\mu \frac{\partial}{\partial p'_\mu} \frac{\vec{\delta}}{\delta \psi_L^N(p')} \text{STr} \left[\tilde{\partial}_t \left(\frac{\Delta \Gamma_k^{(2)}}{\Gamma_{k0}^{(2)} + R_k} \right)^2 \right] \frac{\overleftarrow{\delta}}{\delta \psi_L^N(q')} \Big|_{\substack{\Delta \phi = \psi = W = c = 0 \\ p' = q' = 0}},$$

where we expanded the logarithm and only keep the second order since all other orders do not survive the projection. The matrix calculation is straightforward and the momenta have to be treated as in our first model. We find the same terms as in

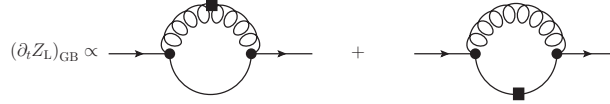


Figure 5.5: Gauge-bosonic contributions to the equation for the left-handed fermionic anomalous dimension.

Chap. 3 and one additional term for the gauge bosons. This new part reads

$$(\partial_t Z_{L,k})_{\text{GB}} = \int \frac{d^d p}{(2\pi)^d} p^2 \tilde{\partial}_t \left[-2d_\gamma Z_L^2 g^2 \sum_{a=1}^N \sum_{i=1}^{N^2-1} T_{aN}^i T_{Na}^i \frac{Z_R(1+r_F)}{Z_L Z_R P_F + \delta^{aN} v^2 h_k^2} \frac{Z_F \frac{\partial}{\partial p^2} P_{\text{GB}}}{(Z_F P_{\text{GB}} + m_i^2)^2} \right].$$

This can be interpreted graphically as shown in Fig. 5.5. The threshold functions and the dimensionless quantities enable us to write this equation in a compact notation:

$$\begin{aligned} \eta_L = & \frac{8v_d}{d} \tilde{h}_k^2 \left[m_{12}^{(\text{FB})d} (\tilde{h}_k^2 \kappa_k, \tilde{u}' + 2\kappa_k \tilde{u}'') + m_{12}^{(\text{FB})d} (\tilde{h}_k^2 \kappa_k, \tilde{u}') \right] \\ & - 8v_d d_\gamma \tilde{g}^2 \sum_{a=1}^N \sum_{i=1}^{N^2-1} T_{aN}^i T_{Na}^i m_{1,2}^{(\text{FGB})d} (\delta^{aN} \kappa_k h_k^2, \tilde{m}_i^2). \end{aligned} \quad (5.6)$$

Since the right-handed fermions do not couple to the gauge bosons the equation for the right-handed anomalous dimension does not change:

$$\begin{aligned} \eta_R = & \frac{8v_d}{d} h_k^2 [m_{12}^{(\text{FB})d} (h_k^2 \kappa_k, u'_{\text{kvev}} + 2\kappa_k u''_{\text{kvev}}) + m_{12}^{(\text{FB})d} (h_k^2 \kappa_k, u'_{\text{kvev}}) \\ & + 2(N_L - 1) m_{12}^{(\text{FB})d} (0, u'_{\text{kvev}})]. \end{aligned} \quad (5.7)$$

Thus we are equipped with all equations we need to turn to the analysis of possible fixed points.

5.3 Fixed-Point Analysis for $N_L = 2$

The flow equations are much more involved compared to Chap. 3. Thus we are not able to solve the equations analytically. The numerical method requires a suitable starting point. There was no acceptable fixed point in the system without gauge bosons in the symmetric regime which we could use as a starting point. Therefore we restrict ourselves to the regime of spontaneous symmetry breaking for the investigations in this section. We can use the flow equation of the effective potential, Eq. (5.2), to derive the flow equations for the vacuum expectation value κ_k and the bosonic self-interactions λ_i . Together with the flow equation for the Yukawa coupling, Eq. (5.4), and the equations for the anomalous dimensions, Eqs. (5.5), (5.6)

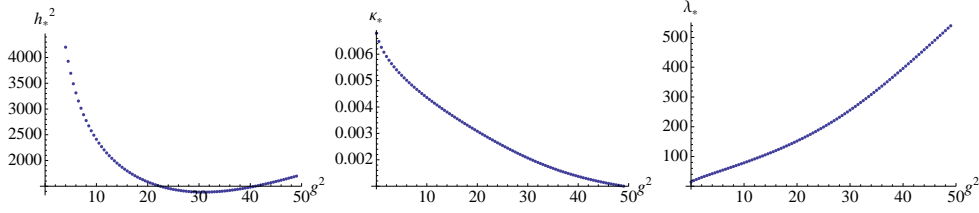


Figure 5.6: Fixed-point values of h^2 , κ_k and λ depending on the gauge coupling g^2 which is used as an external parameter.

and (5.7), we get a large system of coupled nonlinear equations. Nevertheless a numerical solution of the system is possible. We shall use the leading order fixed points of Chap. 3 as a starting point for the Newton method.

A detailed analysis of the fixed-point structure is beyond the scope of this work and thus we concentrate on the special case $N_L = 2$. Therefore our model includes three Goldstone bosons which are removed from the spectrum of the theory by three gauge bosons. These three gauge bosons acquire a mass. We start with an investigation of the leading order derivative expansion. Truncating our polynomial expansion of the effective potential at λ_2 leads to the following nonlinear system of equations:

$$\begin{aligned}\beta_h &= \partial_t h^2(h^2, \kappa_k, \lambda, g^2) = 0 \\ \beta_\kappa &= \partial_t \kappa_k(h^2, \kappa_k, \lambda, g^2) = 0 \\ \beta_\lambda &= \partial_t \lambda(h^2, \kappa_k, \lambda, g^2) = 0.\end{aligned}$$

Here the gauge coupling g^2 serves as another external parameter, besides N_L , which has to be chosen by hand. For $g^2 = 0$ this is the system of Chap. 3 and the results are the same. There was exactly one fixed point for $N_L = 2$. Varying the gauge coupling g^2 leads to a changed fixed point as depicted in Fig. 5.6. One can see that the very high fixed-point value of h^2 which was caused by the Goldstone contributions is lowered by the gauge boson contributions. This helps us to get a fixed point in next to leading order which was not possible up to now.

We use the leading order fixed-point values which depend on g^2 as a starting point and use the Newton method. The results for h^2 , κ and λ of the full system including

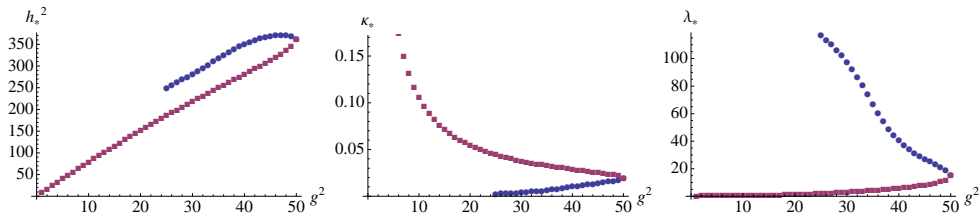


Figure 5.7: Fixed-point values of h^2 , κ_k and λ depending on the gauge coupling g^2 , used as an external parameter, in next to leading order.

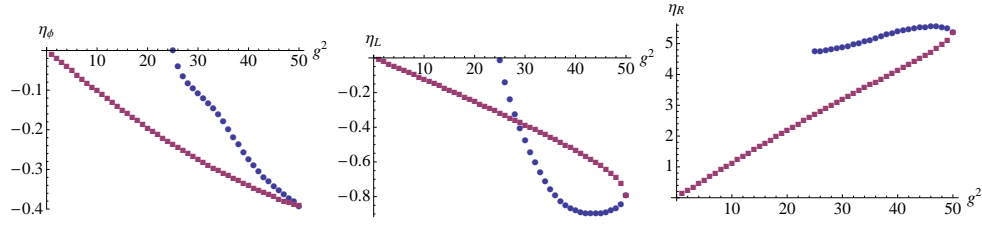


Figure 5.8: Fixed-point values of h^2 , κ_k and λ depending on the gauge coupling g^2 which is used as an external parameter.

the anomalous dimensions η_ϕ, η_L and η_R and neglecting η_F are given in Fig. 5.7. The corresponding values of the anomalous dimensions are depicted in Fig. 5.8. Note that the value of the anomalous dimension of the right-handed fermions η_R is two orders of magnitude smaller than the value of Chap. 3 (see Fig. 3.9). The fixed-point values marked by red squares can be obtained as follows: One starts with the leading order fixed point for $g^2 = 20$ and the result of the Newton method is the next to leading order fixed point for $g^2 = 20$. This one can be used as a new starting point with a slightly changed value of g^2 and so on. Iterating this procedure provides us with the fixed points depicted in Fig. 5.7 (red squares). The fixed points marked by the blue circles result by the same procedure with the leading order starting point at $25 \leq g^2 \leq 32$ or $g^2 = 41$.

Using these fixed-point values we can calculate the critical exponents along the line to Chap. 3. The results for the blue labelled fixed points for $25 < g^2 < 50$ are depicted in Fig. 5.9. Note that there is only one positive critical exponent corresponding to one relevant direction. Thus our system again is predictive. We can construct an asymptotic safety scenario which solves the triviality problem by construction. For some values of g^2 also the hierarchy problem is weakened since the largest critical exponent is smaller than two.

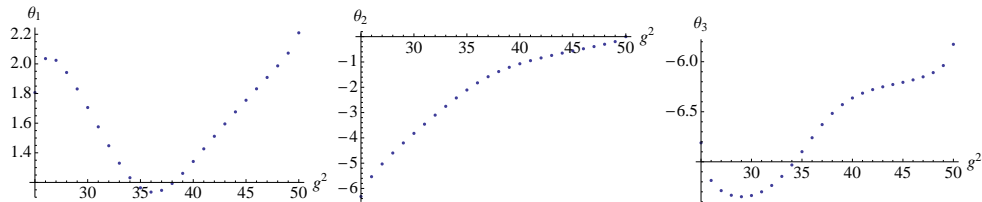


Figure 5.9: Critical exponents θ^I depending on the external parameter g^2 .

Chapter 6

Conclusion and Outlook

We have studied three different Yukawa models with the aid of the Wetterich equation. This work is based on a work about simple Yukawa systems [26]. The model containing one real bosonic field and one left-handed and one right-handed fermion, was extended by replacing the real bosonic field by a N_L -component, complex bosonic field. Furthermore the left-handed fermion was replaced by a N_L -component, left-handed fermion. The following left-right asymmetry allowed a balancing of bosonic and fermion contributions to the flow equations. This system can be seen as a toy model which mimics the Higgs sector of the Standard Model.

This toy model was investigated in leading order derivative expansion. In the symmetric regime there was no reliable fixed point. Nevertheless there were fixed points in the spontaneously symmetry broken regime. We found one reliable fixed point for $N_L < 4$. For $3 < N_L < 30$ there was a second fixed point besides the one which already exists for $N_L < 4$. For $N_L > 29$ there was either one or none fixed point. The calculation of the critical exponents showed that there are two positive critical exponents for the fixed point which already exists for $N_L < 4$. These critical exponents correspond to two relevant directions. The other fixed point only has one positive critical exponent and thus only one relevant direction. We constructed an asymptotic safety scenario with one relevant and two irrelevant directions for $N_L = 10$ as an example. The corresponding fixed point is stable under extension of the effective potential to higher orders in the polynomial expansion. Fixing the vacuum expectation value of the bosonic field to $v = 246\text{GeV}$ provided us with predictions for the top mass ($m_{\text{top}} = 5.78v$) and the Higgs mass ($m_{\text{Higgs}} = 0.97v$) of our toy model. In next to leading order we were not able to find fixed points. There are contributions of the Goldstone bosons to the flow equations which prevent the extension to next to leading order. Nevertheless the balancing due to the left-right asymmetry worked. Furthermore Goldstone bosons are not included in the Standard Model Higgs sector. They are typical for our toy model. This "failure" might be circumvented by including gauge degrees of freedom.

Our model not only resembles the Standard Model Higgs sector but also has similarities with three-dimensional models like the Nambu-Jona-Lasinio model. We investigated the $U(N_L)_L \otimes U(1)_R \otimes \mathcal{P} \otimes \mathcal{C} \otimes \mathcal{T}$ symmetry in three dimensions and classified all possible four-fermion-interaction terms. We found that there are one

scalar condensation channel, two pseudo-scalar channels, two vector-boson channels and one pseudo-vector-boson channel. The scalar channel is similar to the Standard Model Higgs scalar. Thus the three-dimensional model is connected to the previous Standard Model like system by Hubbard-Stratonovich transformation. Nevertheless the fixed-point behaviour of this system is totally different from the four-dimensional model. This time there is a next to leading order fixed point in the symmetric regime for $N_L \in \{1, 2\}$. Furthermore we found fixed points for $N_L > 2$ in the spontaneously symmetry broken regime. As in the four-dimensional model the fixed points are stable under extension of the effective potential to higher orders in the polynomial expansion. The model exhibits a second order phase transition from the symmetric to the spontaneously symmetry broken phase similar to the well known phase transition of the Nambu-Jona-Lasinio model. The critical behaviour at this phase transition is characterised by the critical exponents. The results show that the critical exponents are comparable with those of the $O(2N_L)$ model. This model corresponds to our model with vanishing Yukawa coupling. The difference of the critical exponents due to the fermionic contributions is rather small.

After this short side trip to the three-dimensional fermionic models we turned our attention back to the toy model which mimics the Higgs sector of the Standard Model. Since the Goldstone bosons prevented an asymptotic safety scenario in next to leading order derivative expansion we included gauge fields in our model. These new fields should remove the troublesome Goldstone bosons from the spectrum of the theory. We derived the flow equations and restricted ourselves to the spontaneously symmetry broken regime. Increasing the gauge coupling g as an external parameter leads to a decreasing of the troublesome, high fixed-point value of the Yukawa coupling in leading order derivative expansion. This enabled us to use the Newton method and find two different types of fixed points in next to leading order. For $25 < g^2 < 50$ the critical exponents of one type of fixed points corresponds to one relevant and otherwise irrelevant directions. Thus we can construct an asymptotic safety scenario which solves the triviality problem by construction. The hierarchy problem is weakened for those g^2 values where the highest critical exponent is smaller than two. Furthermore the theory is predictive since there is only one physical parameter which has to be fixed by experiment, namely the one which corresponds to the relevant direction.

Nevertheless there are still some unresolved questions which should be considered in future work. First of all the stability of the fixed points during the extension of the effective potential to higher orders of polynomial expansion should be investigated. Also the dependence of the fixed points on the number of left-handed fermions should be studied. The anomalous dimension of the right-handed fermion is larger than one ($\eta_R \sim 5$). It is not clear if this is special for our model or a problem of principle and should be considered in future work. Furthermore predictions of the theory for the Higgs mass should be calculated and compared to the results of the four-dimensional model without gauge bosons.

Appendix A

Fluctuation Matrix

The different parts of the fluctuation matrix read (primes denote ρ derivatives)

$$\begin{aligned}
(\Gamma_{\phi_1\phi_1})_{ab} &= \frac{\overrightarrow{\delta}}{\delta\phi_1^a(-p)} \Gamma_k \frac{\overleftarrow{\delta}}{\delta\phi_1^b(q)} = Z_{\phi,k} q^2 \delta^{ab} \delta(p-q) \\
&\quad + \int d^d x e^{ix(q-p)} [\delta^{ab} U'_k + U''_k \phi_1^a(x) \phi_1^b(x)], \\
(\Gamma_{\phi_1\phi_2})_{ab} &= \frac{\overrightarrow{\delta}}{\delta\phi_1^a(-p)} \Gamma_k \frac{\overleftarrow{\delta}}{\delta\phi_2^b(q)} = \int d^d x U''_k e^{ix(q-p)} \phi_1^a(x) \phi_2^b(x) = (\Gamma_{\phi_2\phi_1})_{ba}, \\
(\Gamma_{\phi_2\phi_2})_{ab} &= \frac{\overrightarrow{\delta}}{\delta\phi_2^a(-p)} \Gamma_k \frac{\overleftarrow{\delta}}{\delta\phi_2^b(q)} = Z_{\phi,k} q^2 \delta^{ab} \delta(p-q), \\
(\Gamma_{\phi_1\psi_L})_{ab} &= \frac{\overrightarrow{\delta}}{\delta\phi_1^a(-p)} \Gamma_k \frac{\overleftarrow{\delta}}{\delta\psi_L^b(q)} = \frac{h_k}{\sqrt{2}} \delta^{ab} \bar{\psi}_R(q-p), \\
(\Gamma_{\phi_1\bar{\psi}_L})_{ab} &= \frac{\overrightarrow{\delta}}{\delta\phi_1^a(-p)} \Gamma_k \frac{\overleftarrow{\delta}}{\delta\bar{\psi}_L^b(-q)} = \frac{h_k}{\sqrt{2}} \delta^{ab} \psi_R^T(p-q), \\
(\Gamma_{\phi_1\psi_R})_a &= \frac{\overrightarrow{\delta}}{\delta\phi_1^a(-p)} \Gamma_k \frac{\overleftarrow{\delta}}{\delta\psi_R(q)} = -\frac{h_k}{\sqrt{2}} \bar{\psi}_L^a(q-p), \\
(\Gamma_{\phi_1\bar{\psi}_R})_a &= \frac{\overrightarrow{\delta}}{\delta\phi_1^a(-p)} \Gamma_k \frac{\overleftarrow{\delta}}{\delta\bar{\psi}_R(-q)} = -\frac{h_k}{\sqrt{2}} \psi_L^{aT}(p-q), \\
&\quad + \int d^d x e^{ix(q-p)} [\delta^{ab} U'_k + U''_k \phi_2^a(x) \phi_2^b(x)], \\
(\Gamma_{\phi_2\psi_L})_{ab} &= \frac{\overrightarrow{\delta}}{\delta\phi_2^a(-p)} \Gamma_k \frac{\overleftarrow{\delta}}{\delta\psi_L^b(q)} = -i \frac{h_k}{\sqrt{2}} \delta^{ab} \bar{\psi}_R(q-p), \\
(\Gamma_{\phi_2\bar{\psi}_L})_{ab} &= \frac{\overrightarrow{\delta}}{\delta\phi_2^a(-p)} \Gamma_k \frac{\overleftarrow{\delta}}{\delta\bar{\psi}_L^b(-q)} = i \frac{h_k}{\sqrt{2}} \delta^{ab} \psi_R^T(p-q), \\
(\Gamma_{\phi_2\psi_R})_a &= \frac{\overrightarrow{\delta}}{\delta\phi_2^a(-p)} \Gamma_k \frac{\overleftarrow{\delta}}{\delta\psi_R(q)} = -i \frac{h_k}{\sqrt{2}} \bar{\psi}_L^a(q-p),
\end{aligned}$$

$$\begin{aligned}
 (\Gamma_{\phi_2 \bar{\psi}_R})_a &= \frac{\overrightarrow{\delta}}{\delta \phi_2^a(-p)} \Gamma_k \frac{\overleftarrow{\delta}}{\delta \bar{\psi}_R^T(-q)} = i \frac{h_k}{\sqrt{2}} \psi_L^{aT}(p-q), \\
 (\Gamma_{\psi_L \phi_1})_{ab} &= \frac{\overrightarrow{\delta}}{\delta \psi_L^{aT}(-p)} \Gamma_k \frac{\overleftarrow{\delta}}{\delta \phi_1^b(q)} = -\frac{h_k}{\sqrt{2}} \delta^{ab} \bar{\psi}_R^T(q-p), \\
 (\Gamma_{\psi_L \phi_2})_{ab} &= \frac{\overrightarrow{\delta}}{\delta \psi_L^{aT}(-p)} \Gamma_k \frac{\overleftarrow{\delta}}{\delta \phi_2^b(q)} = i \frac{h_k}{\sqrt{2}} \delta^{ab} \bar{\psi}_R^T(q-p), \\
 (\Gamma_{\psi_L \bar{\psi}_L})_{ab} &= \frac{\overrightarrow{\delta}}{\delta \psi_L^{aT}(-p)} \Gamma_k \frac{\overleftarrow{\delta}}{\delta \bar{\psi}_L^{bT}(-q)} = -Z_{L,k} \delta^{ab} \not{q}^T \delta(p-q), \\
 (\Gamma_{\psi_L \bar{\psi}_R})_a &= \frac{\overrightarrow{\delta}}{\delta \psi_L^{aT}(-p)} \Gamma_k \frac{\overleftarrow{\delta}}{\delta \bar{\psi}_R^T(-q)} = -h_k \phi^{a\dagger}(p-q), \\
 (\Gamma_{\bar{\psi}_L \phi_1})_{ab} &= \frac{\overrightarrow{\delta}}{\delta \bar{\psi}_L^a(p)} \Gamma_k \frac{\overleftarrow{\delta}}{\delta \phi_1^b(q)} = -\frac{h_k}{\sqrt{2}} \delta^{ab} \psi_R(p-q), \\
 (\Gamma_{\bar{\psi}_L \phi_2})_{ab} &= \frac{\overrightarrow{\delta}}{\delta \bar{\psi}_L^a(p)} \Gamma_k \frac{\overleftarrow{\delta}}{\delta \phi_2^b(q)} = -i \frac{h_k}{\sqrt{2}} \delta^{ab} \psi_R(p-q), \\
 (\Gamma_{\bar{\psi}_L \psi_L})_{ab} &= \frac{\overrightarrow{\delta}}{\delta \bar{\psi}_L^a(p)} \Gamma_k \frac{\overleftarrow{\delta}}{\delta \psi_L^b(q)} = -Z_{L,k} \delta^{ab} \not{q} \delta(p-q), \\
 (\Gamma_{\bar{\psi}_L \psi_R})_a &= \frac{\overrightarrow{\delta}}{\delta \bar{\psi}_L^a(p)} \Gamma_k \frac{\overleftarrow{\delta}}{\delta \psi_R(q)} = -h_k \phi^a(p-q), \\
 (\Gamma_{\psi_R \phi_1})_a &= \frac{\overrightarrow{\delta}}{\delta \psi_R^T(-p)} \Gamma_k \frac{\overleftarrow{\delta}}{\delta \phi_1^a(q)} = \frac{h_k}{\sqrt{2}} \bar{\psi}_L^{aT}(q-p), \\
 (\Gamma_{\psi_R \phi_2})_a &= \frac{\overrightarrow{\delta}}{\delta \psi_R^T(-p)} \Gamma_k \frac{\overleftarrow{\delta}}{\delta \phi_2^a(q)} = i \frac{h_k}{\sqrt{2}} \bar{\psi}_L^{aT}(q-p), \\
 (\Gamma_{\psi_R \bar{\psi}_L})_a &= \frac{\overrightarrow{\delta}}{\delta \psi_R^T(-p)} \Gamma_k \frac{\overleftarrow{\delta}}{\delta \bar{\psi}_L^{aT}(-q)} = h_k \phi^a(p-q), \\
 \Gamma_{\psi_R \bar{\psi}_R} &= \frac{\overrightarrow{\delta}}{\delta \psi_R^T(-p)} \Gamma_k \frac{\overleftarrow{\delta}}{\delta \bar{\psi}_R^T(-q)} = -Z_{R,k} \not{q}^T \delta(p-q), \\
 (\Gamma_{\bar{\psi}_R \phi_1})_a &= \frac{\overrightarrow{\delta}}{\delta \bar{\psi}_R(p)} \Gamma_k \frac{\overleftarrow{\delta}}{\delta \phi_1^a(q)} = \frac{h_k}{\sqrt{2}} \psi_L^a(p-q), \\
 (\Gamma_{\bar{\psi}_R \phi_2})_a &= \frac{\overrightarrow{\delta}}{\delta \bar{\psi}_R(p)} \Gamma_k \frac{\overleftarrow{\delta}}{\delta \phi_2^a(q)} = -i \frac{h_k}{\sqrt{2}} \psi_L^a(p-q), \\
 (\Gamma_{\bar{\psi}_R \psi_L})_a &= \frac{\overrightarrow{\delta}}{\delta \bar{\psi}_R(p)} \Gamma_k \frac{\overleftarrow{\delta}}{\delta \psi_L^a(q)} = h_k \phi^{a\dagger}(p-q), \\
 \Gamma_{\bar{\psi}_R \psi_R} &= \frac{\overrightarrow{\delta}}{\delta \bar{\psi}_R(p)} \Gamma_k \frac{\overleftarrow{\delta}}{\delta \psi_R(q)} = -Z_{R,k} \not{q} \delta(p-q).
 \end{aligned}$$

Appendix B

Extended Fluctuation Matrix

The relevant parts of the extended fluctuation matrix which differ from the old one read

$$\begin{aligned}
(\Gamma_{\phi_1\phi_1})_{ab} &= \frac{\overrightarrow{\delta}}{\delta\phi_1^a(-p)}\Gamma_k\frac{\overleftarrow{\delta}}{\delta\phi_1^b(q)} = Z_\phi\alpha v^2 g^2\delta(p-q)(T_{Na}^iT_{bN}^i + T_{Nb}^iT_{aN}^i) \\
&\quad + Z_{\phi,k}q^2\delta^{ab}\delta(p-q) + \int d^d x e^{ix(q-p)}[\delta^{ab}U'_k + U''_k\phi_1^a(x)\phi_1^b(x)], \\
(\Gamma_{\phi_1\phi_2})_{ab} &= \frac{\overrightarrow{\delta}}{\delta\phi_1^a(-p)}\Gamma_k\frac{\overleftarrow{\delta}}{\delta\phi_2^b(q)} = (\Gamma_{\phi_2\phi_1})_{ab} \\
&= \int d^d x U''_k e^{ix(q-p)}\phi_1^a(x)\phi_2^b(x) - iZ_\phi\alpha v^2 g^2\delta(p-q)(T_{Na}^iT_{bN}^i - T_{Nb}^iT_{aN}^i), \\
(\Gamma_{\phi_2\phi_2})_{ab} &= \frac{\overrightarrow{\delta}}{\delta\phi_2^a(-p)}\Gamma_k\frac{\overleftarrow{\delta}}{\delta\phi_2^b(q)} = Z_\phi\alpha v^2 g^2\delta(p-q)(T_{Na}^iT_{bN}^i + T_{Nb}^iT_{aN}^i) \\
&\quad + Z_\phi q^2\delta^{ab}\delta(p-q) + \int d^d x e^{ix(q-p)}[\delta^{ab}U'_k + U''_k\phi_2^a(x)\phi_2^b(x)], \\
(\Gamma_{\phi_1 W})_{ai}^\rho &= \frac{\overrightarrow{\delta}}{\delta\phi_1^a(-p)}\Gamma_k\frac{\overleftarrow{\delta}}{\delta W_\rho^i(q)} = -\frac{Z_\phi}{\sqrt{2}}vgq^\rho\delta(p-q)(T_{Na}^i - T_{aN}^i) \\
&\quad + \frac{Z_\phi g}{\sqrt{2}}\left[(q^\rho - 2p^\rho)T_{ab}^i\phi^b(p-q) + (2p^\rho - q^\rho)\phi^{b\dagger}(p-q)T_{ba}^i\right], \\
(\Gamma_{\phi_2 W})_{ai}^\rho &= \frac{\overrightarrow{\delta}}{\delta\phi_2^a(-p)}\Gamma_k\frac{\overleftarrow{\delta}}{\delta W_\rho^i(q)} = -i\frac{Z_\phi}{\sqrt{2}}vgq^\rho\delta(p-q)(T_{Na}^i + T_{aN}^i) \\
&\quad + \frac{iZ_\phi g}{\sqrt{2}}(2p^\rho - q^\rho)\left[T_{ab}^i\phi^b(p-q) + \phi^{b\dagger}(p-q)T_{ba}^i\right],
\end{aligned}$$

$$\begin{aligned}
 (\Gamma_{W\phi_1})_{ia}^\rho &= \frac{\vec{\delta}}{\delta W_\rho^i(-p)} \Gamma_k \frac{\overleftarrow{\delta}}{\delta \phi_1^a(q)} = \frac{Z_\phi}{\sqrt{2}} v g p^\rho \delta(p-q) (T_{Na}^i - T_{aN}^i) \\
 &\quad + \frac{Z_\phi g}{\sqrt{2}} \left[(2q^\rho - p^\rho) T_{ab}^i \phi^b(p-q) + (p^\rho - 2q^\rho) \phi^{b\dagger}(p-q) T_{ba}^i \right], \\
 (\Gamma_{W\phi_2})_{ia}^\rho &= \frac{\vec{\delta}}{\delta W_\rho^i(-p)} \Gamma_k \frac{\overleftarrow{\delta}}{\delta \phi_2^a(q)} = i \frac{Z_\phi}{\sqrt{2}} v g p^\rho \delta(p-q) (T_{Na}^i + T_{aN}^i) \\
 &\quad + \frac{i Z_\phi g}{\sqrt{2}} (p^\rho - 2q^\rho) \left[T_{ab}^i \phi^b(p-q) + \phi^{b\dagger}(p-q) T_{ba}^i \right], \\
 (\Gamma_{WW})_{ij}^{\rho\gamma} &= \frac{\vec{\delta}}{\delta W_\rho^i(-p)} \Gamma_k \frac{\overleftarrow{\delta}}{\delta W_\gamma^j(q)} = Z_F \delta^{ij} \delta(p-q) \left[p^2 \delta^{\rho\gamma} - p^\rho p^\gamma \left(1 - \frac{Z_\phi}{\alpha Z_F} \right) \right] \\
 &\quad + Z_\phi g^2 \delta^{\rho\gamma} \int \frac{d^d r}{(2\pi)^d} \phi^{a\dagger}(r) \left[T_{ab}^i T_{bc}^j + T_{ab}^j T_{bc}^i \right] \phi^c(p-q-r), \\
 (\Gamma_{c\bar{c}})_{ij} &= \frac{\vec{\delta}}{\delta c^{iT}(-p)} \Gamma_k \frac{\overleftarrow{\delta}}{\delta \bar{c}^{jT}(-q)} = p^2 \delta^{ij} \delta(p-q) + 2\alpha v g^2 T_{Na}^j T_{ab}^i \phi^b(p-q), \\
 (\Gamma_{\bar{c}c})_{ij} &= \frac{\vec{\delta}}{\delta \bar{c}^i(p)} \Gamma_k \frac{\overleftarrow{\delta}}{\delta c^j(q)} = -p^2 \delta^{ij} \delta(p-q) - 2\alpha v g^2 T_{Na}^i T_{ab}^j \phi^b(p-q), \\
 (\Gamma_{W\psi_L})_{ia} &= \frac{\vec{\delta}}{\delta W_\rho^i(-p)} \Gamma_k \frac{\overleftarrow{\delta}}{\delta \psi_L^a(q)} = -Z_L g \bar{\psi}_L^{bT}(q-p) \gamma_\rho T_{ba}^i.
 \end{aligned}$$

Appendix C

Threshold Functions

For a compact notation we use the so-called threshold functions. For comparison see [31, 37, 39]. We use $P_B(p) = p^2(1 + r_{kB}(p))$, $P_F(p) = p^2(1 + r_{kF}(p))^2$ and $v_d^{-1} = 2^{d+1}\pi^{d/2}\Gamma(d/2)$. For the calculation of the flow equations, we use the following threshold integrals:

$$\begin{aligned}
l_n^d(\omega) &= \frac{n + \delta_{n,0}}{4} v_d^{-1} k^{2n-d} \int \frac{d^d p}{(2\pi)^d} \times \\
&\quad \left[\left(\frac{1}{Z_{\phi,k}} \partial_t R_k(p) \right) (P_B(p) + \omega k^2)^{-(n+1)} \right], \\
l_{n,L/R}^{(F)d}(\omega) &= \frac{n + \delta_{n,0}}{2} v_d^{-1} k^{2n-d} \int \frac{d^d p}{(2\pi)^d} \times \\
&\quad \left[\frac{P_F(p)}{1 + r_{kF}(p)} \left(\frac{1}{Z_{L,k}} \partial_t (Z_{L,k} r_{kF}) \right) (P_F(p) + \omega k^2)^{-(n+1)} \right], \\
l_{n_1, n_2}^{(FB)d}(\omega_1, \omega_2) &= -\frac{1}{4} v_d^{-1} k^{2(n_1+n_2)-d} \int \frac{d^d p}{(2\pi)^d} \times \\
&\quad \frac{1}{\tilde{\partial}_t (P_F(p) + \omega_1 k^2)^{n_1} (P_B(p) + \omega_2 k^2)^{n_2}}, \\
l_{n_1, n_2, n_3}^{(FB)d}(\omega_1, \omega_2, \omega_3) &= -\frac{k^{2(n_1+n_2+n_3)-d}}{4v_d} \int \frac{d^d p}{(2\pi)^d} \times \\
&\quad \frac{1}{\tilde{\partial}_t (P_F(p) + k^2 \omega_1)^{n_1} (P_B(p) + k^2 \omega_2)^{n_2} (P_B(p) + k^2 \omega_3)^{n_3}}, \\
l_{nT}^{(GB)d}(\omega) &= \frac{n + \delta^{n0}}{4v_d} k^{2n-d} \int \frac{d^d p}{(2\pi)^d} \frac{\frac{1}{Z_F} \partial_t (Z_F p^2 r_{kGB})}{(P_{GB}(p) + \omega k^2)^{n+1}}, \\
l_{nL}^{(GB)d}(\omega) &= \frac{n + \delta^{n0}}{4v_d} k^{2n-d} \int \frac{d^d p}{(2\pi)^d} \frac{\frac{1}{Z_\phi} \partial_t (Z_\phi p^2 r_{kGB})}{(P_{GB}(p) + \omega k^2)^{n+1}}, \\
l_n^{(G)d}(\omega) &= \frac{n + \delta^{n0}}{4v_d} k^{2n-d} \int \frac{d^d p}{(2\pi)^d} \frac{\partial_t (p^2 r_{kG}(p))}{(P_G(p) + \omega k^2)^{n+1}},
\end{aligned}$$

$$\begin{aligned}
l_{n_1, n_2}^{(\text{BGB})d}(\omega_1, \omega_2) &= -\frac{k^{2(n_1+n_2)-d}}{8v_d} \int \frac{d^d p}{(2\pi)^d} \tilde{\partial}_t \frac{1}{(P_B + \omega_1 k^2)^{n_1} (P_{GB} + \omega_2 k^2)^{n_2}}, \\
m_{n_1, n_2}^d(\omega_1, \omega_2) &= -\frac{1}{4} v_d^{-1} k^{2(n_1+n_2-1)-d} \int \frac{d^d p}{(2\pi)^d} p^2 \times \\
&\quad \tilde{\partial}_t \left[\frac{\frac{\partial}{\partial p^2} P_B(p)}{(P_B(p) + \omega_1 k^2)^{n_1}} \frac{\frac{\partial}{\partial p^2} P_B(p)}{(P_B(p) + \omega_2 k^2)^{n_2}} \right], \\
m_2^{(\text{F})d}(\omega) &= -\frac{1}{4} v_d^{-1} k^{6-d} \int \frac{d^d p}{(2\pi)^d} p^2 \tilde{\partial}_t \left[\frac{\frac{\partial}{\partial p^2} P_F(p)}{(P_F(p) + \omega k^2)^2} \right]^2, \\
m_4^{(\text{F})d}(\omega) &= -\frac{1}{4} v_d^{-1} k^{4-d} \int \frac{d^d p}{(2\pi)^d} p^4 \tilde{\partial}_t \left[\frac{\partial}{\partial p^2} \frac{1 + r_{kF}(p)}{P_F(p) + \omega k^2} \right]^2, \\
m_{n_1, n_2}^{(\text{FB})d}(\omega_1, \omega_2) &= -\frac{1}{4} v_d^{-1} k^{2(n_1+n_2-1)-d} \int \frac{d^d p}{(2\pi)^d} p^2 \times \\
&\quad \tilde{\partial}_t \left[\frac{1 + r_{kF}(p)}{(P_F(p) + \omega_1 k^2)^{n_1}} \frac{\frac{\partial}{\partial p^2} P_B(p)}{(P_B(p) + \omega_2 k^2)^{n_2}} \right], \\
m^{(\text{FBG})}(\omega_1, \omega_2, \omega_3) &= -\frac{k^{4-d}}{4v_d} \int \frac{d^d p}{(2\pi)^d} \tilde{\partial}_t \frac{p^2 (1 + r_F)}{(P_B + \omega_1 k^2) (P_F + \omega_2 k^2) (P_{GB} + \omega_3 k^2)}, \\
m_{n_1, n_2}^{(\text{BGB})d}(\omega_1, \omega_2) &= -\frac{k^{2(n_1+n_2-1)-d}}{4v_d} \int \frac{d^d p}{(2\pi)^d} \tilde{\partial}_t \frac{p^2 \frac{\partial}{\partial p^2} P_{GB}}{(P_B + \omega_1 k^2)^{n_1} (P_{GB} + \omega_2 k^2)^{n_2}}, \\
m_4^{(\text{BGB})d}(\omega_1, \omega_2) &= -\frac{k^{4-d}}{4v_d} \int \frac{d^d p}{(2\pi)^d} p^4 \tilde{\partial}_t \frac{\left(\frac{\partial}{\partial p^2} P_B \right) \left(\frac{\partial}{\partial p^2} P_{GB} \right)}{(P_B + \omega_1 k^2)^2 (P_{GB} + \omega_2 k^2)^2}, \\
m_{n_1, n_2}^{(\text{FGB})d}(\omega_1, \omega_2) &= -\frac{k^{2(n_1+n_2-1)-d}}{4v_d} \int \frac{d^d p}{(2\pi)^d} p^2 \tilde{\partial}_t \left(\frac{1 + r_F}{(P_F + \omega_1 k^2)^{n_1}} \frac{\frac{\partial}{\partial p^2} P_{GB}}{(P_{GB} + \omega_2 k^2)^{n_2}} \right).
\end{aligned}$$

Here $\tilde{\partial}_t$ only acts on the regulator R_k (neither r_{kB} nor r_{kF}). For explicit calculations we use the following bosonic regulator:

$$r_{kB}(p) = \left(\frac{k^2}{p^2} - 1 \right) \theta \left(1 - \frac{p^2}{k^2} \right),$$

where θ is the Heviside function. The fermionic regulator is determined by

$$(1 + r_{kB}(p)) = (1 + r_{kF}(p))^2.$$

In [43] is shown, that these regulators are optimal in the sense that they maximise the gap C in

$$\min_{q^2 \geq 0} (\Gamma_k^{(2)} + R_k) = Ck^2 > 0.$$

For the ghost regulator and the gauge bosonic regulator we choose $r_{kGB}(p) = r_{kG}(p) = r_{kB}(p)$. Using this and analytically perform the integrals we end up with

the following threshold functions:

$$\begin{aligned}
l_n^d(\omega) &= \frac{2(\delta_{n,0} + n)}{d} \left(1 - \frac{\eta_\phi}{d+2}\right) \frac{1}{(1+\omega)^{n+1}}, \\
l_{n,L/R}^{(F)d}(\omega) &= \frac{2(\delta_{n,0} + n)}{d} \left(1 - \frac{\eta_{L/R}}{d+1}\right) \frac{1}{(1+\omega)^{n+1}}, \\
l_{n_1,n_2}^{(FB)d}(\omega_1, \omega_2) &= \frac{2}{d} \frac{1}{(1+\omega_1)^{n_1} (1+\omega_2)^{n_2}} \times \\
&\quad \left[\frac{n_1}{1+\omega_1} \left(1 - \frac{\frac{1}{2}(\eta_R + \eta_L)}{d+1}\right) + \frac{n_2}{1+\omega_2} \left(1 - \frac{\eta_\phi}{d+2}\right) \right], \\
l_{n_1,n_2,n_3}^{(FB)d}(\omega_1, \omega_2, \omega_3) &= \frac{2}{d} \frac{1}{(1+\omega_1)^{n_1} (1+\omega_2)^{n_2} (1+\omega_3)^{n_3}} \times \\
&\quad \left[\frac{n_1}{1+\omega_1} \left(1 - \frac{\frac{1}{2}(\eta_L + \eta_R)}{d+1}\right) \right. \\
&\quad \left. + \frac{n_2}{1+\omega_2} \left(1 - \frac{\eta_\phi}{d+2}\right) + \frac{n_3}{1+\omega_3} \left(1 - \frac{\eta_\phi}{d+2}\right) \right], \\
l_{nT}^{(GB)d}(\omega) &= \frac{2(\delta_{n,0} + n)}{d} \left(1 - \frac{\eta_F}{d+2}\right) \frac{1}{(1+\omega)^{n+1}}, \\
l_{nL}^{(GB)d}(\omega) &= \frac{2(\delta_{n,0} + n)}{d} \left(1 - \frac{\eta_\phi}{d+2}\right) \frac{1}{(1+\omega)^{n+1}}, \\
l_n^{(G)d}(\omega) &= \frac{2(\delta_{n,0} + n)}{d} \frac{1}{(1+\omega)^{n+1}}, \\
l_{n_1,n_2}^{(BGB)d}(\omega_1, \omega_2) &= \frac{1}{d(1+\omega_1)^{n_1} (1+\omega_2)^{n_2}} \times \\
&\quad \left[\frac{n_1}{1+\omega_1} \left(1 - \frac{\eta_\phi}{d+2}\right) + \frac{n_2}{1+\omega_2} \left(1 - \frac{\eta_F}{d+2}\right) \right], \\
m_{n_1,n_2}^d(\omega_1, \omega_2) &= \frac{1}{(1+\omega_1)^{n_1} (1+\omega_2)^{n_2}}, \\
m_2^{(F)d}(\omega) &= \frac{1}{(1+\omega)^4}, \\
m_4^{(F)d}(\omega) &= \frac{1}{(1+\omega)^4} + \frac{1 - \frac{1}{2}(\eta_R + \eta_L)}{d-2} \frac{1}{(1+\omega)^3} \\
&\quad - \left(\frac{1 - \frac{1}{2}(\eta_R + \eta_L)}{2d-4} + \frac{1}{4} \right) \frac{1}{(1+\omega)^2},
\end{aligned}$$

$$\begin{aligned}
m_{n_1, n_2}^{(\text{FB})d}(\omega_1, \omega_2) &= \left(1 - \frac{\eta_\phi}{d+1}\right) \frac{1}{(1+\omega_1)^{n_1}(1+\omega_2)^{n_2}}, \\
m^{(\text{FBG})}(\omega_1, \omega_2, \omega_3) &= \frac{1}{(1+\omega_1)(1+\omega_2)(1+\omega_3)} \times \\
&\quad \left[-\frac{1-\eta_\psi}{d+1} - \frac{\eta_\psi}{d+2} + \frac{\frac{\eta_\phi}{d+3} + \frac{2-\eta_\phi}{d+1}}{1+\omega_1} \right. \\
&\quad \left. + \frac{\frac{2(1-\eta_\psi)}{d+1} + \frac{2\eta_\psi}{d+2}}{1+\omega_2} + \frac{\frac{\eta_F}{d+3} + \frac{2-\eta_F}{d+1}}{1+\omega_3} \right], \\
m_{n_1, n_2}^{(\text{BGB})d}(\omega_1, \omega_2) &= \frac{1}{(1+\omega_1)^{n_1}(1+\omega_2)^{n_2}}, \\
m_4^{(\text{BGB})d}(\omega_1, \omega_2) &= \frac{1}{(1+\omega_1)^2(1+\omega_2)^2}, \\
m_{n_1, n_2}^{(\text{FGB})d}(\omega_1, \omega_2) &= \frac{\left(1 - \frac{\eta_F}{d+2}\right)}{(1+\omega_1)^{n_1}(1+\omega_2)^{n_2}}.
\end{aligned}$$

Bibliography

- [1] M. Luscher and P. Weisz. Scaling Laws and Triviality Bounds in the Lattice ϕ^4 Theory. 1. One Component Model in the Symmetric Phase. *Nucl. Phys.*, B290:25, 1987.
- [2] M. Luscher and P. Weisz. Scaling Laws and Triviality Bounds in the Lattice ϕ^4 Theory. 2. One Component Model in the Phase with Spontaneous Symmetry Breaking. *Nucl. Phys.*, B295:65, 1988.
- [3] M. Luscher and P. Weisz. Scaling Laws and Triviality Bounds in the Lattice ϕ^4 Theory. 3. N Component Model. *Nucl. Phys.*, B318:705, 1989.
- [4] A. Hasenfratz, K. Jansen, C. B. Lang, T. Neuhaus, and H. Yoneyama. The Triviality Bound of the Four Component ϕ^4 Model. *Phys. Lett.*, B199:531, 1987.
- [5] D. J. E. Callaway. Triviality Pursuit: Can Elementary Scalar Particles Exist? *Phys. Rept.*, 167:241, 1988.
- [6] U. M. Heller, H. Neuberger, and P. M. Vranas. Large N analysis of the Higgs mass triviality bound. *Nucl. Phys.*, B399:271–348, 1993, hep-lat/9207024.
- [7] O. J. Rosten. Triviality from the Exact Renormalization Group. *JHEP*, 07:019, 2009, hep-th/0808.0082.
- [8] M. Gell-Mann and F. E. Low. Quantum electrodynamics at small distances. *Phys. Rev.*, 95:1300–1312, 1954.
- [9] M. Gockeler et al. Is there a Landau pole problem in QED? *Phys. Rev. Lett.*, 80:4119–4122, 1998, hep-th/9712244.
- [10] M. Gockeler et al. Resolution of the Landau pole problem in QED. *Nucl. Phys. Proc. Suppl.*, 63:694–696, 1998, hep-lat/9801004.
- [11] H. Gies and J. Jaeckel. Renormalization flow of QED. *Phys. Rev. Lett.*, 93:110405, 2004, hep-ph/0405183.
- [12] J. Kuti, L. Lin, and Y. Shen. Upper bound on the higgs-boson mass in the standard model. *Phys. Rev. Lett.*, 61(6):678–681, Aug 1988.

- [13] I-H. Lee, J. Shigemitsu, and R. E. Shrock. Lattice Study of A Yukawa Theory with a real Scalar Field. *Nucl. Phys.*, B330:225, 1990.
- [14] I-H. Lee, J. Shigemitsu, and R. E. Shrock. Study of Different Lattice Formulations of a Yukawa Model with a real Scalar Field. *Nucl. Phys.*, B334:265, 1990.
- [15] J. Smit. Standard Model and Chiral Gauge Theories on the Lattice. *Nucl. Phys. Proc. Suppl.*, 17:3–16, 1990.
- [16] J. Shigemitsu. Higgs - yukawa - chiral models 1. *Nuclear Physics B - Proceedings Supplements*, 20:515 – 527, 1991.
- [17] K. Jansen. Domain wall fermions and chiral gauge theories. *Phys. Rept.*, 273:1–54, 1996, hep-lat/9410018.
- [18] P. Gerhold and K. Jansen. The phase structure of a chirally invariant lattice Higgs- Yukawa model for small and for large values of the Yukawa coupling constant. *JHEP*, 09:041, 2007, hep-lat/0705.2539.
- [19] P. Gerhold and K. Jansen. The phase structure of a chirally invariant lattice Higgs- Yukawa model - numerical simulations. *JHEP*, 10:001, 2007, hep-lat/0707.3849.
- [20] P. Gerhold, K. Jansen, and J. Kallarackal. Higgs mass bounds from a chirally invariant lattice Higgs- Yukawa model with overlap fermions. 2008, hep-lat/0810.4447.
- [21] Z. Fodor, K. Holland, J. Kuti, D. Negradi, and C. Schroeder. New Higgs physics from the lattice. *PoS*, LAT2007:056, 2007, hep-lat/0710.3151.
- [22] M. Harada, Y. Kikukawa, T. Kugo, and H. Nakano. Nontriviality of gauge Higgs-Yukawa system and renormalizability of gauged NJL model. *Prog. Theor. Phys.*, 92:1161–1184, 1994, hep-ph/9407398.
- [23] R. Percacci and D. Perini. Constraints on matter from asymptotic safety. *Phys. Rev.*, D67:081503, 2003, hep-th/0207033.
- [24] R. Percacci and D. Perini. Asymptotic safety of gravity coupled to matter. *Phys. Rev.*, D68:044018, 2003, hep-th/0304222.
- [25] M. Shaposhnikov and C. Wetterich. Asymptotic safety of gravity and the Higgs boson mass. *Phys. Lett.*, B683:196–200, 2010, hep-th/0912.0208.
- [26] H. Gies and M. M. Scherer. Asymptotic safety of simple Yukawa systems. 2009, hep-th/0901.2459.
- [27] H. Gies, S. Rechenberger, and M. M. Scherer. Towards an Asymptotic-Safety Scenario for Chiral Yukawa Systems. 2009, hep-th/0907.0327.

- [28] M. M. Scherer, H. Gies, and S. Rechenberger. An asymptotic-safety mechanism for chiral Yukawa systems. 2009, hep-th/0910.0395.
- [29] H. Gies, L. Janssen, S. Rechenberger, and M. M. Scherer. Phase transition and critical behavior of $d=3$ chiral fermion models with left/right asymmetry. *Phys. Rev.*, D81:025009, 2010, 0910.0764.
- [30] C. Wetterich. Exact evolution equation for the effective potential. *Phys. Lett.*, B301:90–94, 1993.
- [31] J. Berges, N. Tetradis, and C. Wetterich. Non-perturbative renormalization flow in quantum field theory and statistical physics. *Phys. Rept.*, 363:223–386, 2002, hep-ph/0005122.
- [32] J. Polonyi. Lectures on the functional renormalization group method. *Central Eur. J. Phys.*, 1:1–71, 2003, hep-th/0110026.
- [33] J. M. Pawłowski. Aspects of the functional renormalisation group. *Annals Phys.*, 322:2831–2915, 2007, hep-th/0512261.
- [34] H. Gies. Introduction to the functional rg and applications to gauge theories. 2006, hep-ph/0611146.
- [35] B. Delamotte. An introduction to the nonperturbative renormalization group. 2007, cond-mat/0702365.
- [36] H. Sonoda. The Exact Renormalization Group – renormalization theory revisited –. 2007, hep-th/0710.1662.
- [37] D. U. Jungnickel and C. Wetterich. Effective action for the chiral quark-meson model. *Phys. Rev.*, D53:5142–5175, 1996, hep-ph/9505267.
- [38] L. Rosa, P. Vitale, and C. Wetterich. Critical exponents of the Gross-Neveu model from the effective average action. *Phys. Rev. Lett.*, 86:958–961, 2001, hep-th/0007093.
- [39] F. Hofling, C. Nowak, and C. Wetterich. Phase transition and critical behaviour of the $d = 3$ gross-neveu model. *Phys. Rev.*, B66:205111, 2002, cond-mat/0203588.
- [40] H. Gies and C. Wetterich. Renormalization flow of bound states. *Phys. Rev.*, D65:065001, 2002, hep-th/0107221.
- [41] H. Gies and C. Wetterich. Universality of spontaneous chiral symmetry breaking in gauge theories. *Phys. Rev.*, D69:025001, 2004, hep-th/0209183.
- [42] J. Braun. Thermodynamics of QCD low-energy models and the derivative expansion of the effective action. *Phys. Rev.*, D81:016008, 2010, 0908.1543.
- [43] D. F. Litim. Optimised renormalisation group flows. *Phys. Rev.*, D64:105007, 2001, hep-th/0103195.

- [44] S. Weinberg, in C76-07-23.1 HUTP-76/160, Erice Subnucl. Phys., 1, (1976).
- [45] S. Weinberg. Ultraviolet divergences in quantum theories of gravitation. In Hawking, S.W., Israel, W.: General Relativity, 790- 831.
- [46] B. Rosenstein, B. J. Warr, and S. H. Park. The Four Fermi Theory Is Renormalizable in (2+1)- Dimensions. *Phys. Rev. Lett.*, 62:1433–1436, 1989.
- [47] J. M. Schwindt and C. Wetterich. Asymptotically free four-fermion interactions and electroweak symmetry breaking. 2008, hep-th/0812.4223.
- [48] A. Codello and R. Percacci. Fixed Points of Nonlinear Sigma Models in $d > 2$. *Phys. Lett.*, B672:280–283, 2009, hep-th/0810.0715.
- [49] C. de Calan, P. A. Faria da Veiga, J. Magnen, and R. Seneor. Constructing the three-dimensional Gross-Neveu model with a large number of flavor components. *Phys. Rev. Lett.*, 66:3233–3236, 1991.
- [50] H. Gies, J. Jaeckel, and C. Wetterich. Towards a renormalizable standard model without fundamental Higgs scalar. *Phys. Rev.*, D69:105008, 2004, hep-ph/0312034.
- [51] H. Gies. Renormalizability of gauge theories in extra dimensions. *Phys. Rev.*, D68:085015, 2003, hep-th/0305208.
- [52] M. Reuter. Nonperturbative Evolution Equation for Quantum Gravity. *Phys. Rev.*, D57:971–985, 1998, hep-th/9605030.
- [53] W. Souma. Non-trivial ultraviolet fixed point in quantum gravity. *Prog. Theor. Phys.*, 102:181–195, 1999, hep-th/9907027.
- [54] O. Lauscher and M. Reuter. Ultraviolet fixed point and generalized flow equation of quantum gravity. *Phys. Rev.*, D65:025013, 2002, hep-th/0108040.
- [55] O. Lauscher and M. Reuter. Is quantum Einstein gravity nonperturbatively renormalizable? *Class. Quant. Grav.*, 19:483–492, 2002, hep-th/0110021.
- [56] P. Forgacs and M. Niedermaier. A fixed point for truncated quantum Einstein gravity. 2002, hep-th/0207028.
- [57] A. Codello, R. Percacci, and C. Rahmede. Ultraviolet properties of $f(R)$ -gravity. *Int. J. Mod. Phys.*, A23:143–150, 2008, hep-th/0705.1769.
- [58] D. Benedetti, P. F. Machado, and F. Saueressig. Asymptotic safety in higher-derivative gravity. *Mod. Phys. Lett.*, A24:2233–2241, 2009, hep-th/0901.2984.
- [59] D. Benedetti, P. F. Machado, and F. Saueressig. Four-derivative interactions in asymptotically safe gravity. 2009, hep-th/0909.3265.
- [60] D. Benedetti, P. F. Machado, and F. Saueressig. Taming perturbative divergences in asymptotically safe gravity. *Nucl. Phys.*, B824:168–191, 2010, hep-th/0902.4630.

-
- [61] A. Eichhorn, H. Gies, and M. M. Scherer. Asymptotically free scalar curvature-ghost coupling in Quantum Einstein Gravity. *Phys. Rev.*, D80:104003, 2009, hep-th/0907.1828.
- [62] A. Eichhorn and H. Gies. Ghost anomalous dimension in asymptotically safe quantum gravity. 2010, 1001.5033.
- [63] R. Percacci. Asymptotic safety. 2007, hep-th/0709.3851.
- [64] S. Weinberg. Living with infinities. 2009, hep-th/0903.0568.
- [65] K. Moriyasu. *An elementary Primer for Gauge Theory*. Worls Scientific Publishing, 1983.
- [66] T. Kugo. *Eichtheorie*. Springer-Verlag, 1997.
- [67] C. Becchi. Introduction to gauge theories. 1996, hep-ph/9705211.
- [68] M.E. Peskin and D.V. Schroeder. *An Introduction to Quantum Field Theory*. Westview Press, 1995.
- [69] M. Kaku. *Quantum Field Theory*. Oxford University Press, 1993.
- [70] F. Mandl and G. Shaw. *Quantenfeldtheorie*. Aula-Verlag, 1993.
- [71] M. Gomes, R. S. Mendes, R. F. Ribeiro, and A. J. da Silva. Gauge structure, anomalies and mass generation in a three- dimensional Thirring model. *Phys. Rev.*, D43:3516–3523, 1991.
- [72] Y. Nambu and G. Jona-Lasinio. Dynamical model of elementary particles based on an analogy with superconductivity. I. *Phys. Rev.*, 122:345–358, 1961.
- [73] Y. Nambu and G. Jona-Lasinio. Dynamical model of elementary particles based on an analogy with superconductivity. II. *Phys. Rev.*, 124:246–254, 1961.
- [74] W. E. Thirring. A soluble relativistic field theory. *Annals Phys.*, 3:91–112, 1958.
- [75] S. Christofi, S. Hands, and C. Strouthos. Critical flavor number in the three dimensional Thirring model. *Phys. Rev.*, D75:101701, 2007, hep-lat/0701016.
- [76] I. F. Herbut, V. Juricic, and B. Roy. Theory of interacting electrons on the honeycomb lattice. *Phys. Rev.*, B79:085116, 2009, cond-mat.str-el/0811.0610.
- [77] F. Benitez et al. Solutions of renormalization group flow equations with full momentum dependence. *Phys. Rev.*, E80:030103, 2009, cond-mat.stat-mech/0901.0128.

Acknowledgements

I would like to thank Prof. Dr. Holger Gies for the supervision of this thesis and his support during the work. Furthermore I would like to thank Dr. Jens Braun for being the second supervisor and reviewing the work. Special thanks go to Dipl. Phys. Michael M. Scherer for his support and many illuminating discussions. Thanks also go to the rest of the group of Prof. Dr. Holger Gies for helpful discussions and a nice year as a part of this group. It would be remiss of me not to express my gratitude to my parents and my wife who supported me during the whole study.